Role of eddies in the Bay of Bengal circulation and hydrography and in the distribution of nutrients and chlorophyll

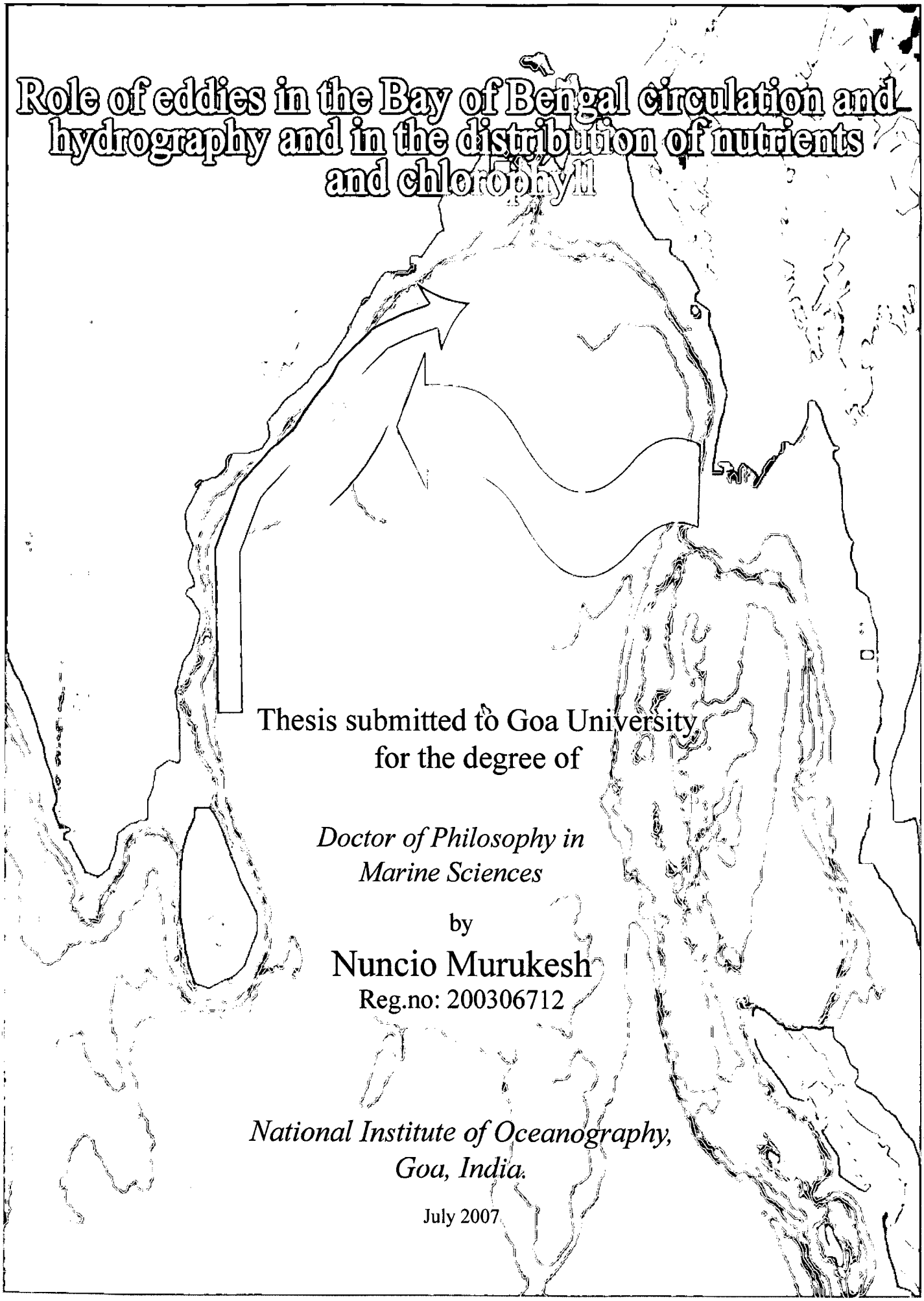

Thesis submitted to Goa University
for the degree of

Doctor of Philosophy in
Marine Sciences

by

Nuncio Murukesh
Reg.no: 200306712

National Institute of Oceanography,
Goa, India.

July 2007

Role of eddies in the Bay of Bengal circulation and hydrography and in the distribution of nutrients and chlorophyll

Thesis submitted to

Goa University

For the degree of

Doctor of Philosophy

in

Marine Sciences

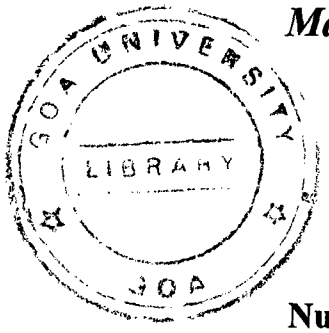

by

Nuncio Murukesh
Reg.no: 200306712

National Institute of Oceanography,
Goa, India.

July 2007

List of Contents

Statement

As required under the University ordinance 0.19.8(vi), I state that this thesis entitled "Role of eddies in the Bay of Bengal circulation and hydrography and in the distribution of nutrients and chlorophyll" is my original contribution and it has not been submitted on any previous occasion.

The literature related to the problem investigated has been cited. Due acknowledgements have been made wherever facilities and suggestions have been availed off.

Nuncio Murukesh

National Institute of Oceanography
Dona Paula, Goa

Place: Dona Paula

Date: 13 July 2007

Certificate

This is to certify that the thesis entitled "The role of eddies in the Bay of Bengal circulation and hydrography and in the distribution of nutrients and chlorophyll" submitted by Shri. Nuncio Murukesh for the award of the degree of Doctor of Philosophy in Marine Science is based on original studies carried out by him under my supervision. The thesis or any part thereof has not been previously submitted for any other degree or diploma in any institution.

Dr. S. Prasanna Kumar

Research Supervisor

National Institute of Oceanography

Dona Paula, Goa

Place: Dona Paula

Date: 13 July 2007

All the suggestions of the experts have been incorporated.

R R Rao

7 Feb. 08

Acknowledgements

Though I encountered eddies in one of the data analysis and synthesis session of MR-LR programme, I had no idea whether it would make it into this volume. But plans were working out differently. Soon I came to know that Dr Prasanna Kumar is ready to take a student and by that time I received a decent fellowship from Council of Scientific and Industrial research, which have been my all means of living through these years, and I happily boarded the train to Goa. Even after, this was only one of the topics under consideration, before he finally showed the green signal. The Head of the Department, HRDG and the Director, NIO forwarded my proposal with out any delay and permitted to utilize the institute's resources. During these years Dr Prasanna has not only been a good supervisor but a good friend and a great motivator who thinks about me more than I ever would. The interactions we had, leapfrogged my insight on how oceans function as a single entity. He allowed me to use the BOBPS data set which forms the basis of the present study and instilled courage to go ahead in difficult times. After a year, Goa University kindly permitted to register my study under the Marine Science Department and offered their services and Dr. Ramesh Pai was appointed as co-guide. His comments and suggestions have made me to go that extra mile and his presence has ensured an efficient link between me and the university. Dr G.N. Nayak, HOD Marine Science has been prompt in the university related matters and critically monitored the progress of my work.

Back in NIO, Remote sensing lab offered a calm place to ruminate. Dr's VSN Murty and Babu never hesitated to spend time whenever required and Dr Fernandes happily shared his knowledge, so too was Dr Ramesh Kumar but, in return I had to share responsibilities of NIO's cultural activities. Dr Vethamony had painstakingly gone through my half-yearly reports and offered valuable suggestions. Dr Rajan of NCAOR and Dr Sujatha Kaisare of NIO functioned as external members for the review committee along with the HRDG of the institute. Their critical comments helped to see science from a common man's perspective. All through these years I've been a seagoing ocean researcher. It was the BOBPS colleagues who made each of my voyages memorable. Their technical and scientific acumen has generated a reliable data set from one of the least explored regions of the world oceans.

This research would not have been possible without the backing of an efficient library. The huge repository of information stunningly kept at the finger tips has not only downsized many tedious hours of searching references but made learning an exhilarating experience. An efficient LAN and Internet has made possible downloading of many data sets kept in the public domain which are used in the present study and communicating science faster. I would have had a tough time keeping my records without an efficient administrative section, which made it all the more easier. The publication and reprography division had every solution to make the figures more appealing.

Sreejith had done the first installation of Linux for me, which still runs perfect. There was all smiles, when I approached him in my initial days with my qualms to get the code

running. Then I relied on Sudheesh, as Sreejith left NIO, who took time from his own work to fix the bugs. Almeida was the first one to give a space in one of their workstations and Michael patiently heard my queries on GMT and FORTRAN during my initial days. Dr. Muraleedharan, Mr. Sathe and Mr. Saran had eased the toughest of the times. It turned out to be a happy experience every time as I let loose my thoughts to Mohammed. He listened patiently, offered suggestions and solutions. Things became easier as Gourish joined the group and provided able system administration and Jayu always lend a hand, though she fell victim of reckless conversations I had with my guide. Within and away from the department there were many who struck the right chords and made it all worthwhile. Initially there was Shoby, Sumesh, Anil, Sree Kumar and Swapna. Soon joined Ramesh, Krishnan, Roxy, Rajani, Diju, Reny, Kuldeep and Deepthi. Yatheesh & Aparna and Sudheesh & Srijitha many a times extended their warm hospitality. They made my stay in Goa a pleasant one and NIO colony a home away from home.

Finally it's my family members whose care and affection kept me going. My sister excused me a lot for not having been in time and my parents who let me to choose a path in which I find satisfaction. They ask quite often, how far I've been progressed? Finally I can say I' m done with. To them I dedicate this thesis.

Abstract

Eddies are ubiquitous in the ocean and are products of geophysical turbulence. They develop from the hydrodynamic instabilities and are known to alter the physical and biochemical properties of the ocean. In the north Indian Ocean (NIO), these changes in the hydrodynamical and biochemical properties are a response to the seasonal reversal of monsoon winds. Off the twin seas of the NIO, the Arabian Sea (AS) responds to this seasonal reversal more directly, whereas its eastern counterpart the Bay of Bengal (BOB) deviates from the norm. Apart from the seasonal reversal of the monsoon winds, BOB is influenced by the remote forcing via Rossby waves and coastally trapped Kelvin waves. Though the presence of eddies were reported in the BOB as early as 1950's, their genesis and evolution have not been subjected to intense scrutiny. Present study is an attempt in this direction and to decipher their role.

Recently concluded Bay of Bengal Process Studies (BOBPS) had two observational transects, along the central as well the western boundary of BOB, which was repeatedly sampled for 3 seasons during summer 2001, fall intermonsoon 2002 and spring inermonsoon 2003. Analysis of the thermohaline structure showed many undulations which can be characterized as eddies along both transects. They altered the ambient temperature by 2-6°C and salinity by 0.2 to 1 psu. Eddies observed along the western boundary and along the central BOB are found to have different origins.

Along the western boundary the cyclonic eddy designated as northern coastal eddy (NCE) was found to be a robust feature occurring every year. Satellite derived sea-level anomaly data during 2001 and 2003 showed that the NCE was formed in February from an instability in the northward flowing western boundary current. This instability was governed by a local positive wind-stress curl close to the western boundary and offshore negative wind-stress curl, and remote forcing via the westward propagating Rossby waves. NCE had a life span of about 5 months.

Eddies encountered along the central BOB appeared to have a different origin. It has been found that a gradient in sea-level anomaly, which is a manifestation of the horizontal density gradient, was generated out of a variety of physical processes (viz, large scale circulation, westward propagating Rossby waves and the wind forcing), which drives a vertical shear and baroclinic instability. However, this explanation does not hold good for all the eddies observed, especially those found during spring intermonsoon. The life cycle of these eddies is marked with splitting and coalescing. Evolution of these eddies studied using the satellite sea-level anomalies showed that they have a life span of about 1-5 months.

Analysis of heat and salt content showed that the heat content is dramatically influenced by the presence of eddies and was about 2-3 times the seasonal variability. The impact of eddies was not pronounced in the salt content. In the Bay of Bengal winds are comparatively weak hence the Ekman transport computed from the observed winds were found to be smaller (<1Sv) than the geostrophic transport which was about 2-8 Sv when

integrated in the upper 150 m depth. The geostrophic transport also was dominated by eddies. Enhanced heat and salt transports was noticed near these eddies which reached up to 600 x 10^{12} J/m/day and 200 x 10^{12} Kg/m/day respectively. This resulted in enhanced east-west and offshore-onshore transport of heat and salt.

Eddies not only influenced the thermohaline characteristics of the BOB, but showed its influence in the distribution of water-column nutrients as well as chlorophyll concentrations. Eddy-pumping supplied the much needed nutrients to the upper layers which in turn enhanced the chlorophyll concentrations by 2 to 6 times the ambient values in the BOB. Thus, the study show that eddies are ubiquitous in the BOB in all the seasons and play a key role in altering the physical, chemical and biological characteristics of this basin. The eddy-induced enhanced biological productivity in the BOB provides an explanation to the paradox of comparable rates of annual organic flux to the deeper ocean between biologically low productive BOB and a high productive Arabian Sea.

Chapter 1 - Introduction

1.1 An overview of eddies

A 'traditional' picture of oceanic fields of temperature, salinity, density and current shows that the changes occurring in time and in space are slow and smooth. This notion of slowly and smoothly changing ocean was rendered illusory with the advent of high resolution sampling techniques. They revealed that the oceanic motions vary abruptly in time and in space and are more energetic. This variability arises from a host of features, like rings, vortices, lens, meanders, jets, filaments etc. Physical oceanographers group them in a generic term 'eddies' [*Robinson,* 1983]. However, in oceanographic literature it is the circulating water columns that are commonly referred to as eddies. These features having dimensions of the order of Rossby deformation radius (~100 km) are called mesoscale eddies and received great attention during the later half of the 20^{th} century.

At planetary scales in the northern hemisphere, a northward moving parcel of water would turn right under the influence of Coriolis force. Consequently, water converges in a clockwise (anticyclonic) rotating eddy and diverges in an anticlockwise (cyclonic) eddy, leading to downwelling and upwelling respectively at their centers (Figure 1.1.1).

An examination of global picture of satellite sea-level anomaly (SLA) (Figure 1.1.2) shows that along the western boundaries of the ocean SLA tends to be heterogeneous, consisting of positive as well as negative anomalies, indicating strong eddy activity.

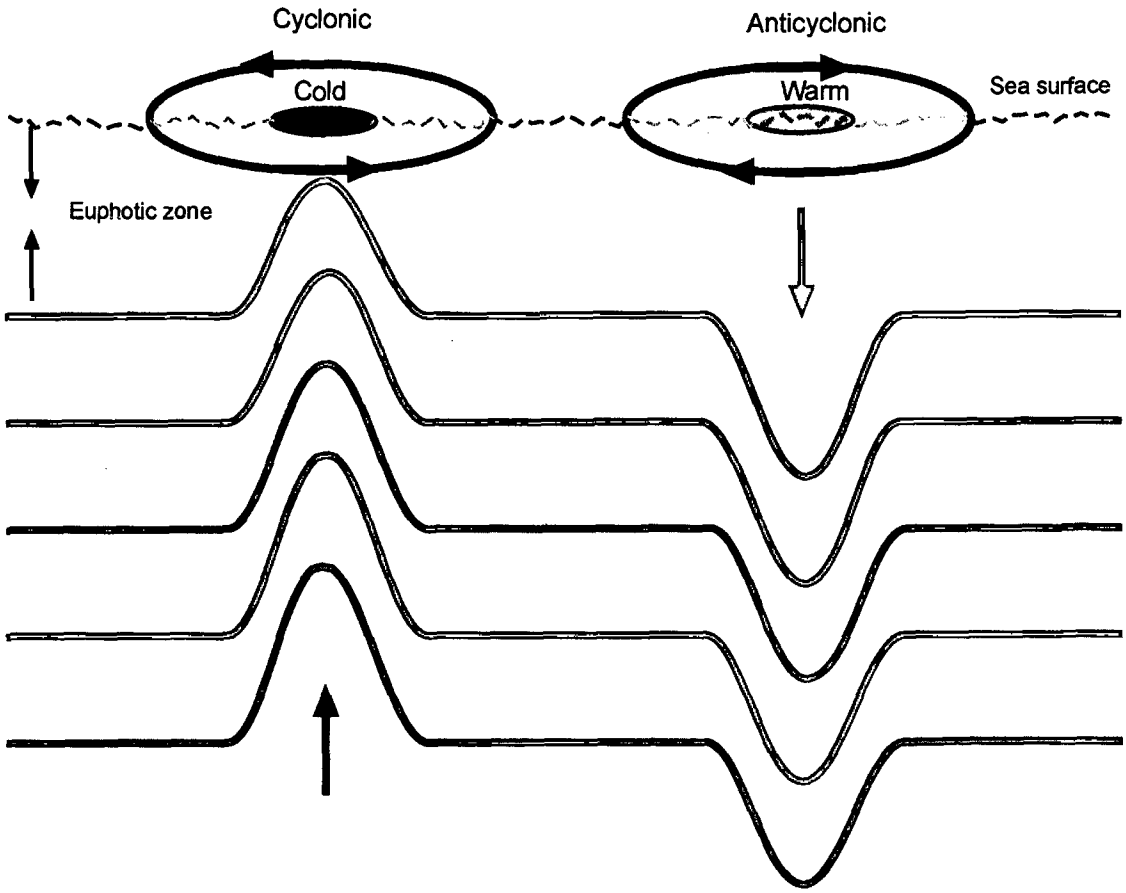

Figure1.1.1 Schematics of a cyclonic and an anticyclonic eddy. In a cyclonic eddy the thermocline is uplifted due to the divergence at its centre, whereas the thermocline is depressed in an anticyclonic eddy due to convergenence. This results in upwelling and downwelling respectively at their centres.

These are locations where currents are intense as a result of conservation of potential vorticity. These flows are called western boundary currents. These intense current regions are found to be the major eddy generating regions of the world.

For example the Gulf Stream (north Atlantic), Kuroshio (north Pacific), Somali current (north Indian Ocean), East Australian current (south Pacific), the Agulhas current (south Indian Ocean) are well known regions of eddy generation. The eddy kinetic energy found in these regions is several folds greater that the rest of the ocean [*Wyrtki et al.*, 1976]

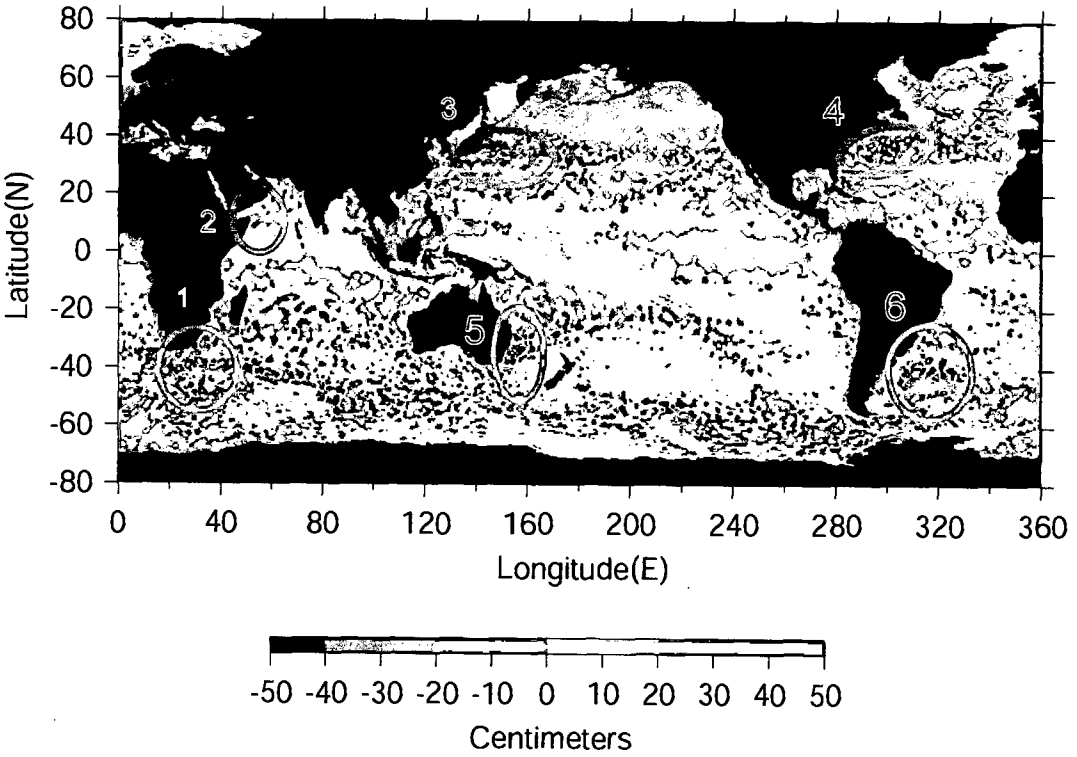

Figure 1.1.2 Sea-level anomaly obtained from AVISO live access sever (see chapter 2 for details) showing the major eddy dominated regions of the world. 1) Agulhas 2) Somali 3) Gulf stream 4) Kuroshio 5) East Australian current region 6)The Brazil-Malvinas confluence All these regions are located along the western boundary of the oceans and are characterised by intense current system known as the western boundary currents.

The causative factors for eddy generation in these regions are instabilities of these currents. These instabilities are categorized as barotropic and baroclinic instabilities, arising from the horizontal and vertical shear respectively of the horizontal currents [*Pedlosky,* 1979]. In case of baroclinic instability, the vertical shear can be related to the horizontal density gradient by the thermal wind relationship [*Pond and Pickard,* 1978]. Hence regions with horizontal gradients in density are susceptible to baroclinic instability. Barotropic instability, on the other hand, is depth independent and arises in currents with no vertical shear [*Pedlosky*, 1979]. A quantitative approximation of these instabilities can be made by computing the barotropic and baroclinic fluxes [*eg. Boning and Budich,* 1992]. The advantage with this approximation is that one can pinpoint what

type of instability is operating in a given region, but gives no idea of what are the mechanisms that generates such instability. *Stammer* [1997] using satellite altimetry showed baroclinic instability as the major mechanism of generating eddy energy in the ocean. Once generated they tend to propagate westwards because of the acquisition of relative vorticity by the displaced water parcel [*Cushman et al.,* 1990].

Eddies generated from the Gulf stream were the first to be studied experimentally and dates back to 1793 [*Robinson,* 1983]. The cold core eddies of these regions have a dimension of approximately 200 km and extends beyond 1000 m depth. These eddies are called rings and are the most energetic eddies studied till date. Studies showed that they develop from meanders towards the south of the stream [*Fuglister and Worthington,* 1947; *Iselin and Fuglister,* 1948] and play a significant role in removing salt and contributing to the primary productivity of the region [*The ring group,* 1981]. Warm core eddies too form in the region but towards the north of the Gulf Stream. Another eddy dominated region of World Ocean is the northwest Pacific, which is known for the poleward flowing Kuroshio current, a well known western boundary current. The Kuroshio current also generates warm and cold core eddies similar to the Gulf Stream [*Richardson,* 1983]. In the Indian Ocean, the best studied regions for eddies are the Somali and Agulhas current. Eddies in the Agulhas region play a vital role in inter-basin exchange of water across Indian and Atlantic oceans [*Lutjeharms*, 2006].

The first scientifically designed experiment to map eddies *in situ* and understand their dynamics was conducted in 1970 by USSR in the North Equatorial current code named as

POLYGON-70. The experiment used a suite of direct measurements to elucidate the, generating mechanism, energy level, spatial structure and the time evolution of the oceanic eddies [*Kamenkovich et al.,* 1986]. Subsequently, US lead Mid Ocean Dynamic Experiment (MODE) in the southwest of Bermuda in 1973 which revealed that ocean eddies are part of an energetic and structured variability field superposed on weaker gyre-scale circulation [*The MODE group*, 1978]. The USSR-US joint venture POLYMODE was the single largest experiment of its kind which investigated in more detail the dynamics of synoptic eddies in open ocean [*Kamenkovich et al.,* 1986]. During its execution many cyclonic as well as anticyclonic eddies of the dimension of deformation radius and smaller were encountered and studied. These experiments were conducted by occupying a pre-determined region in the ocean. Recent advancements in satellite altimetry allowed oceanographers to track eddies and study them individually. The recently concluded Mixing of Agulhas Ring Experiment (MARE) was one such kind in the Agulhas region which dealt with the role of eddies in inter-ocean exchange between Indian and Atlantic Ocean[*van Aken et al.,* 2003]. All these experiments unequivocally conclude that eddies are an important dynamical entity of ocean circulation.

1.2 The north Indian Ocean

The regions of eddy generation, except Somali current, discussed above are away from the tropics and the current systems have a permanent existence. How ever, the Northern Indian Ocean (NIO) is different from the rest. It is landlocked approximately at the tropic of cancer. During summer, the heating of Asian land mass generates large land-sea pressure difference, which drives the Monsoon winds. These winds, having an annual

periodicity, are southwesterly during summer (June-September) and northeasterly during winter (November-February), and are considered to be the primary forcing mechanism of the NIO. As a result, much of the studies on the variability of the NIO revolve around the monsoonal reversal.

One of the most extensively studied regions in the NIO is the Somali current, which lies along the western margin of the Arabian Sea (AS). Here eddies develop in close association with the development of the boundary current [*Robinson, 1983*]. With the onset of summer monsoon strong anti-cyclonic gyre is established along the east coast of Africa [*Schott*, 1983], the western limb of which is the Somali current and is characterized by strong vertical shears [*Swallow and Bruce* , 1966]. The 'Prime eddy' generated out of this current deepens the isotherms resulting in a loss of heat of the order of 10^{20} calories from the upper ocean to the deeper layers [*Bruce*, 1979].

Its eastern counterpart, the Bay of Bengal (BOB), is one of the least studied basins of the world ocean. Though lying in the same latitudinal belts both the seas are markedly different. On an average BOB is warmer and less saline and AS is cooler and more saline [*Levitus*, etal 1994, also see Figure 1.2.2 & 1.2.3]. This primarily arises from the fact that in the AS evaporation exceeds precipitation, whereas, in the BOB it is the precipitation that exceeds the evaporation (~ 2 m yr^{-1}) [*Prasad, 1997*]. Three major river systems - the Ganges-Bhramaputra, Irrawadi-Salween and the Krishna-Godavari - drain into the BOB. The total runoff from the peninsular rivers, which peaks during summer monsoon, amounts up to about 1.625×10^{25} m^3/yr [*Subramanian, 1993*] (Figure 1.2.1). This huge

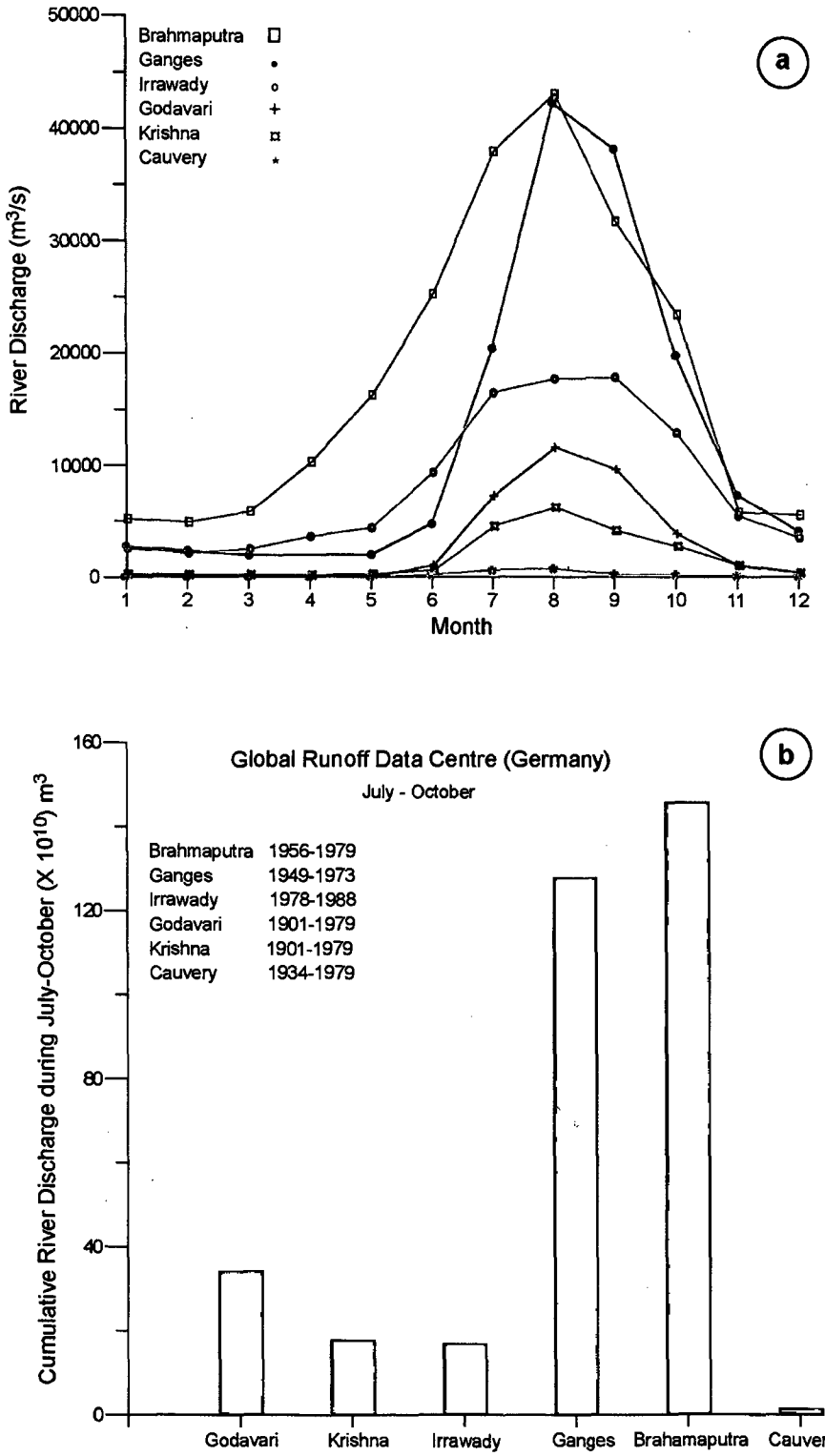

Figure. 1.2.1 Climatology of (a) monthly mean river discharge (m^3/s) and (b) cumulative dischage (m^3) during July to October of rivers Ganges, Brahmaputra, Irrawady, Godavari, Krishna and Cauvery. The river dischage data was obtained from Global Runoff Data Center, Germany (http://grdc.bafg.de/servlet/is/2781/).

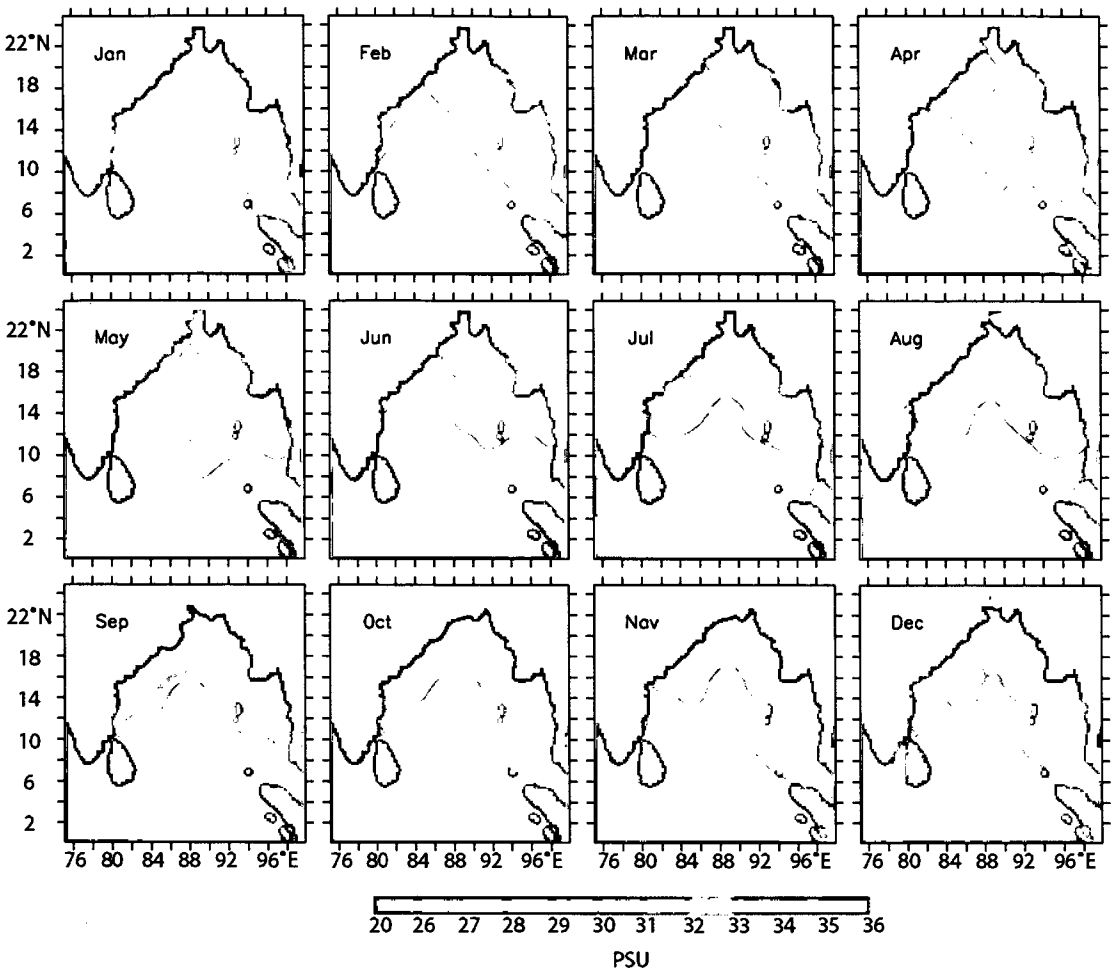

Figure 1.2.2 Surface salinity (psu) in the BOB obtained from the WOA01 climatology [*Conkright et al.*, 2002]. Northern regions of the BOB is fresher through out the year than the southen BOB due to high river discharge.

quantity of river runoff coupled with the excess precipitation induces large changes in the salinity, which is predominantly felt along its peripheries (Figure 1.2.2). However, the temperature shows much less variability except during winter (Figure 1.2.3). Low salinity with comparatively weak winds makes the BOB a highly stratified basin. The stability parameter in the BOB is 3-4 times greater than that in the AS [*Prasanna Kumar et al., 2002*] making it increasingly difficult to perturb the BOB except during the cyclonic storm period.

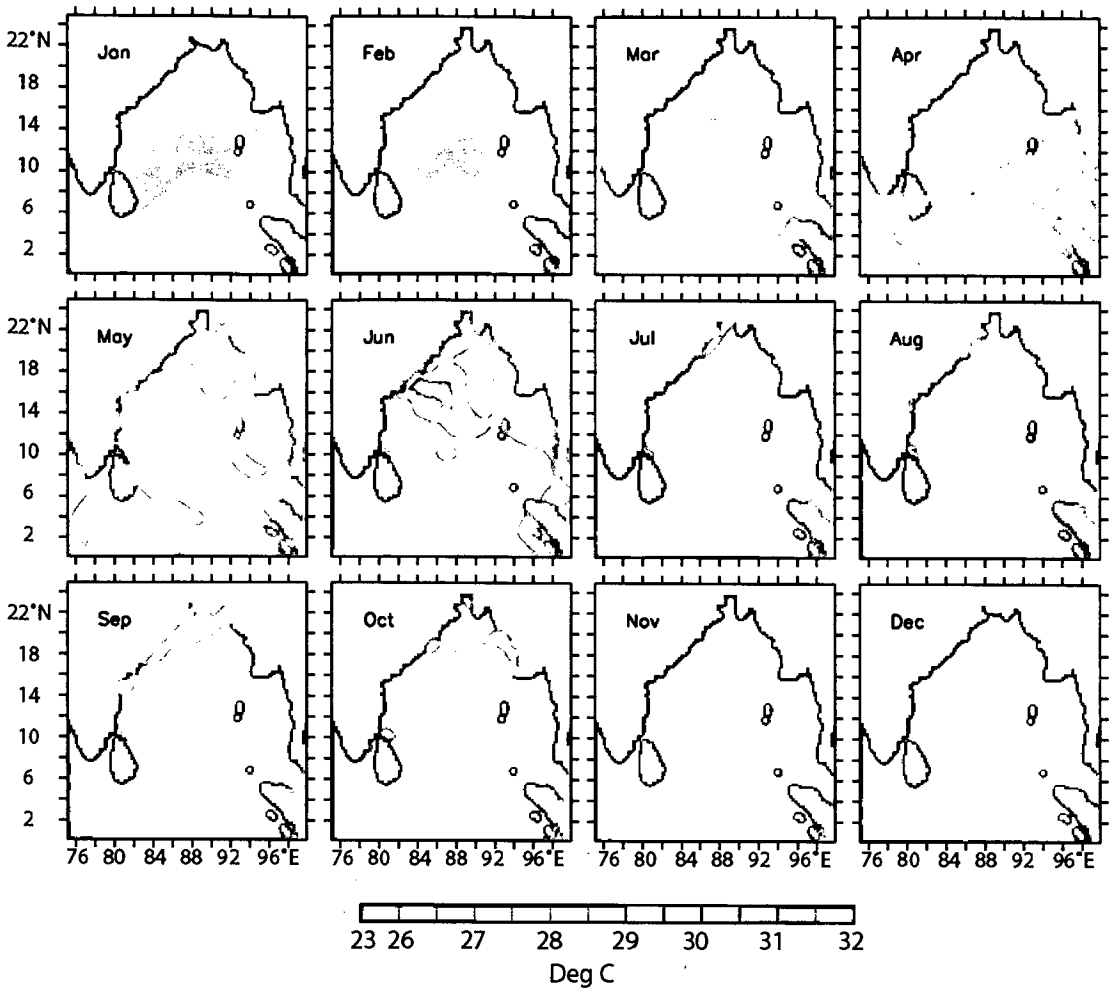

Figure 1.2.3 Sea surface temperature (°C) in the BOB obtained from the WOA01 climatology [*Conkright, et al.*, 2002].

Intense current regimes can be found in BOB too. The most striking one is the northward flowing East India Coastal Current (EICC) [*Shetye et al.*, 1993] during spring intermonsoon (March-May) (Figure 1.2.4). Despite low wind speeds (~4 m/s) this current attains a peak velocity of ~100 cm/s. This is in direct contrast with the AS where maximum current speeds are obtained during summer monsoon when the winds are stronger. This contrast is explained in terms of the role of remote forcing by the westward propagating Rossby waves and coastally trapped Kelvin waves in the

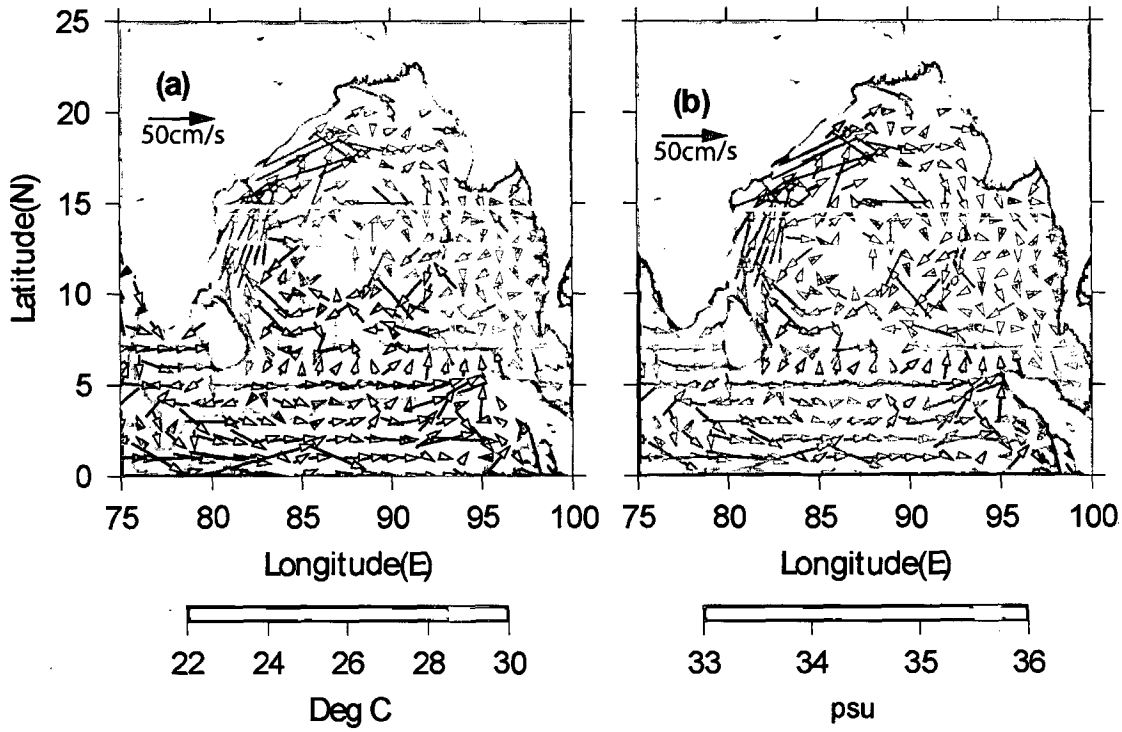

Figure 1.2.4. Monthly mean climatology of (a) temperature (°C) and (b) salinity (psu) from WOA01 [*Conkright et al.*, 2002] overlaid with one-degree surface current vectors derived from NOAA ship drift data during April.

establishment of this current [*Potemra et al.*, 1991, *Yu* et al., 1991, *Vinayachandran et al.*, 1996; *McCreary et al.*, 1996; *Shankar et al.*, 1996; *Shankar et al.*, 2002]. Studies indicate that this current is highly sheared in the vertical [*Babu et al., 2003*], which is an important aspect when dealing with the instabilities. During fall intermonsoon (October), however, this current is equatorward. Another region of intense current is the southern BOB during summer when the southwest monsoon current flows into the BOB. This current flows around the Sri Lankan dome (SLD), a wind driven sea-level low [*Vinayachandran et al., 1998*], carrying cold and high-saline waters into the warm and less-saline southern BOB during summer monsoon. Presence of SLD and the warmer and less-saline water to the east of it gives a frontal characteristic to the southern BOB during summer monsoon (Figure 1.2.5).

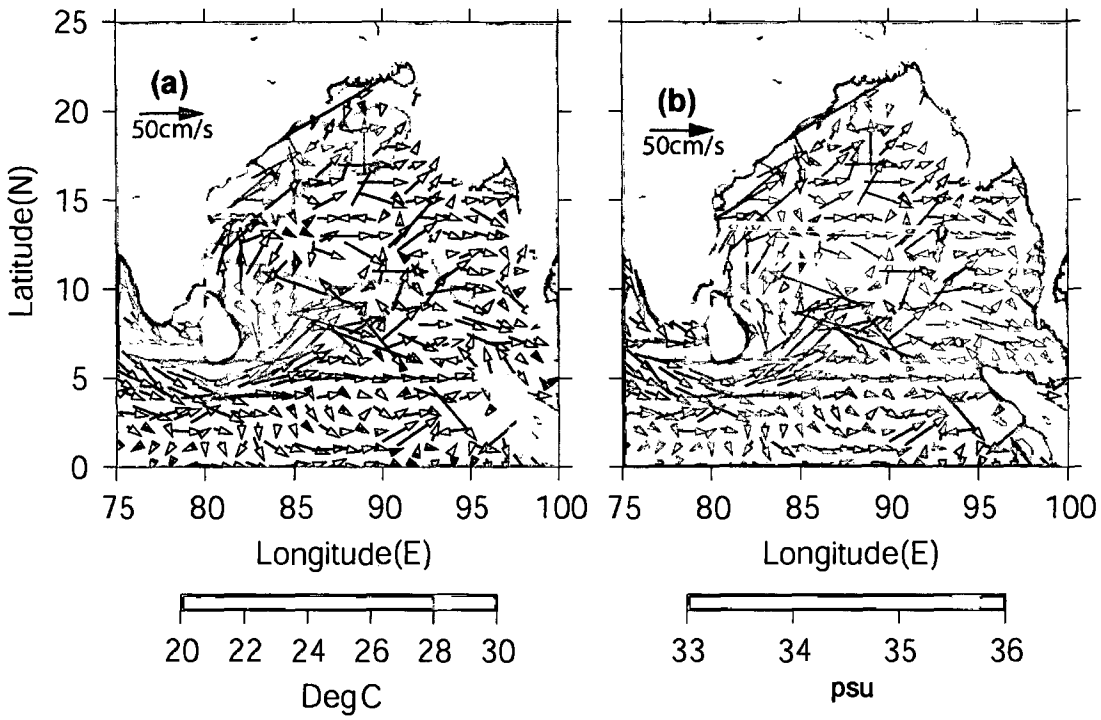

Figure 1.2.5. Monthly mean climatology of (a) temperature (°C) and (b) salinity (psu) from WOA01 [*Conkright et al.*, 2002] overlaid with one-degree surface current vectors derived from NOAA ship drift data during July.

1.3 Eddies in the BOB

The important characteristics of the BOB that emerged from earlier studies are the occurrence of intense currents along the western boundary and in the southern Bay, the high stratification arising from warm and low-salinity waters, presence of westward propagating Rossby waves and coastally trapped Kelvin waves. Apart from the above features of the BOB, there had been reports of occurrence of eddy in the BOB way back in 1957. *Ramasastry and Balaramurty* [1957] reported the presence of eddy off Vishakhapatnam along the western boundary of the BOB during March-April and October-November. They noticed strong cross-shore temperature gradients during these seasons. Subsequently, *Rao and Sastry* [1981] reported cyclonic and anti-cyclonic flows and linked the nutrient distribution with these flows. Though indications of a western

boundary current was present in the earlier studies [eg, *Ramasastry and Balaramurty, 1957* and *La Fond, 1957*] it's presence was established by Legeckis [*1987*] based on satellite derived sea surface temperature (SST) data using Advanced Very High Resolution Radio meter and delineated two warm core eddies in the central and northern Bay during February 1985. Based on remote sensing (altimetry) and *in situ* observations *Gopalan et al.* [*2000*] showed strong inter-annual variability in the spatial location and intensity of eddies. Recent studies too indicated presence of eddies near the western boundary of the BOB during March-August [*Babu et al.*, 1991; *Murty et al.*, 1993; *Shetye et al.*, 1993; *Sanilkumar et al.*, 1997; *Babu et al.*, 2003 ; *Prasanna Kumar et al., 2004*]. The *in situ* measurements show that these eddies mostly confines with in the upper 500 m of the water column [eg. Babu etal *1991*, *Prasanna Kumar et al.*, 2004] and have horizontal dimension of 200 to 300 km. A comparison of eddies at various locations is given in the following table (Table 1.1).

Table 1.1. Details of spatial scales associated with eddies observed at different geographic locations.

Region	Depth of sampling	Vertical extent of eddies	Horizontal dimension	Author
Gulf stream	2000 m 800 m	~ 2000 m ~ 800 m	~ 200 km ~200 km	Iselin, 1936, Richardson et al., 1978
Kuroshio	500 m	~500 m	~ 200 km	Bernstein et al ., 1977
East Australian current	900 m	~900 m	~ 200 km	Nilsson and Cresswell, 1980
Agulhas retroflection	?	> 2000 m	~ 200 km	Duncan, 1968
Somali Current	450 m	450 m	~400-600 km	Bruce, 1979
Bay of Bengal	1000 m 500 m	100-400 m 500 m	~ 350 km ~ 200 km	Babu et al., 1991 Sanilkumar et al, 1997

Though the presence of eddies in the BOB is revealed in many studies, very few of them have directly addressed their generation and evolution [*Prasanna Kumar et al., 1992* and Babu et al., *1991*]. The present thesis is an attempt in that direction.

1.4. Outline of the thesis

Recently concluded Bay of Bengal Process studies had two observational tracks - one along central BOB and another in the western boundary. Examination of the hydrographic data along these track showed many undulations which can be characterized as eddies. This data has been supplemented with the satellite derived sea-level anomaly (SLA) to characterize eddies and to give a spatial context to the observed along-track hydrography and forms the content of chapter 2. The evolution and generating mechanisms of eddies along the western boundary and the open BOB forms chapter 3 and 4 respectively. After describing their characteristics and establishing their origin and evolution, the chapter 5 deals with their role in the hydrography and circulation. In chapter 6 the eddy mediated changes in the distribution of nutrients and chlorophyll are discussed. Chapter7 summarizes the major out comes of the study.

Chapter 2 - Data and methods

2.1 Introduction

In order to understand the characteristics of the eddies in the BOB and address their origin and evolution, a suite of data sets, both in situ as well as remote sensing, were utilized. *In situ* data used in this study is collected on board Indian research vessel ORV Sagar Kanya (SK) during 2001-2003 under a national programme Bay of Bengal Process Study (BOBPS).

2.2 *In situ* data

The *in situ* data used in the present study is the temperature and salinity profiles collected at stations along 88°E in the central BOB from 7°N to 20°N, and along the western boundary from 11°N to 20°N (Figure 2.2.1) during 3 seasons - summer monsoon (SK166, 10-July-2001 to 1-August-2001), fall intermonsoon (SK182, 17-September-2002 to 11-October-2002) and spring intermonsoon (SK191, 16-April-2003 to 6-May-2003) intermonsoon . Temperature and salinity profiles up to 1000 m depth were taken at one-degree latitude interval along the central and western boundary tracks using a Seabird 9/11 plus CTD (Conductivity-Temperature-Depth) system. The station interval along the western boundary was, however more than one degree. The raw data was processed using the software 'Seasoft' version 4.2.17. CTD salinity was calibrated against water samples collected simultaneously by a rosette sampler fitted with 10/30-L Go-Flo bottles and analyzed with a Guildline 8400 Autosal. Using the temperature and salinity profiles

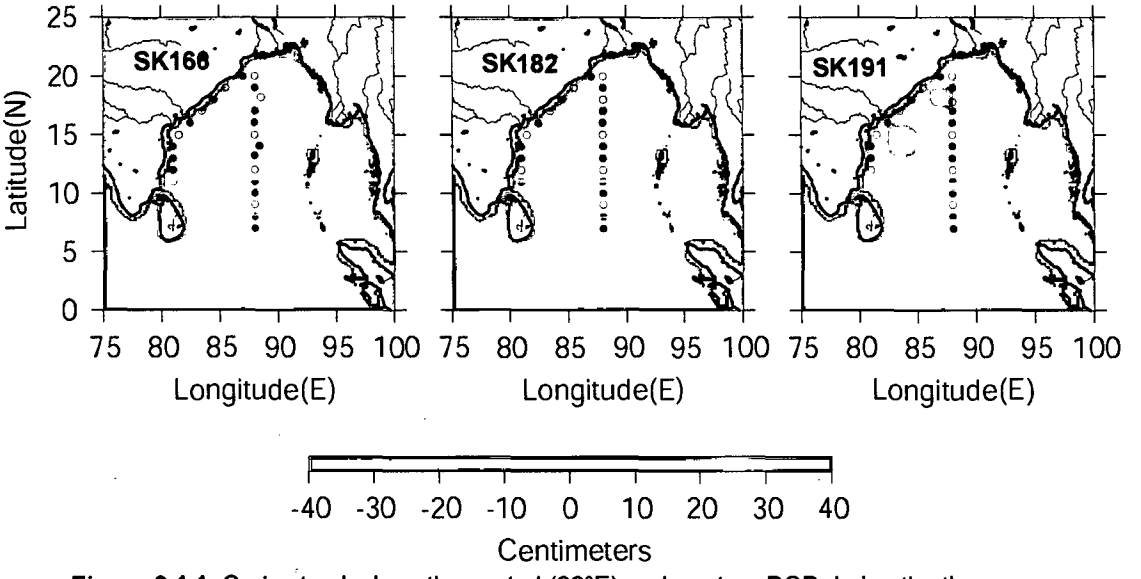

Figure 2.1.1 Cruise track along the central (88°E) and western BOB during the three seasons, summer monsoon (SK 166, 10 July - 1 August 2001), fall intermonsoon(SK 182, 17 September - 11 October 2002) and spring intermonsoon (April-May-2003) overlaid on average SLA for the period of each cruise.

geostrophic currents were computed w.r.t 1000m using the temperature and salinity data following Helland-Hansen method [*Pond and Pickard*, 1978].

In addition to the *in situ* data from the above mentioned 3 cruises, monthly mean climatology of temperature and salinity on a 0.25 x 0.25 degree grid from World Ocean atlas (WOA) 2001 [*Conkright et al., 2002*] is also used for computation of heat and salt content anomalies (discussed in chapter 5).

From the surface meteorological parameters (air temperature, wet bulb temperature, pressure, and wind speed and direction) measured at stations along both central and western boundary tracks in all the 3 seasons, wind data were used for the computation of Ekman volume transport (E_v) using the following relationship.

$$E_v = \tau/\rho f$$

where τ is the windstress at the surface, ρ is the sea water density and f is the Coriolis parameter. Windstress is computed using a constant drag coefficient of 1.3×10^{-3} (see chapter 5 for more details).

The data on nitrate, phosphate, silicate and chlorophyll *a* was taken from BOBPS data CD (Indian Oceanographic Data Centre product, National Institute of Oceanography, Goa, March 2007). The nutrient data (nitrate, phosphate and silicate) of BOBPS was generated from the water samples collected in the upper 1000 m from 19 discreet depths (near surface, 10, 20, 30, 40, 50, 75, 100, 125, 150, 200, 300, 400, 500, 600, 700, 800, 900 and 1000 m) using 10/30L Go-Flo bottles attached to the CTD rosette and analyzed with a SKALAR auto-analyzer during summer and with spectrophotometer following *Grasshoff et al.* [1983] during fall and spring intermonsoons. In both cases, sensitivity for nitrate, silicate and phosphate was 0.1, 0.5 and 0.03μM respectively. The chlorophyll *a* data of BOBPS was obtained from water samples collected in the upper 120 m from 8 discrete depths (near surface, 10, 20, 40, 60, 80, 100 and 120 m) and concentrations measured using a TURNER design fluorometer.

2.3 Remote sensing data

The spatial structure and the evolution of eddies were examined by analyzing 7-day snap-shots of the merged sea-level anomalies of Topex-Posiedon/ERS 1/2 satellites obtained from AVISO live access server (http://las.aviso.oceanobs.com) having a spatial resolution of $1/3^{rd}$ of a degree during the period October 1992 to January 2004 [*Le Traon et al.* 1998].

This is a proven tool in studying the mesoscale features of the ocean [*Le Traon and Dibarboure,* 1999]. They show that the error associated with this amounts to about 3-6% of the variance of the signal. In the BOB the mean error is ~ 3 cm. Velocities from the sea-level anomalies were computed assuming the geostrophic relation

$$2\Omega\sin(\phi).V = g\tan(i)$$

where Ω is the earth's angular velocity, ϕ is the latitude, V is the velocity and tan(i) is the slope of the sea surface [*Pond and Pickard*, 1978]. The error associated with the velocity computation amounts to ~ 20 % of the variance [*Le Traon and Dibarboure,* 1999], which is small, but not negligible.

Twice daily Quik SCAT wind-stress (*Large and Pond* algorithm) obtained from PODAAC [*JPL Publication*, 2003] and Southampton Oceanography Center surface fluxes [*Josey et al., 2002*] was used to compute the curl of the wind-stress and is given by

$$\text{Curl}(\tau) = \partial\tau_y/\partial x - \partial\tau_x/\partial y$$

where τ_x and τ_y are eastward and north ward components of wind-stress.

Eddies formed out of baroclinic instability processes tend to follow the typical length scale, Rossby deformation radius (L_R), a relative measure of stratification and the Coriolis force (discussed in chapter 3). L_R is computed assuming a two layer ocean using the formula, $(\Delta\rho\rho_0^{-1}gh)^{0.5} f^{-1}$ [*Kamenkovich et al.*, 1986] where $\Delta\rho$ is the density drop across the main pycnocline, ρ_0 a reference density, h is the depth of the pycnocline, f the Coriolis parameter .

Chapter 3 - Eddies along the western boundary of the Bay of Bengal

3.1. Introduction

The western boundary of the BOB was sampled three timed during summer (22 to 30 of July 2001), fall intermonsoon (30 September to 11 October 2002) and spring intermonsoon (27 April to 5 May 2003). The seasonal variability of the thermohaline structure along the western boundary of the OB was examined to decipher the occurrence of eddies and its spatio-temporal characteristics. For this purpose the sequence of seasons rather than year is followed in explaining the observed features along the western Bay of Bengal. Cyclonic and anticyclonic eddies are characterized by doming and depressions in the thermohaline structure. These domings and depressions along with the geostrophic velocities computed w.r.t 1000 m is used for the identification of eddies from the hydrography. Further, sea-level anomalies from satellite altimeter are used to confirm observed features and to track its evolution with time.

3.2. Thermohaline structure

3.2.1 Spring intermonsoon 2003

Thermal structure showed a warmer and thicker isothermal layer with upper waters in excess of 30°C in the south, south of 16°N (Figure 3.2.1.1a). Towards the north the isothermal layer was shallower and about 1°C colder. Important features of the thermal structure were the doming of isotherms centered at 14°N and 18°N respectively and a depression centered at 15.5°N. The doming was more pronounced in the deeper layers (below 250 m) in the former case, while that for the latter was in the upper thermocline

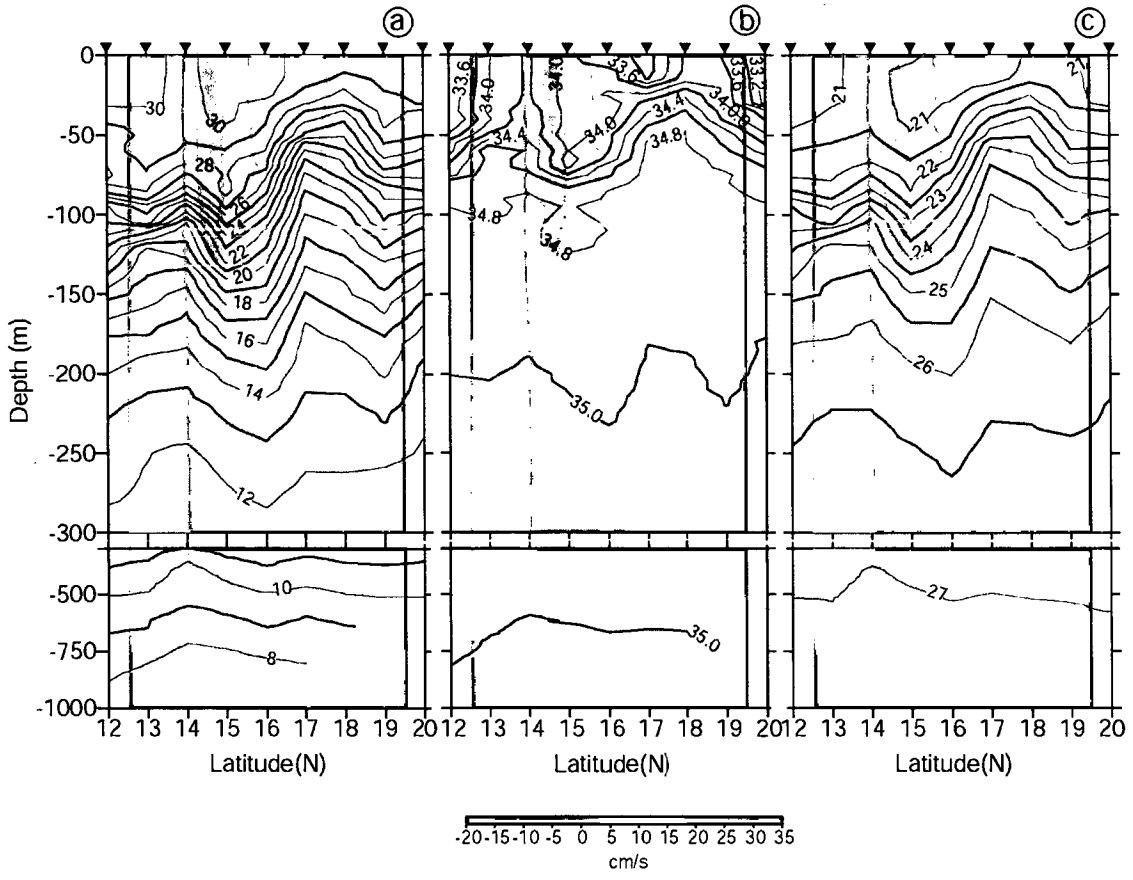

Figure 3.2.1.1 Vertical sections of (a) temperature (°C), (b) salinity (psu), and (c) sigma-t (kg/m^3) overlaid on the geostrophic velocity (cm/s) w.r.t 1000 m along the western boundary in the BOB during spring intermonsoon (April-May) 2003. Filled inverted triangles indicate the position of CTD stations.

(upper 250 m). For example, the 10°C isotherm shoaled by about 150 m in the former case, while it was only about 30 m for the latter. On the contrary the 20°C isotherm shoaled maximum, by about 75 m, in the latter case and it was only less than 30 m for the former. In the case of the depression 20°C isotherm was depressed by about 30 m. The doming centered at 14°N and 18°N depressed the ambient temperature at 100 m by 3°C and 6°C respectively, whereas the depression increased the temperature by one degree. The salinity distribution also reflected features similar to that of temperature with higher salinity, ~ 34 psu (practical salinity unit), in the south and about 0.5 psu fresher towards the north (Figure 3.2.1.1b). Consistent with thermal structure, isohalines also showed

doming which was visible only below 50 m centered at 14°N but was evident even at 20 m centered at 18°N. The doming of isohaline at 14°N and 18°N increased the salinity at 50 m by 0.4 psu and 0.8 psu respectively. The 34 psu contour was pushed down to a depth of about 75 m in the center of the depression. The density (sigma-t) distribution (Figure 3.2.1.1c) essentially reflected a structure similar to that of temperature and salinity.

The geostrophic velocities computed w.r.t 1000 m from the hydrographic data revealed an eastward current south of 14°N attaining a maximum velocity of 30 cm/s followed by a weak westward flow with a peak value of 20 cm/s towards the north up to 16°N (Figure 3.2.1.1 shading). Once again eastward and westward velocities were encountered at the southern and northern side of 18°N respectively. The westward currents, however, were much smaller (~10 cm/s) in the later case. These opposing flows and the doming in the property distribution appear to be a part of the cyclonic circulation feature centered at 14°N and 18°N respectively along the western boundary.

3.2.2. Summer Monsoon 2001

The prominent feature of the thermohaline structure during summer was the up/down sloping of isolines centered at 17°N (Figure 3.2.2.1.a, b), as in the case of spring intermonsoon, except that the center appears to be shifted southward from its spring position of 18°N. The up-down sloping of isotherm/isohaline noticed in the upper 150 m at 14°N during spring intermonsoon completely disappeared in summer monsoon. However, below 150 m, thermal structure still showed feature similar to Spring intermonsoon. It is clear from the thermohaline structure that the upper layer was

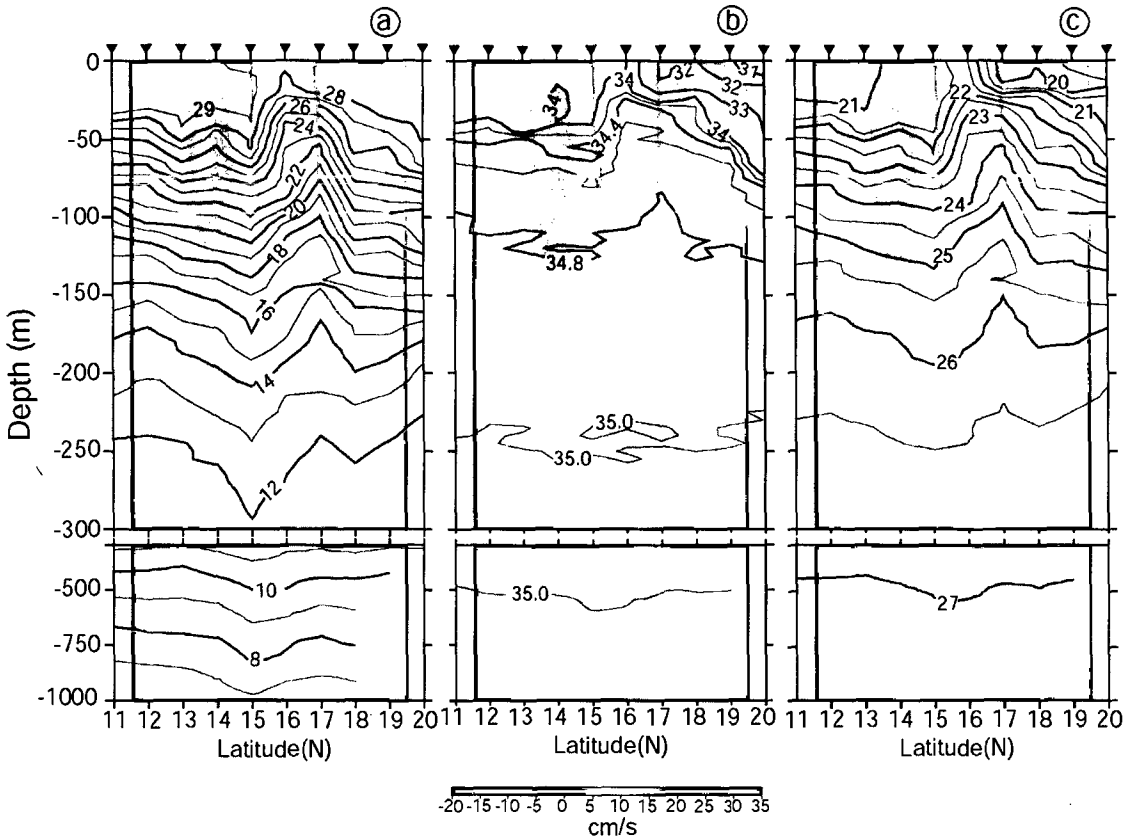

Figure 3.2.2.1 Vertical sections of (a) temperature (°C), (b) salinity (psu), and (c) sigma-t (kg/m^3) overlaid on the geostrophic velocity (cm/s) w.r.t 1000 m along the western boundary in the BOB during summer (July-August) 2001. Note the change in contour interval <33 psu in ⓑ, which is 1 psu. Filled inverted triangles indicate the position of CTD stations.

modified by the presence of the eddy. The isothermal layer which was on an average 30 m deep along the track came very close to the surface under the influence of the eddy centered at 17°N. Though SST along the track was 1°C colder than spring intermonsoon, it retained the spatial pattern with colder SST in the north. During summer monsoon too the 20°C isotherm underwent a maximum displacement, but the magnitude was much less (~40 m). Similarly the eddy depressed the ambient temperature at 100 m by about 3°C which was half that during Spring intermonsoon. Consistent with the thermal structure, isohalines too domed centered around 17°N (Figure 3.2.2.1b). This resulted in the increase of salinity at 50 m by about 0.4 psu at the centre of the eddy. The conspicuous

feature in the haline structure was the presence of fresher waters (~30 psu) in the northern part and the strong vertical gradient of about 4 psu in the upper 50 m. However, in the south salinity was close to 34.5 psu in the upper 50 m. The density (sigma-t) distribution (Figure 3.2.2.1c) essentially depicted a structure similar to that of temperature and salinity.

The geostrophic velocities showed westward flow in the southern parts of the transect that peaked (~ 15 cm/s) at 14°N (Figure 3.2.2.1 shading) in contrast to spring intermonsoon. North of 15°N the flow turned eastward with a velocity of approximately 15 cm/s, which gradually slowed down and reached a minimum value at about 17° N. Once again, the flow increased in its strength to about 10 cm/s in a westward direction at about 18°N. Thus, from the above a cyclonic flow centered about 17°N was discernible which roughly coincided with the doming of the isotherm/isohalines/isopycnals indicating the presence of a cyclonic eddy. However, the westward flow south of 14°N, which replaces the spring-time eastward flow indicated the change in the circulation from cyclonic to anticyclonic. Apart from this, a weak depression centered at 15°N with an anticyclonic flow field is also noticed in the thermal structure.

3.2.3. Fall intermonsoon 2002

Thermal structure showed that SST, in general, was 1°C warmer than that in summer monsoon with water of about 30°C occupying most of the region along the transect expect north of 18°N (Figure 3.2.3.1a). Here again, the conspicuous feature was two domes of isotherms centered at 12°N and 18°N respectively. The 20°C isotherm had undergone maximum displacement of 50 m for the latter, while it was only about 20 m

for the former. On the contrary, the 10°C isotherm underwent a maximum displacement of nearly 100m in the former case, while the latter did not show appreciable change. This indicated that the feature at 18°N was prominent in the upper layers of the water column with not much variability below the thermocline. However, the feature at 12°N was though discernible in the upper thermocline, was most prominent in the deeper layers and extended up to 1000 m. Accordingly, the ambient temperature at 100 m was depressed by about 1°C and 4°C respectively. Vertical section of salinity showed the presence of very low salinity waters (~23 psu) in the north and the effect of freshening was felt as south as 14°N (Figure 3.2.3.1b). This increased the vertical gradient of salinity in the upper 50 m by about 10 psu in the north. The effect of eddy could be inferred from the doming isohaline, which increased the ambient salinity at 50 m by about 1 psu and 0.4 psu for eddies centered at 18°N and 12°N respectively. During fall intermonsoon the eddy was completely overlaid by this freshwater. Thus, the fresh water severely constrained the eddy pumping of saltier waters from subsurface and thereby restricting the eddy signature below the surface layer (below ~15 m). The density (sigma-t) structure also reflected features of temperature and salinity fields (Figure 3.2.3.1c).

Geostrophic velocities showed alternate bands of positive (eastward) and negative (westward) flows all along the track (Figure 3.2.3.1 shading). At 11°N the flow was eastward with a velocity of 15 cm/s, which gradually decreased to a minimum at 12°N and turned to a westward flow of magnitude 15 cm/s centered 13°N. The current once again changed direction towards east at 17°N with its speed decreasing to a minimum at 18°N, followed by another change in direction towards west and increase in its strength

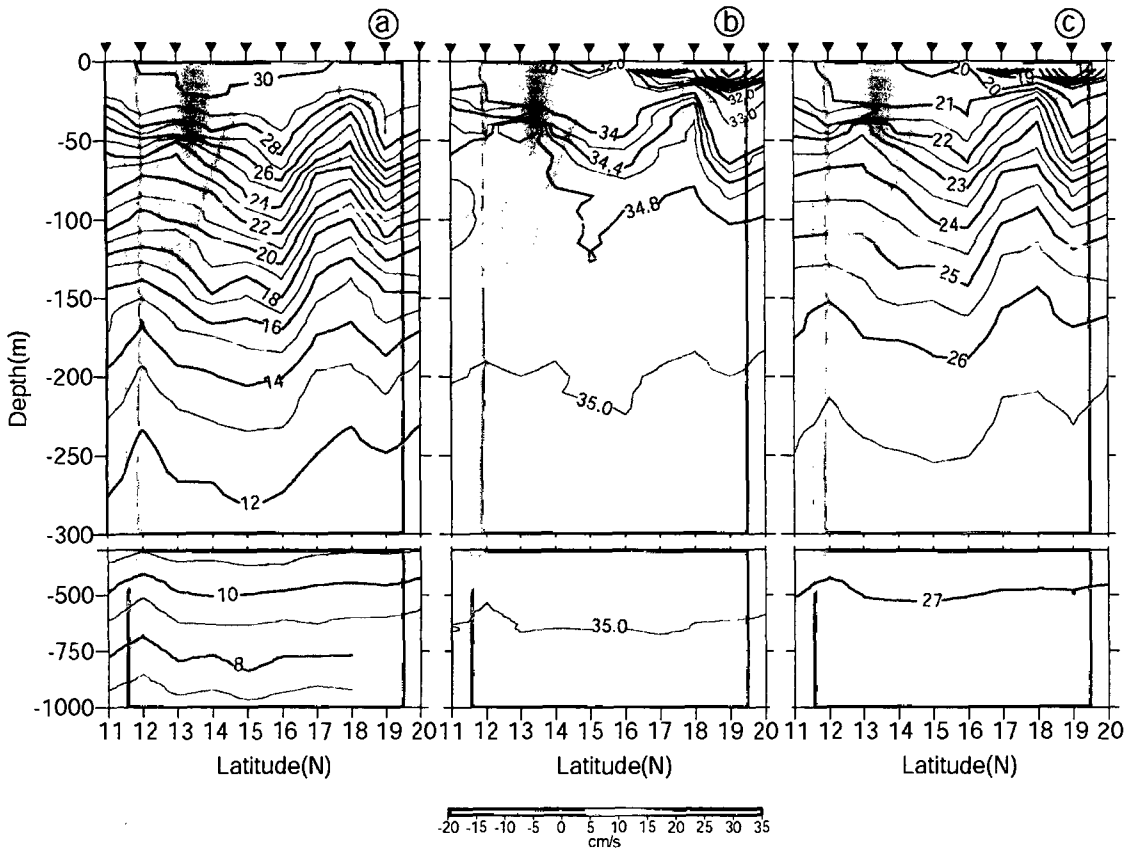

Figure 3.2.3.1 Vertical sections of (a) temperature (°C), (b) salinity (psu), and (c) sigma-t (kg/m^3) overlaid on the geostrophic velocity (cm/s) w.r.t 1000 m along the western boundary in the BOB during fall intermonsoon (September-October) 2002. Note the change in contour interval <34 psu in ⓑ, which is 1 psu and <21 kg/m^3 in c which is 1 kg/m^3. Filled inverted triangles indicate the position of CTD stations.

to about 15 cm/s at 19°N. Thus, from the flow pattern the signatures of two cyclonic eddies centered about 12°N and 18°N along the track was discernible, though in the thermohaline structure only the northern eddy was most visible in the upper layers. During this season too a weak depression and associated anticyclonic flow was noticed in the thermal haline structure centered about 16°N.

Thus, the most prominent feature of the thermohaline structure, in all the three seasons, was the signature of sub-surface cyclonic eddy observed in the northern part of the

western Bay of Bengal (16-19°N). This is designated northern coastal eddy (NCE). A cyclonic eddy during spring and fall intermonsoons in the southern part centered at 14°N and 12°N respectively was also noticed. This has been designated as southern coastal eddy (SCE). A comparison with the sea-level anomaly showed that the depression noticed during the spring intermonsoon was a part of the large scale anticyclonic circulation whereas the one during summer monsoon and fall intermonsoon are anticyclonic eddies.

3.3. Evolution of the northern and southern coastal eddy (NCE, SCE) from sea-level anomaly

Having analyzed the thermohaline structure and identified signatures of eddies from them, it is important to attempt to understand the time evolution of these features in relation to the prevailing circulation. Towards this, seven-day snap shots of the sea-level anomaly maps of the respective years along with the geostrophic flows computed from them were analyzed. Though the sea-level anomaly maps showed several circulation features, the focus of this study is on the NCE and SCE as these were the most dominant feature reflected in the vertical thermohaline structure as well as the geostrophic currents computed from hydrography.

3.3.1. Spring Intermonsoon 2003

Sea-level anomaly pictures showed a small meander in the northeastward western boundary current (WBC), close to the coast at about 17°N, 84°E during early February 2003 (Figure 3.3.1.1), which developed into an elongated cyclonic flow centered at 16°N,

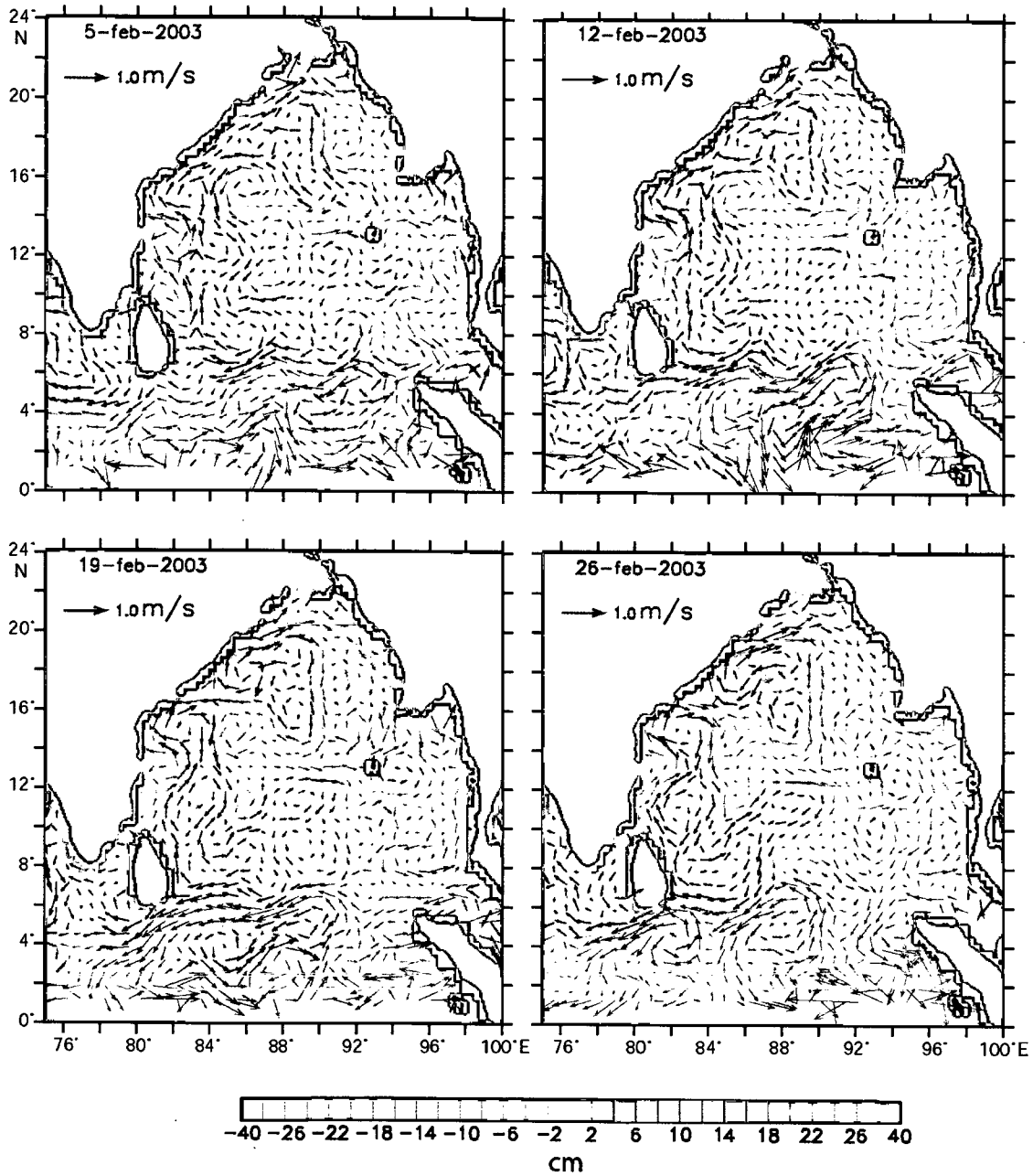

Figure 3.3.1.1 7-day snap-shots of Topex/Poseidon ERS1/2 merged sea-level anomalies overlaid with geostrophic velocities during February 2003.

84.5°E by the last week of March (Figure 3.3.1.2). This cyclonic eddy (NCE) moved onshore, to about 17°N, 84°E by the third week of April (Figure 3.3.1.3) and was sampled from onboard the ship during the last week of April (Figure 3.3.1.4, see Figure 3.2.1.1 for its thermohaline structure). During this period, the eddy was characterized by a negative

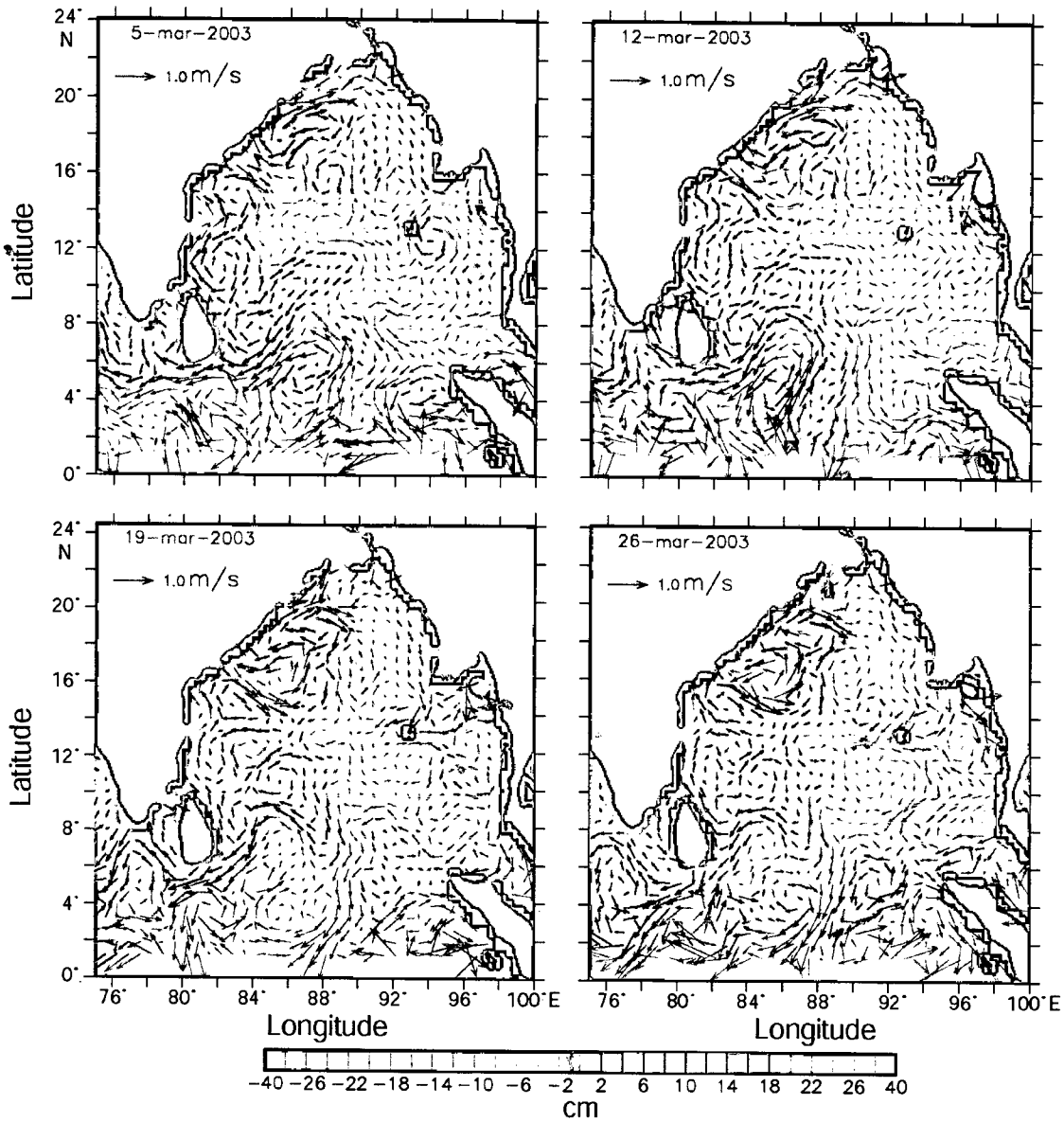

Figure 3.3.1.2. 7-day snap-shots of Topex/Poseidon ERS1/2 merged sea-level anomalies overlaid with geostrophic velocities during March 2003.

sea-level anomaly of about 22 cm and geostrophic velocity of about 30-40 cm/s along its periphery. Subsequently, as the circulation weakened, the eddy moved offshore and coalesced with another cyclonic eddy, by end of May, thereby increasing its strength (Figure 3.3.1.4, bottom right).

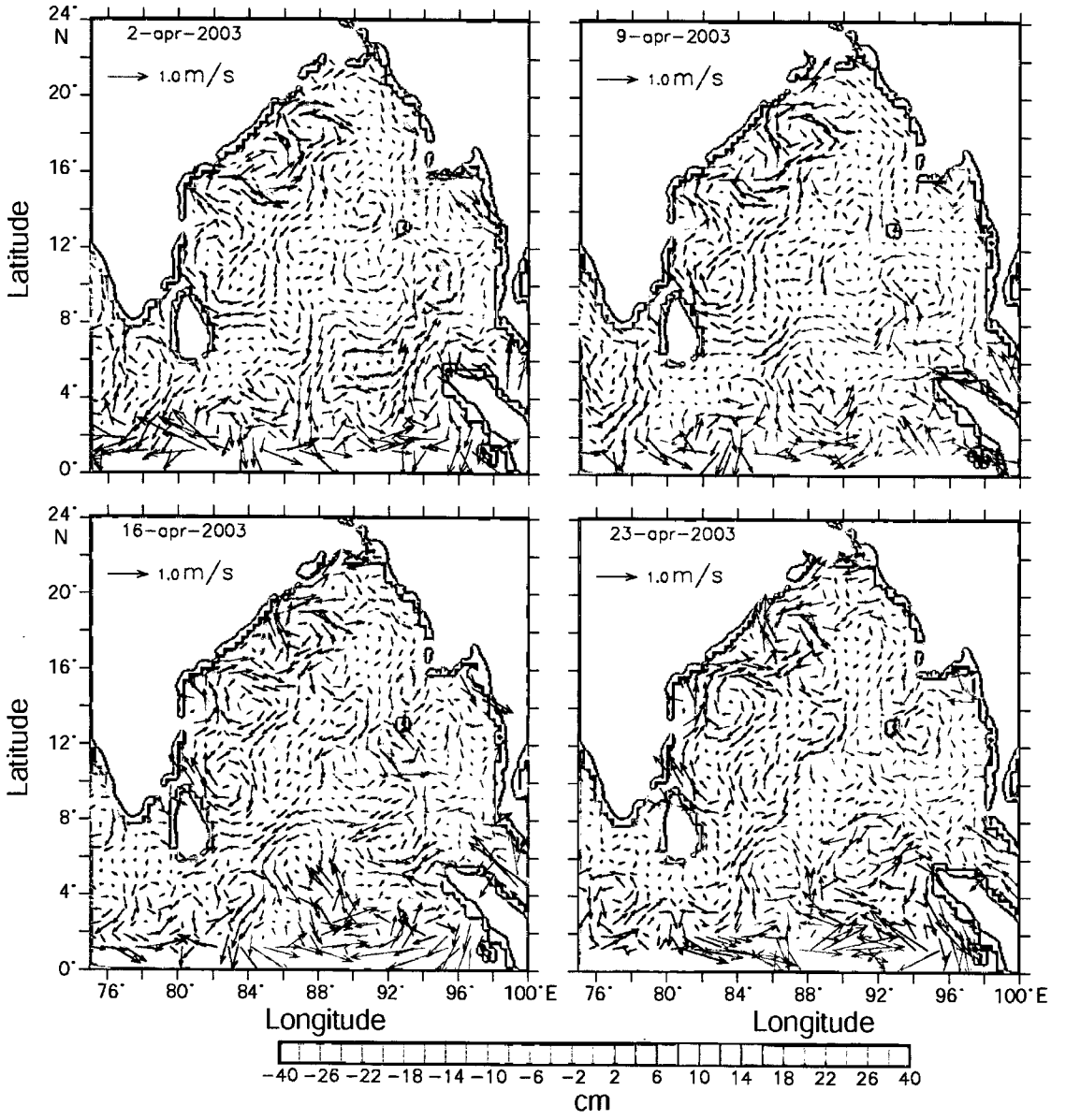

Figure 3.3.1.3. 7-day snap-shots of Topex/Poseidon ERS1/2 merged sea-level anomalies overlaid with geostrophic velocities during April 2003.

In the southern part of the western boundary another cyclonic circulation centered at 13.5°N and 81°E is noticed, which formed in the first week of April (Figure 3.3.1.3).

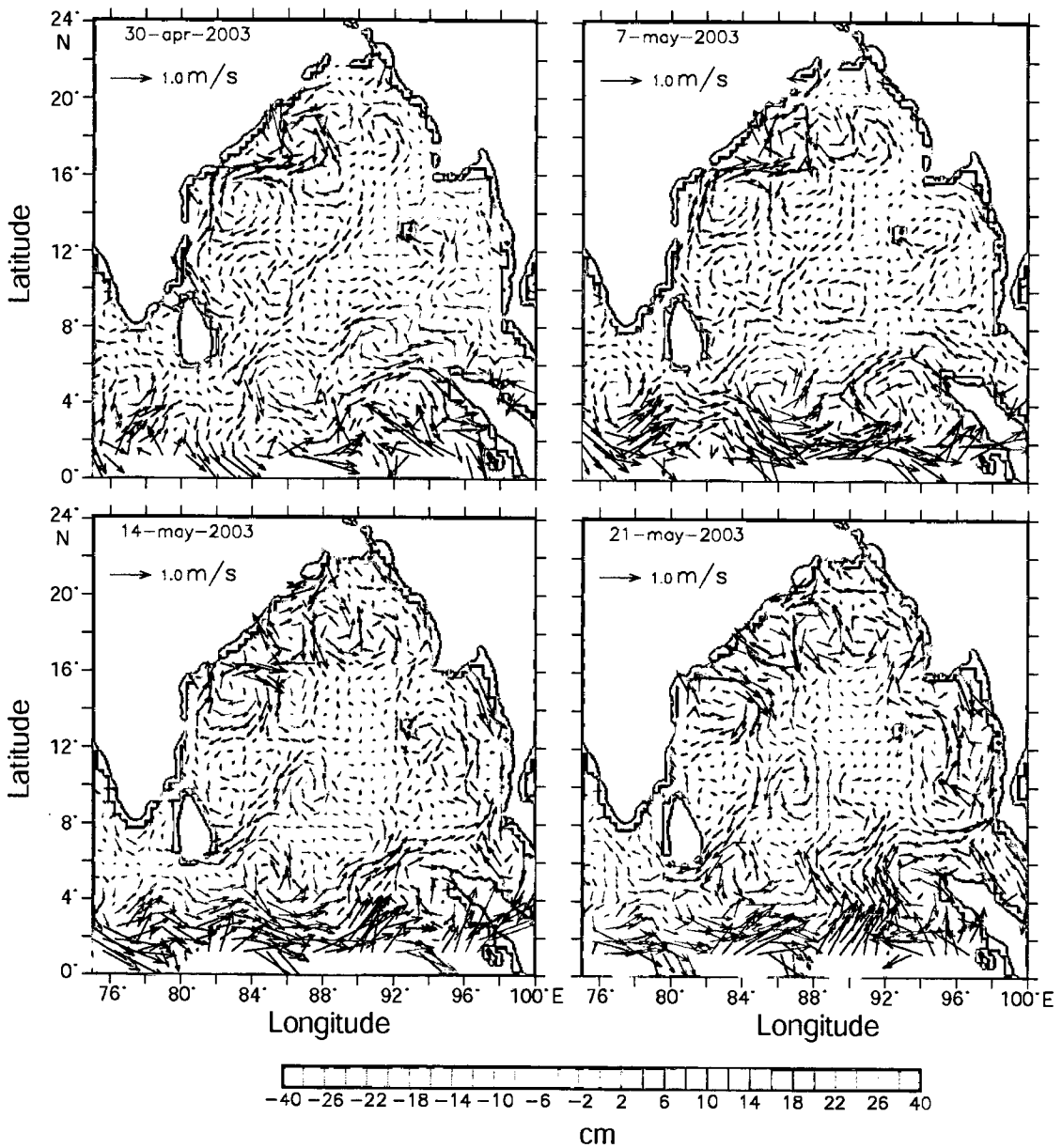

Figure 3.3.1.4. 7-day snap-shots of Topex/Poseidon ERS1/2 merged sea-level anomalies overlaid with geostrophic velocities during April-May 2003.

After persisting for two weeks, it dissipated by the end of April (Figure 3.3.1.4). It is this cyclonic circulation (SCE) that was captured during last week of April 2003 in the hydrographic section centered at 14°N along the western boundary.

3.3.2. Summer monsoon 2001

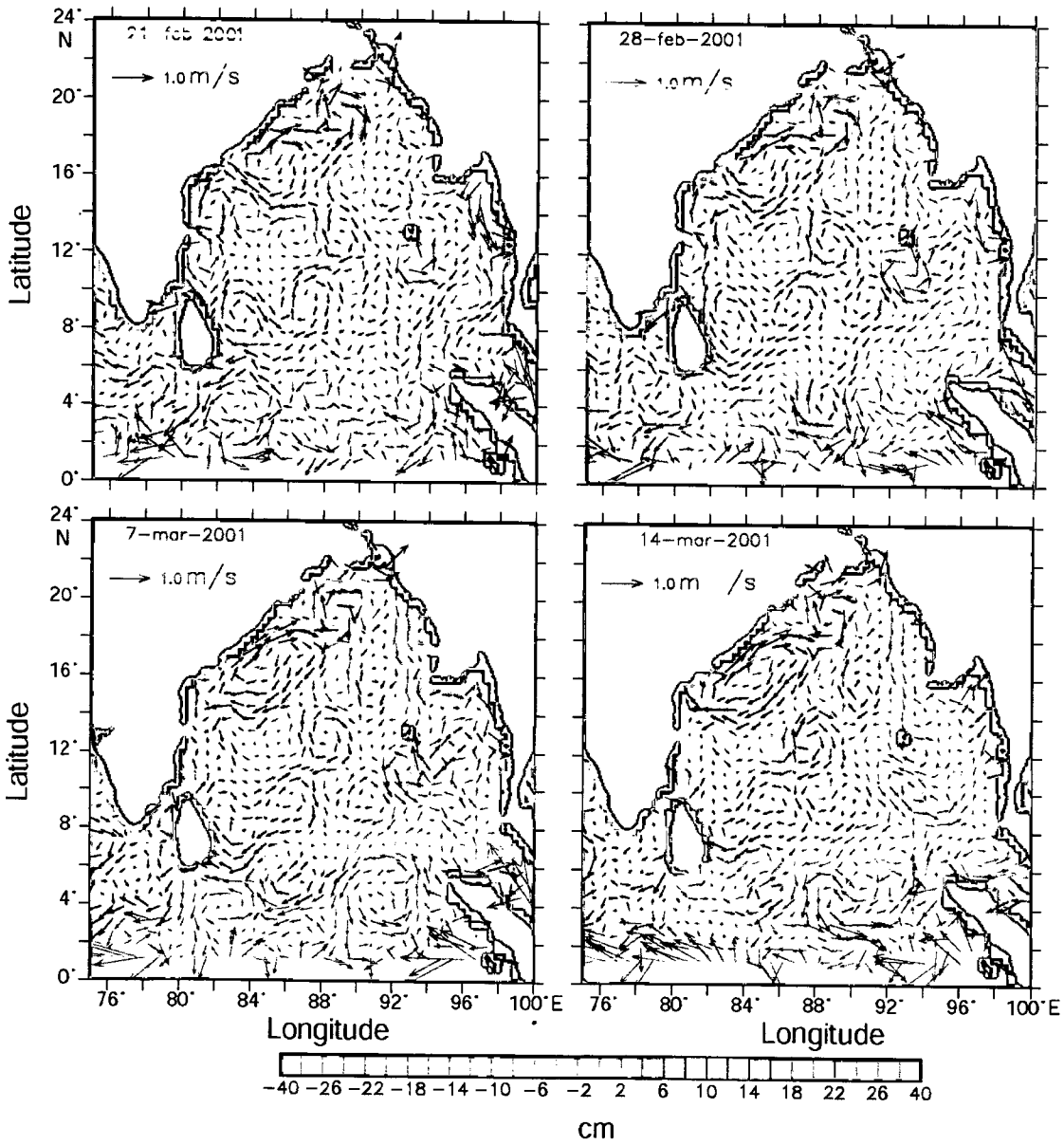

Figure 3.3.2.1. 7-day snap-shots of Topex/Poseidon ERS1/2 merged sealevel anomalies overlaid with geostrophic velocities during February-March 2001.

The eddy observed in summer 2001 (NCE), in the hydrographic section, was also appeared to have formed from a meander in the northeastward current (WBC) during

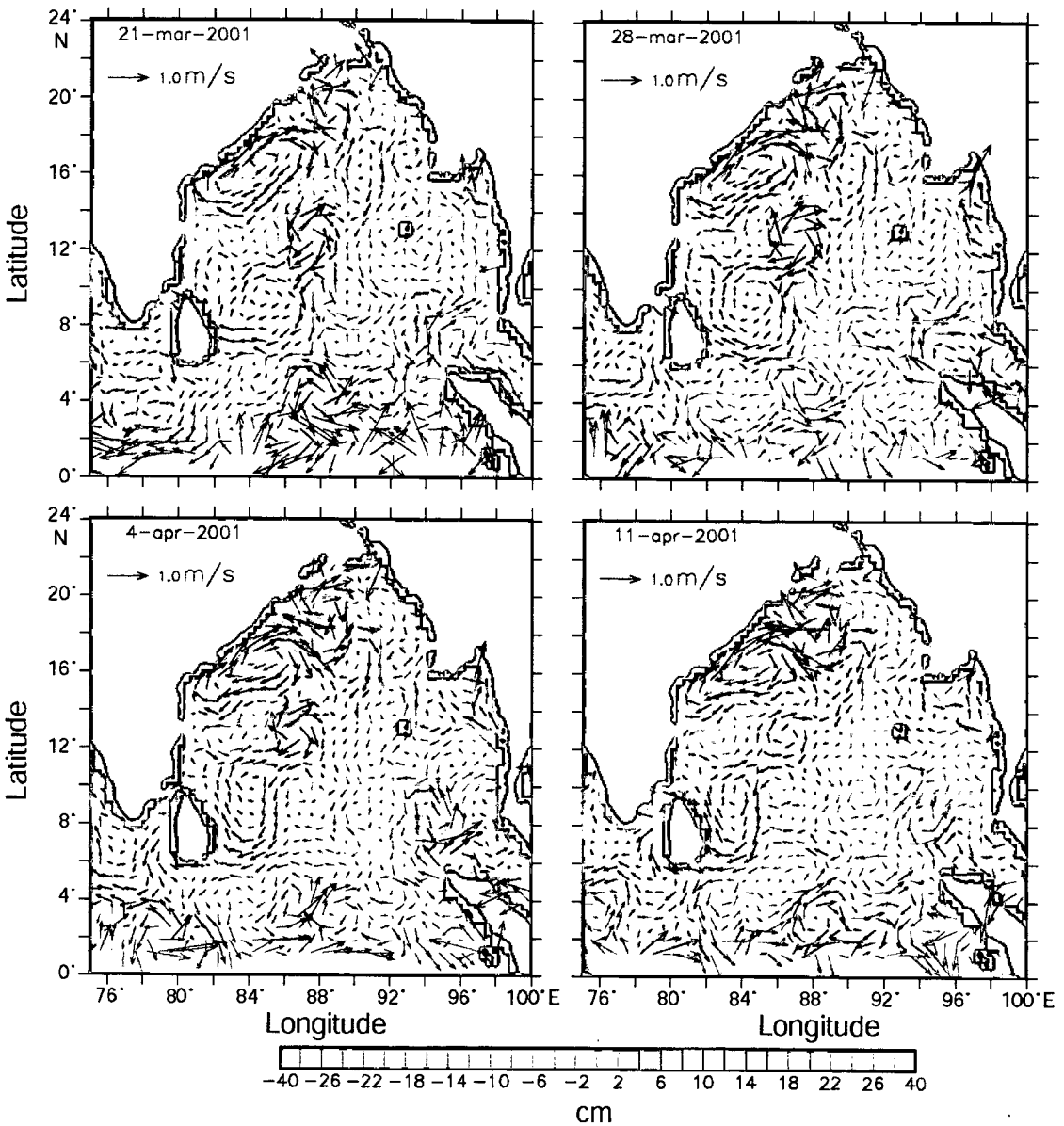

Figure 3.3.2.2. 7-day snap-shots of Topex/Poseidon ERS1/2 merged sealevel anomalies overlaid with geostrophic velocities during March-April 2001.

February (Figure 3.3.2.1) as in the case of 2003 spring intermonsoon eddy. This meander intensified with time and developed into a cyclonic eddy by the end of March 2001 with its centre at 19°N, 87°E (Figure 3.3.2.2). Another cyclonic eddy was also evident in the sea-level anomaly picture with its centre at 17.5°N, 88°E. In mid April, these two cyclonic features coalesced and intensified to from a single cyclonic eddy located at

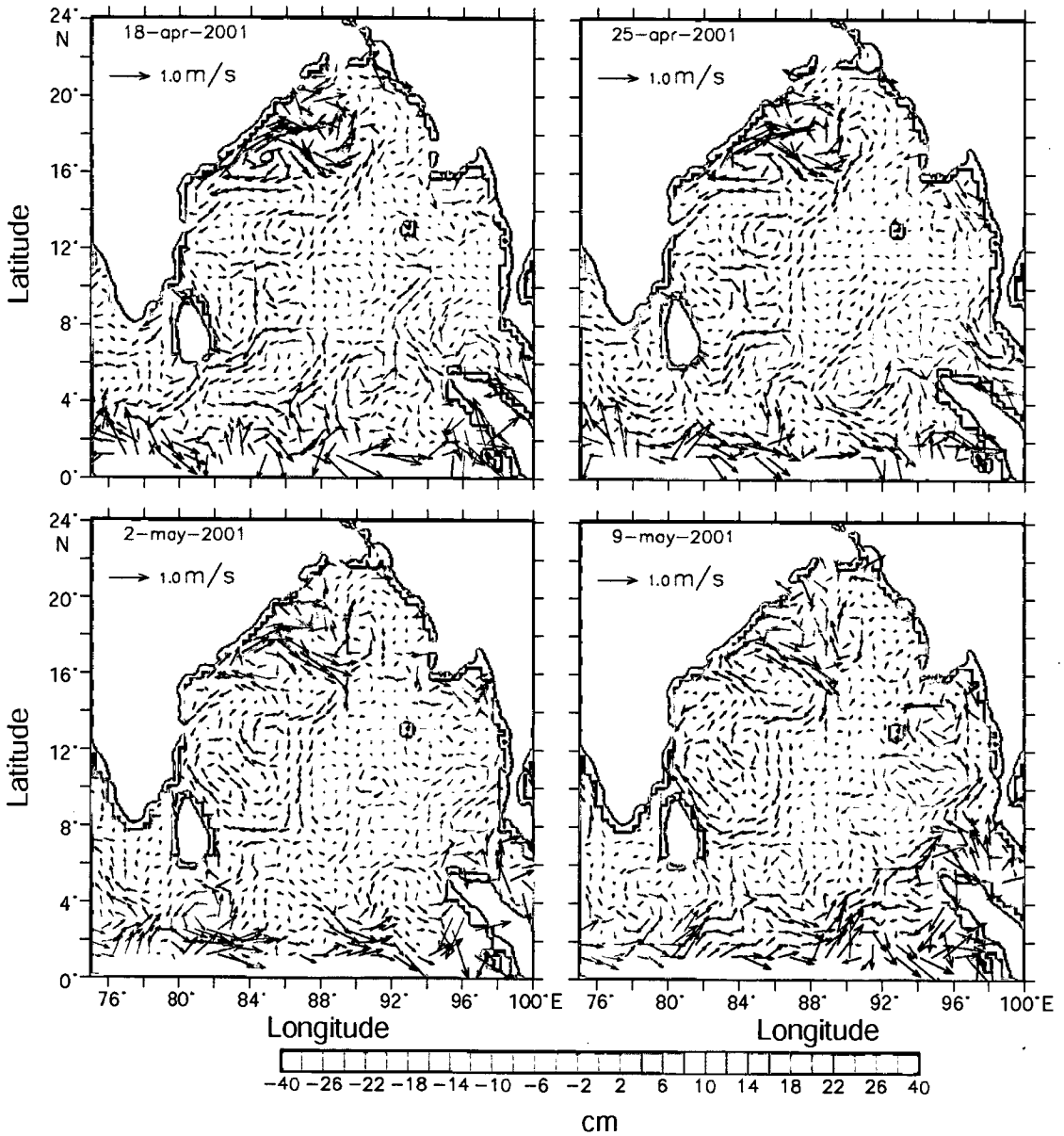

Figure 3.3.2.3. 7-day snap-shots of Topex/Poseidon ERS1/2 merged sealevel anomalies overlaid with geostrophic velocities during April-May 2001.

17.5°N, 88°E (Figure 3.3.2.3). Later, in the second week of May (Figure 3.3.2.4, top left) the single cyclonic eddy split and the northern eddy moved towards the coast while the southern one moved offshore and appeared to coalesce with another weak cyclonic circulation. Subsequently it intensified (Figure 3.3.2.5). During last week of July (Figure 3.3.2.6, bottom left), when the hydrographic measurements were carried out onboard the

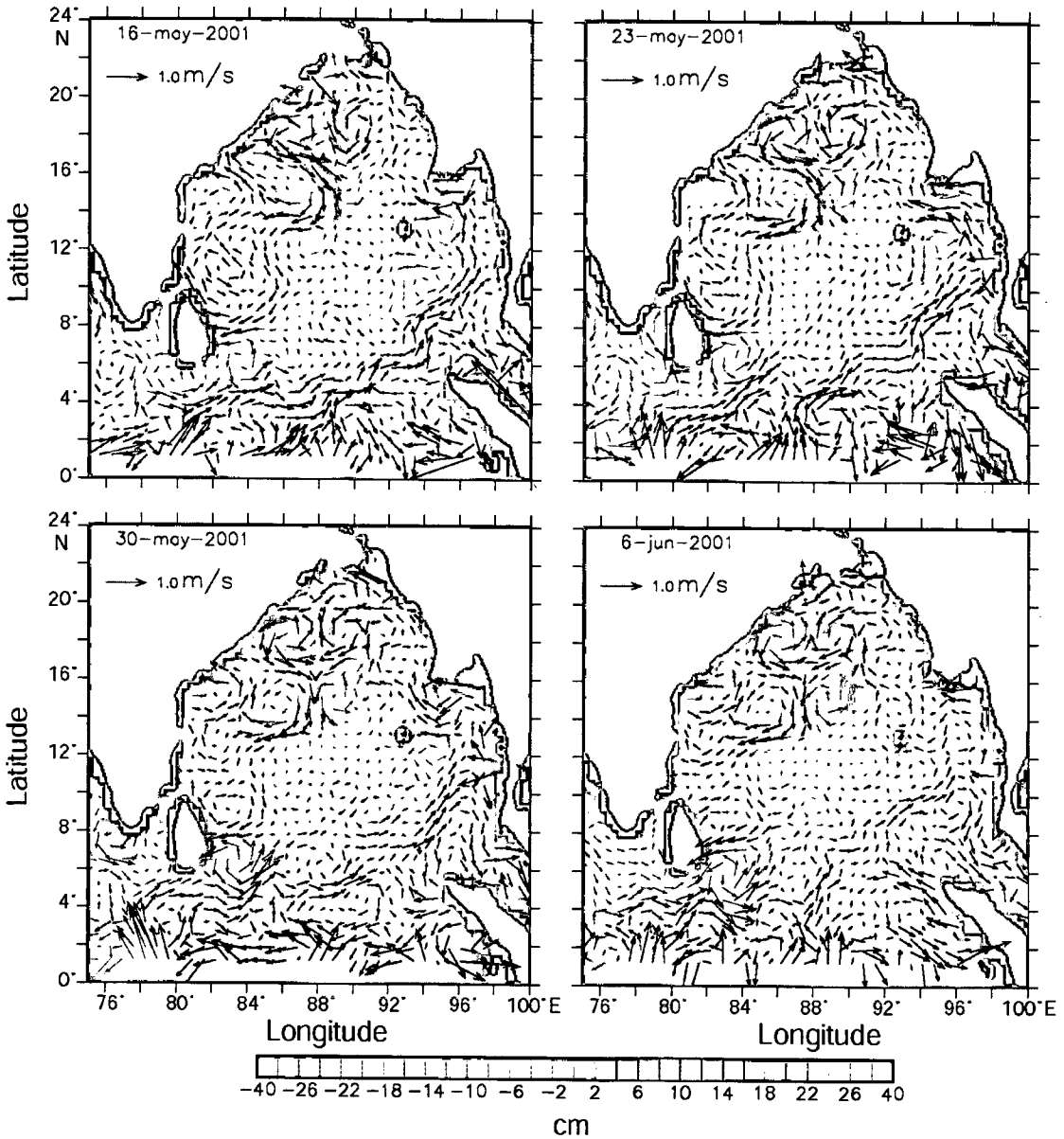

Figure 3.3.2.4. 7-day snap-shots of Topex/Poseidon ERS1/2 merged sealevel anomalies overlaid with geostrophic velocities during May-June 2001.

ship, these two eddies were in a coalesced state and located in a zonal band. Hence the *in situ* measurement picked up the signature of the northern eddy (see Figure 3.2.2.1 for its

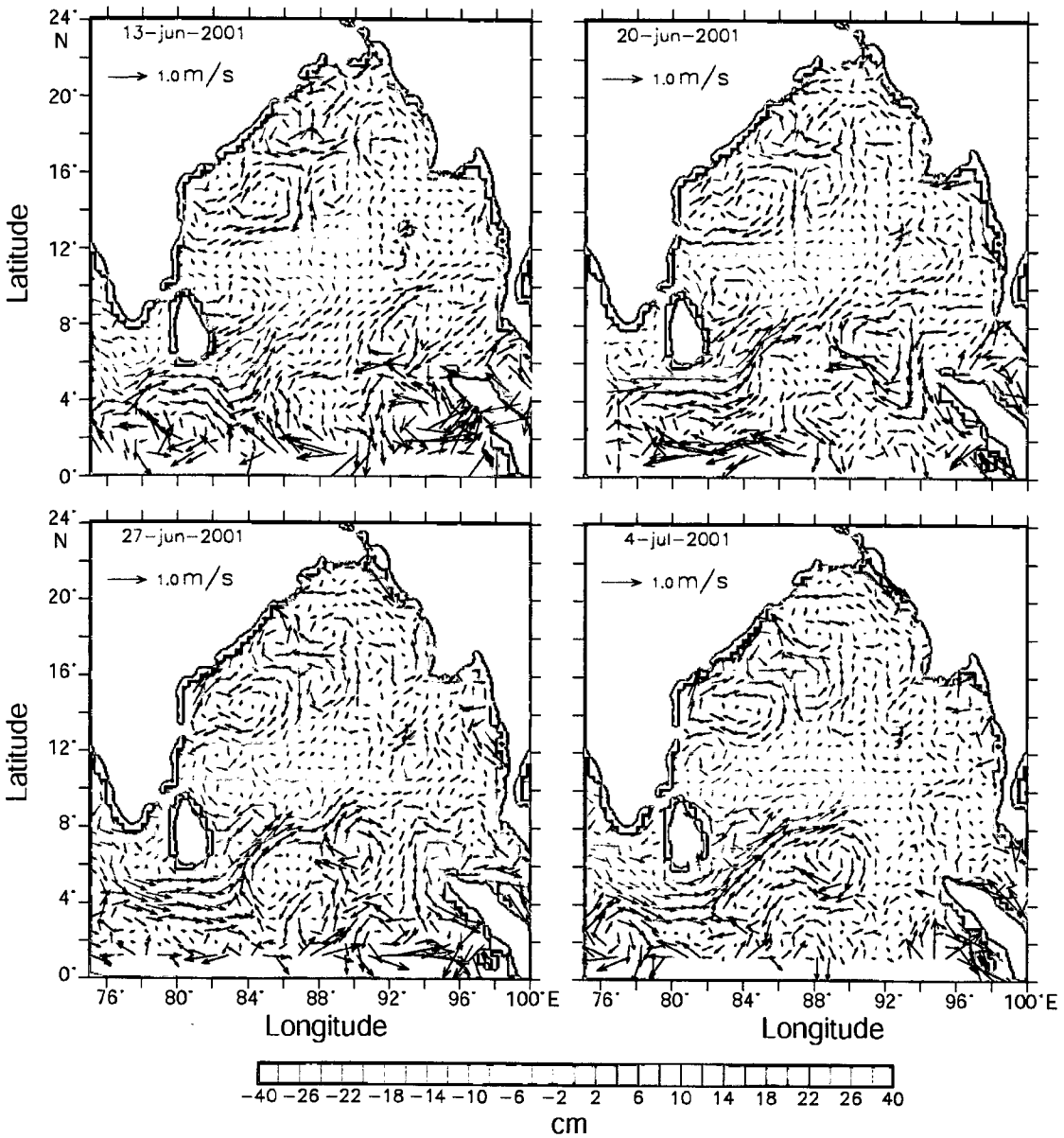

Figure 3.3.2.5 7-day snap-shots of Topex/Poseidon ERS1/2 merged sealevel anomalies overlaid with geostrophic velocities during June-July 2001.

thermohaline structure). The eddy was characterized by a negative sea-level anomaly of 30 cm and geostrophic swirl velocity of 30-40 cm/s along its periphery.

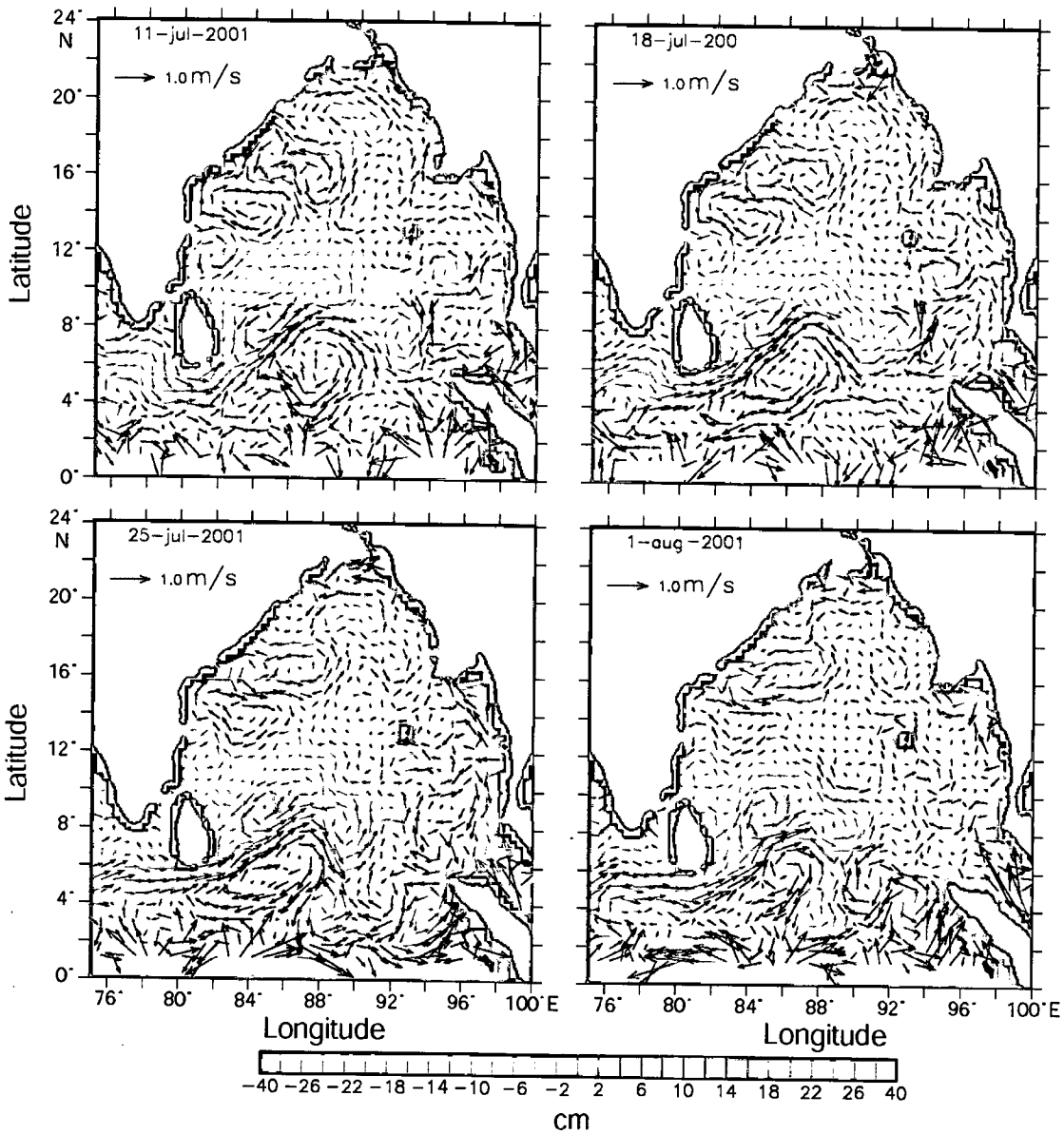

Figure 3.3.2.6. 7-day snap-shots of Topex/Poseidon ERS1/2 merged sealevel anomalies overlaid with geostrophic velocities during July-August 2001.

3.3.3. Fall intermonsoon 2002

Unlike the eddy observed during spring intermonsoon and summer monsoon, the fall intermonsoon eddy (NCE) was not developed from the meander in northeastward flowing WBC. The sea-level anomaly picture showed two cyclonic eddies in the first week of

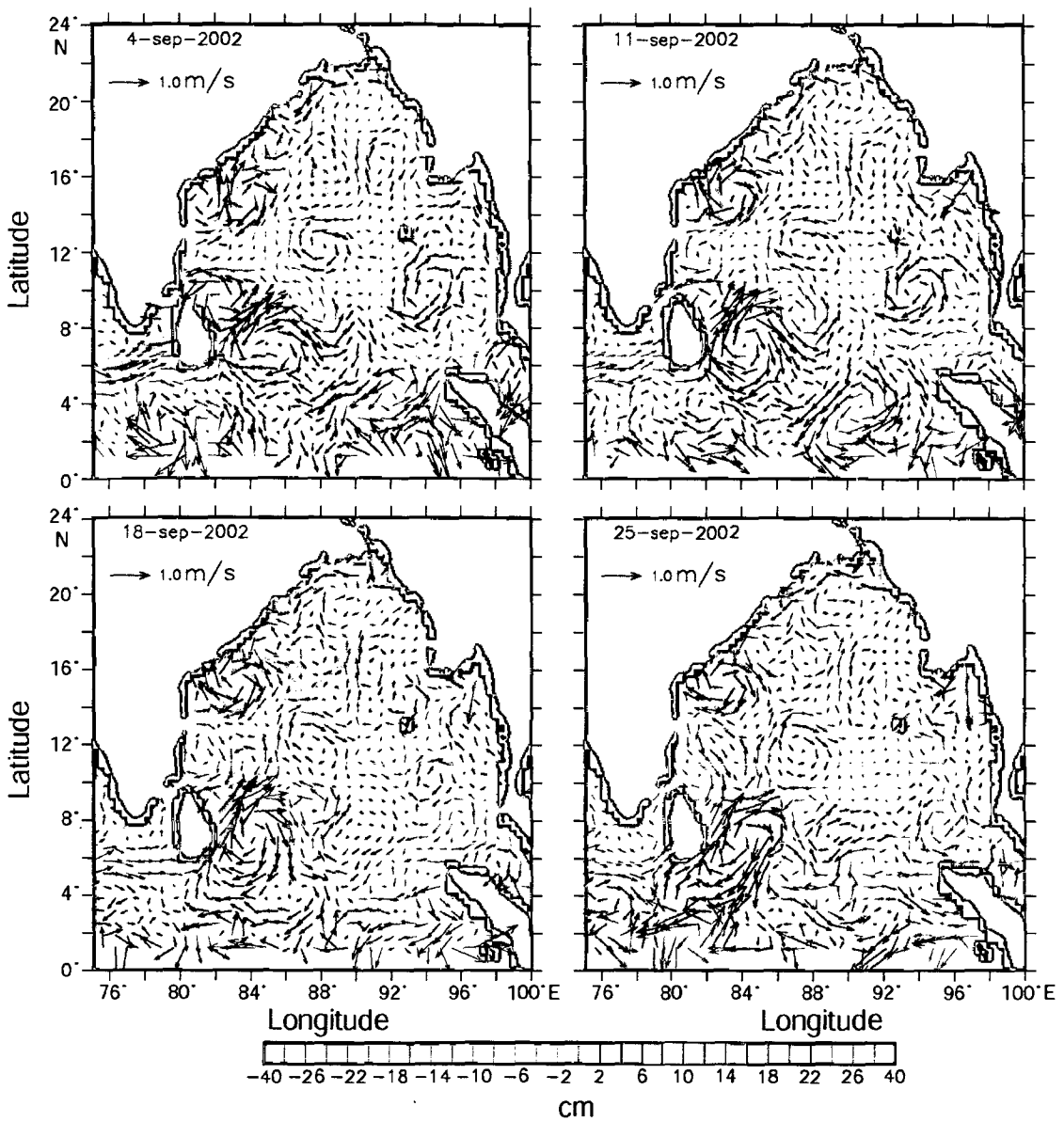

Figure 3.3.3.1. 7-day snap-shots of Topex/Poseidon ERS1/2 merged sealevel anomalies overlaid with geostrophic velocities during September 2002.

September 2002 (Figure 3.3.3.1), which was centered at 18°N, 85°E and 17°N, 88°E respectively. By last week of September, these two eddies moved closer (Figure 3.3.3.1). In early October the shipboard measurements sampled the eddy (NCE) centered at 17°N, 85°E (Figure 3.3.3.2 top left; see Figure 3.2.3.1 for the thermohaline structure). The eddy

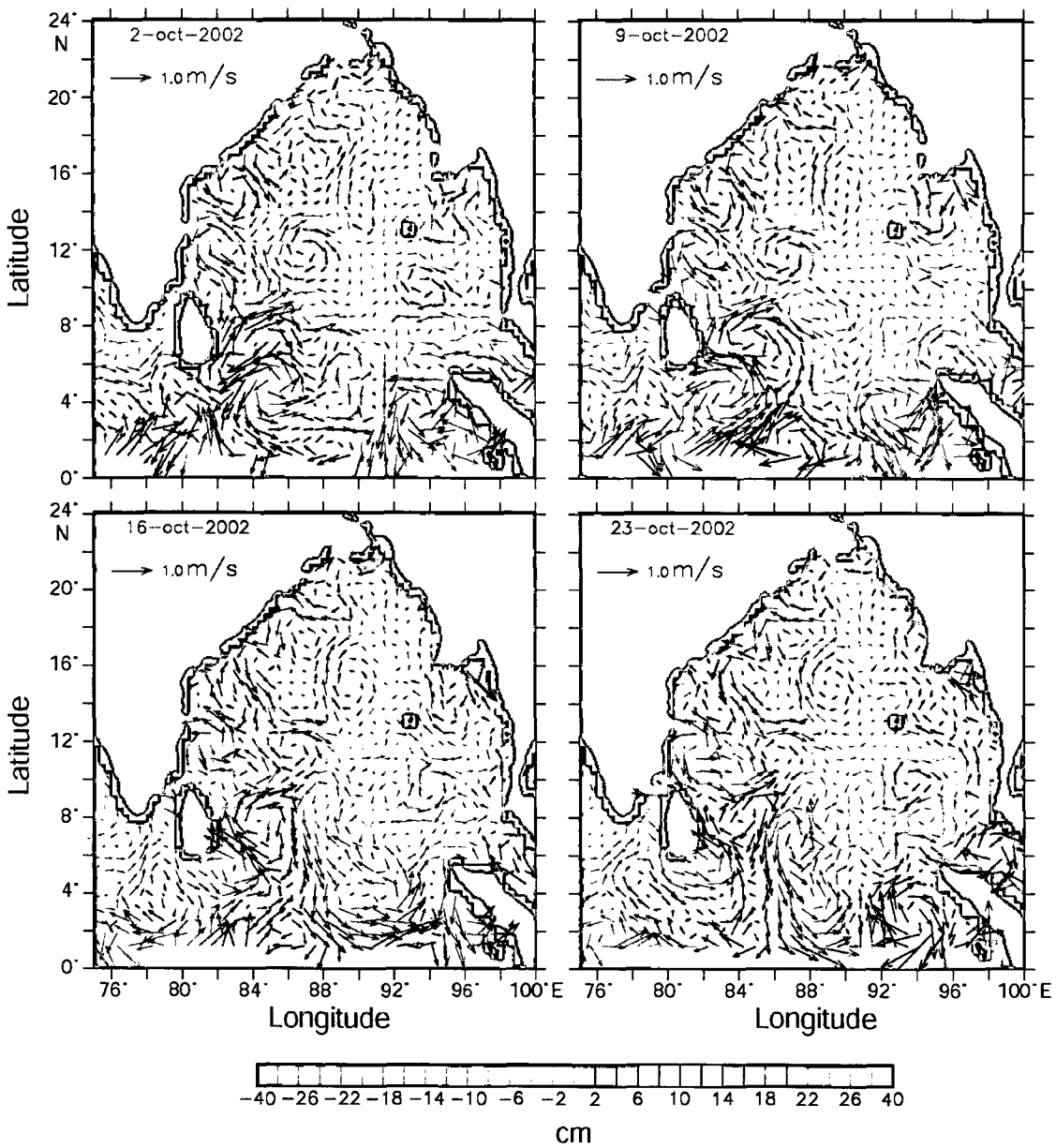

Figure 3.3.3.2. 7-day snap-shots of Topex/Poseidon ERS1/2 merged sealevel anomalies overlaid with geostrophic velocities during October 2002.

centre had a negative sea-level anomaly of 28 cm and geostrophic swirl velocities of 30-40 cm/s along its periphery. Finally both the eddy merged into the cyclonic circulation, which prevailed in the Bay during fall intermonsoon 2002 (Figure 3.3.3.2, bottom left). In the south, the eddy (SCE) centered at 12°N was not discernible during the first week of

September (Figure 3.3.3.1). However, in the third week of September a patch of low sea-level anomaly was seen extending from the northeastern part of Sri Lanka. This patch moved in a northwest direction with time and intensified into a cyclonic eddy (SCE) during October (Figure 3.3.3.2), which was sampled on 9 October 2002 from the ship.

Thus, the sea-level anomaly maps shows that the cyclonic eddies observed in the northern part of the western boundary (NCE), during spring intermonsoon as well as summer monsoon, originated from a meander in the northeastward flowing WBC during Spring intermonsoon. However, at this stage it is difficult to conclude about the origin of NCE during fall intermonsoon from the sea-level anomaly maps. There were two cyclonic eddies observed in the southern part of the western boundary (SCE) during spring and fall intermonsoons respectively. The spring intermonsoon SCE was formed when the anticyclonic circulation offshore of the southern part of the western boundary intensified and approached the coast during the first week of April. However, this feature dissipated within couple of weeks. The SCE seen during fall intermonsoon arises from the intensification of a patch of low sea-level anomaly, which moved from northeastern part of Sri Lanka into the western boundary region during summer. The anticyclonic eddies seen in the thermohaline structure of summer monsoon and fall intermonsoon seems to be the remnant of the large scale anticyclonic circulation that prevails in the BOB during spring intermonsoon. Thus, the hydrographic field along the western boundary of BOB showed the dominance of eddies. The NCE during summer monsoon and spring intermonsoon are generated from the meander in the northeast ward flowing western

boundary current, whereas the SCE during fall intermonsoon appears to have moved from the SLD region into the western boundary of the BOB.

3.4. Mechanisms of generation

Having described the characteristics of the NCE from the *in situ* as well as the satellite data, it is pertinent to examine the potential mechanism/s that could generate eddies during western boundary current regime. Since NCE during spring intermonsoon (NCE-2003) and the summer (NCE-2001) were found to be associated with the meander in the western boundary current, the discussion is focused only to the NCE during the above periods.

The trigger for the eddy generation could be the instability of the western boundary current (WBC). The cross-shore and along-shore dimensions of the WBC in the region of eddy generation are about 150 km and 500 km respectively. A scale analysis of the horizontal motion associated with the WBC showed that $Lr^2/L^2 \leq O(1)$ [*Pedlosky*, 1979], where Lr (~70 Km) is the Rossby deformation radius and L is the horizontal scales of motion, which suggests the role of baroclinic instability in generating eddies.

From the topography of isopycnals (Figure 3.2.1.1c & Figure 3.2.2.1c) the horizontal dimension of the eddy was found to be approximately 352 km during spring intermonsoon 2003 and about 311 km during summer monsoon (core of the eddy was slightly away from the sampling track). The typical value for first mode internal Rossby

deformation radius (Lr) in the northern Bay of Bengal is approximately 70 km (Figure 3.4.1).

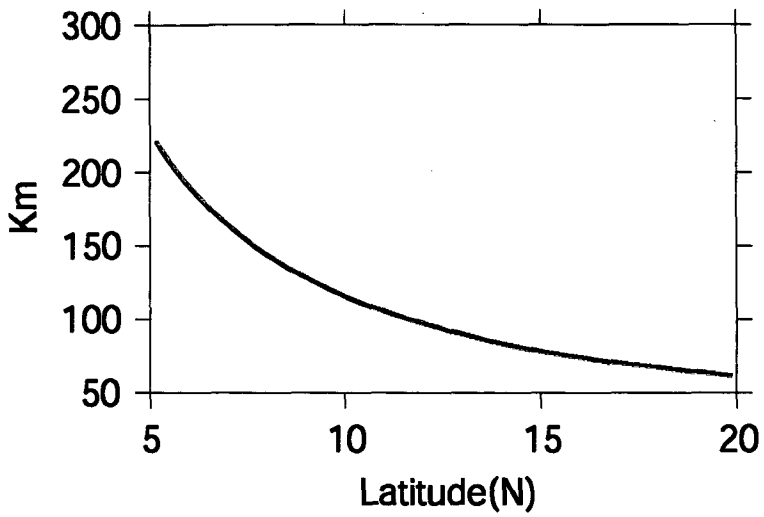

Figure 3.4.1 Rossby deformation in the BOB along 88°E (see Chapter 2 for details of computation).

The wavelength of most unstable baroclinic instability process is given by 2π Lr [*Stammer and Boning*, 1992] and in the northern Bay of Bengal this is about 440 km. From the sea-level anomaly maps the transverse dimension of this eddy was found to be about 430 km. Eddy dimensions obtained from sea-level anomaly maps differed from the hydrography by about 80 km.

However, the computed dimension broadly agrees with the observed one with in the resolvable limits of sea-level anomaly (~37 km) and hydrography (~150 km). The agreement between the theoretical and the observed spatial dimensions suggest the role of baroclinic instability of large-scale currents in generating eddies [*Kamenkovich et al.*, 1986]. In the present case, it is the instability associated with the northeastward flowing spring time WBC of the BOB.

The sea-level anomaly maps showed that the meanders in the northeastward flowing WBC forms in early February, in 2003 (Figure 3.3.1.1), and the signatures of cyclonic circulation was seen towards the end of February which becomes fully developed by the end of March (Figure 3.3.1.2). Thus, time span for the meander to develop into a cyclonic circulation is about three-weeks. A similar time-span was found during 2001 as well (Figure 3.3.2.1 & Figure 3.2.2.2).

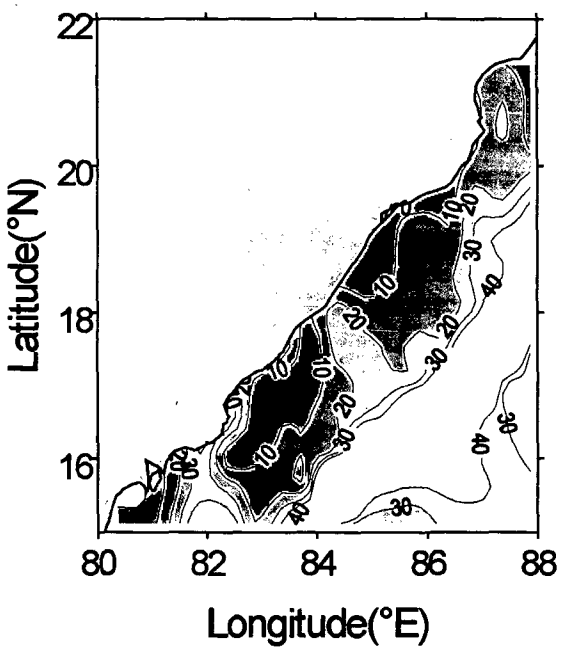

Figure 3.4.2 Barodinic time scale (days) computed from WOA01 climatology [*Conkright et al.*, 2002] along the region where NCE is formed. See text for details.

Following *Stammer* [1998], a baroclinic time scale $\sqrt{Ri} / f$ (where Ri is the Richardson number, f the coriolis parameter) was computed from the WOA01 climatology [*Conkright et al.*, 2002] for 50 to 1000m depth of water column for the northwestern Bay

of Bengal (Figure 3.4.2). The mean vertical shear in the velocity was computed from the cross-shore density differences. However, horizontal density gradient less than 6 x 10^{-8} was discarded, as the corresponding velocity is too small, of the order of 10^{-1} cm/s in the northwestern region. In the northwestern Bay of Bengal (15°N-22°N, 80°E-88°E) baroclinic time scale during February-March varied between less than 20 days near to the coast to more than 100 days off shore. Thus, the observed time-scale for the meander to form a cyclonic circulation, obtained from sea-level anomaly, falls within the theoretical values in the western boundary region. This time scale is associated with the growth rate of baroclinic eddies [*Eady,* 1949; *Stammer*, 1998]. The agreement of the observed time scale with the predicted one suggests, once again, the role of baroclinic instability process in the formation of eddies along the western boundary region of the Bay of Bengal.

An examination of the density structure at 100 m computed from WOA01 climatology [*Conkright et al.,* 2002] reveals the presence of denser waters close to the shore during January and February with strong cross-shore gradients (Figure 3.4.3). The cross-shore density gradient accompanied by vertical shear in the horizontal velocity is a necessary condition for baroclinic instability [*Pedlosky*, 1979]. The possible mechanisms that can lead to this cross-shore density gradient could be (1) topographic changes, (2) wind forcing, and (3) remote forcing, either individually or in combination.

The topography along the western boundary of the Bay of Bengal from 15° to 20°N, obtained from ETOPO data having five-minute resolution showed that the orientation of the coast turns eastward at 16°N.

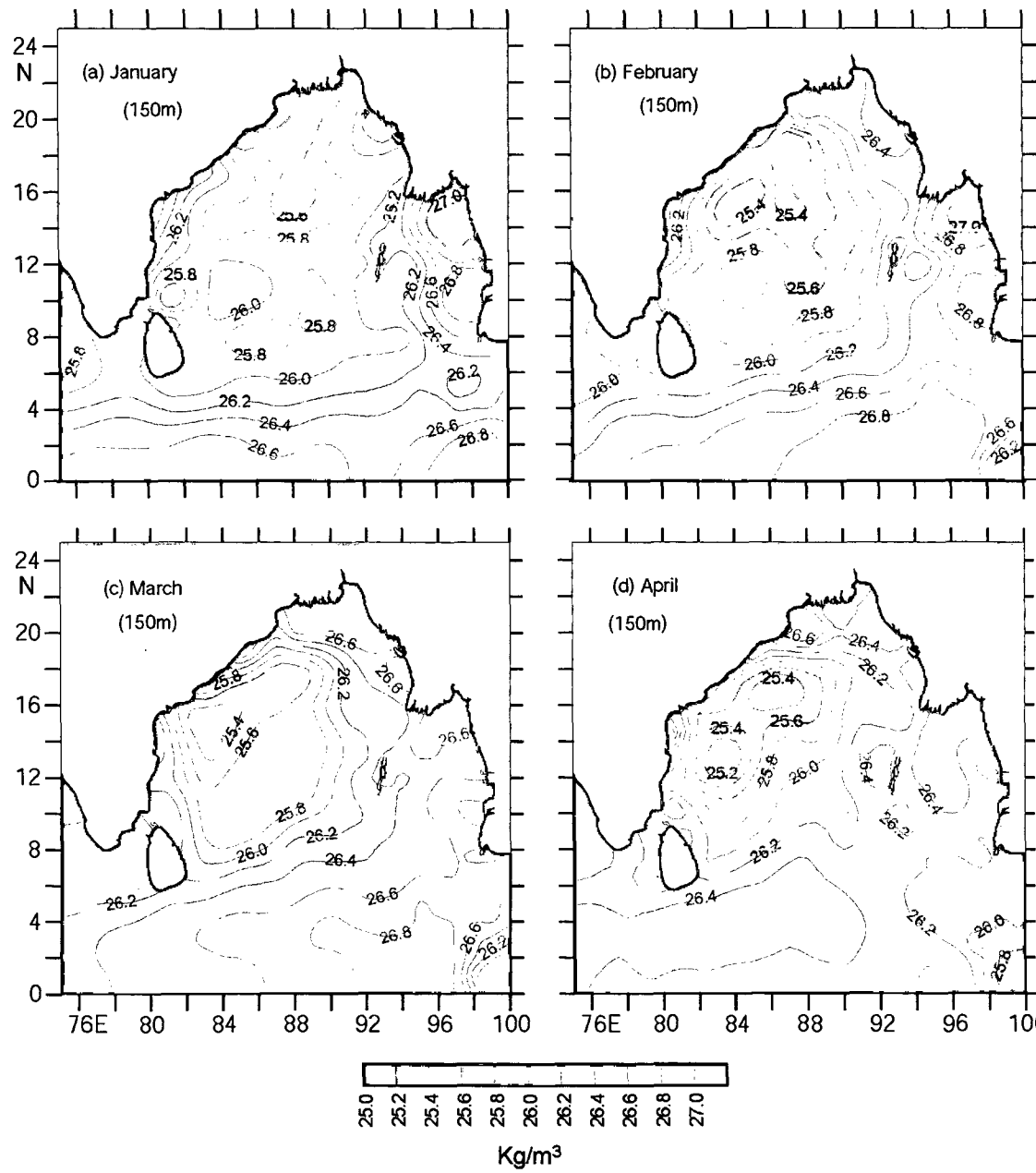

Figure 3.4.3. Basin-wide distribution of monthly mean sigma-t at 150m depth during (a) January, (b) February, (c) March and (d) April derived from WOA01 qaurter-degree climatology [*Conkright et al.*, 2002].

The meandering of the northeastward WBC and the resultant eddy formation took place in the vicinity of 20°N during 2001, where as during 2003 the meander formed at about 17°N, which was away from the eastward turn at 16°N. This would mean that topographic change has little contribution to the formation of eddy. Thus, it seems that

along the western boundary of the Bay of Bengal topographic change is not a necessary condition for the formation of eddies.

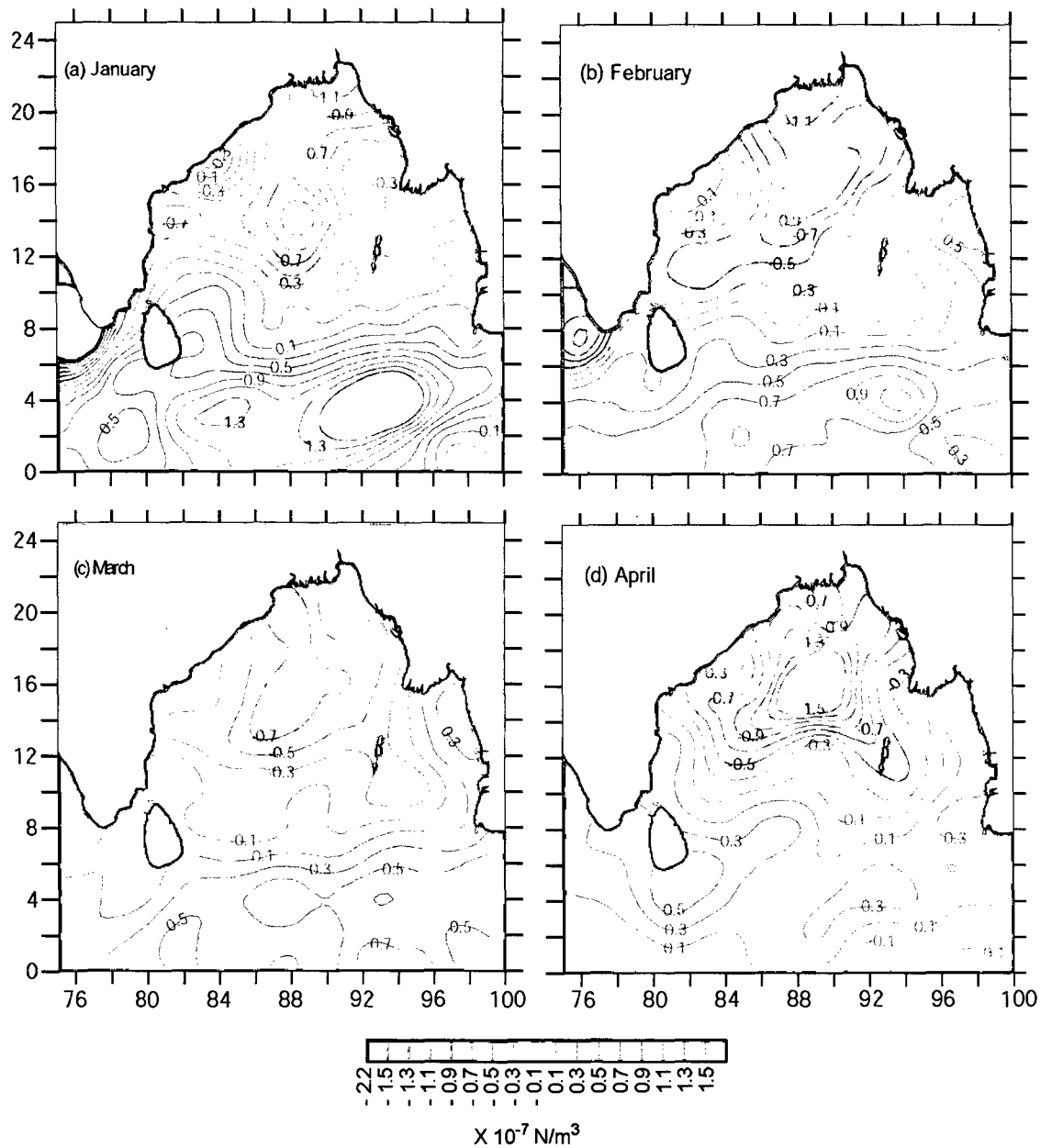

Figure 3.4.4. Curl of wind stress (x 10^{-7} N/m^3) derived from Southampton oceanographic centre monthly mean climatology of wind-stress [*Josey et al.*, 2002]

The basin-wide distribution of monthly mean wind-stress curl computed from SOC climatology [*Josey et al.*, 2002] showed large negative curl in the northern Bay from

January to April having its peak in April (Figure 3.4.4). However, a patch of positive curl was noticed close to the northwestern boundary between 16° and 18°N during January and 14° and 17°N during February.

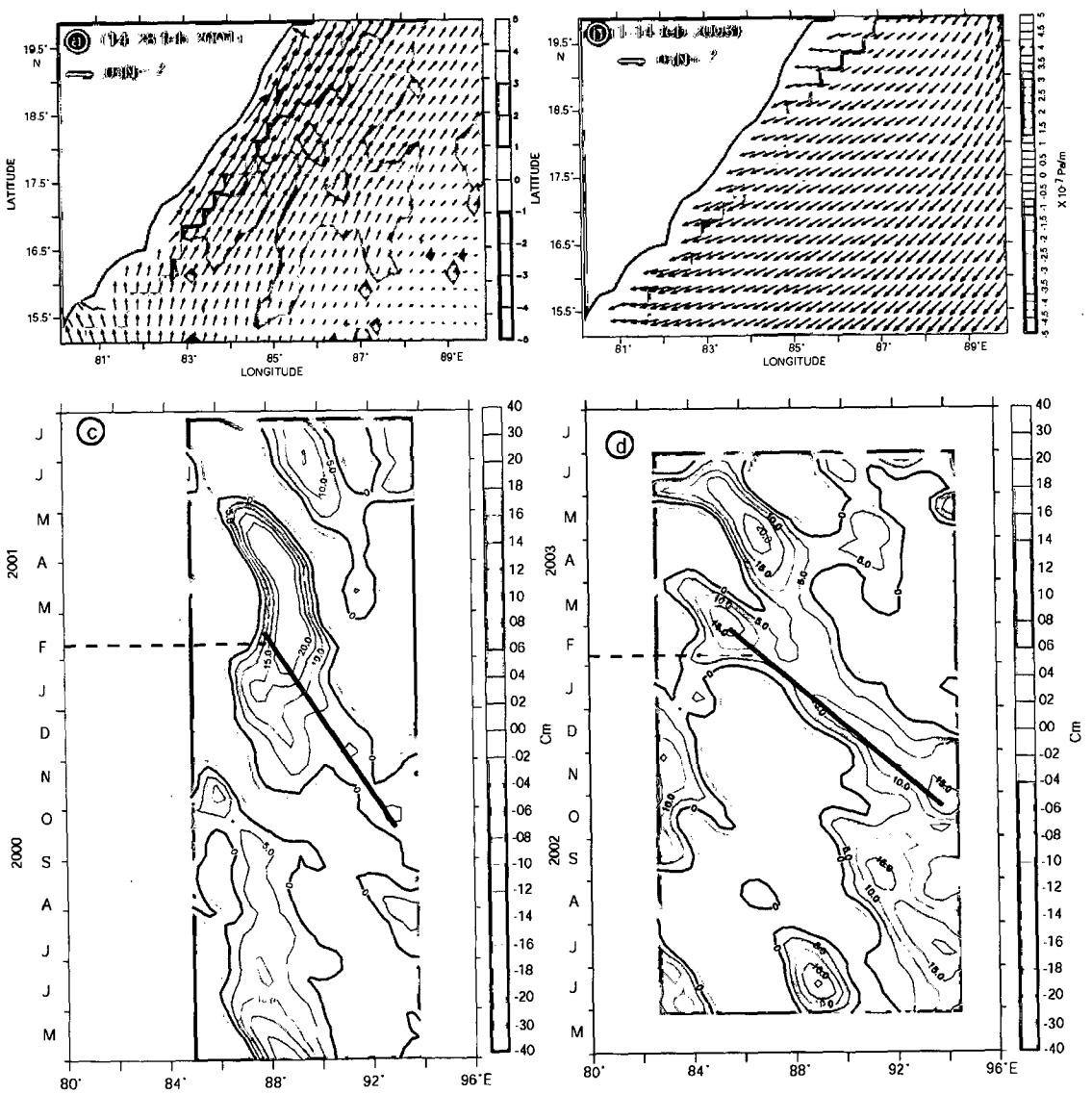

Figure 3.4.5 (a) Curl of wind stress (x 10^{-7} Pa/m) derived from QuikSCAT during 1-14 February 2003 and (b) during 14-28 February 2001), (c) zonally de-meaned merged SLA of Topex/Poseidon-ERS 1/2 series of satellites along 19°N (positive values are contoured) during June 2000 to June 2001, (d) along 17°N (positive values are contoured) during June 2002 to June 2003. Bold slanting line indicates the Rossby wave propagation during respective years. Broken line shows the cross-shore SLA gradient which is a result of upwelling along the western boundary and downwelling offshore.

The QuikSCAT wind-stress (Large-Pond method) curl also showed positive curl close to the western boundary (close to the location of eddies) during 2003 and 2001 (Figure 3.4.5, top left and right). In response to this, one would expect large-scale convergence and downwelling of surface water under the negative wind-stress curl, while divergence and upwelling of subsurface waters close to the coast under the positive wind-stress curl. In fact, *Murty and Varadachari* [1968], *Rao et al.* [1986], *Shetye et al.* [1993] and *Rao* [2002] noticed upwelling signatures very close to the coast during spring intermonsoon. In addition, *Rao* [2002] also showed deepening of pycnocline in the offshore region between 15° and 17°N (see Figure 10 of *Rao*, 2002). Thus, wind-forcing is capable of generating the necessary cross-shore density gradient.

A zonally de-meaned SLA along the latitude of eddy formation during 2003 and 2001 showed a westward propagation of high sea-level anomaly (Figure 3.4.5, bottom) which was also clearly seen in the climatology of SLA in the same latitude (Figure 3.4.6) and indicates the propagation of Rossby waves. This Rossby wave can augment the basin-wide negative wind-stress curl in deepening the pycnocline. Thus, the negative wind-stress curl and Rossby wave act in union to deepen the pycnocline in the offshore region, while the positive wind-stress curl shallows the pycnocline close to the coast. This in turn will generate strong cross-shore density gradient, as is evident from Figure 3.4.3, necessary for the baroclinic instability that leads to eddy generation.

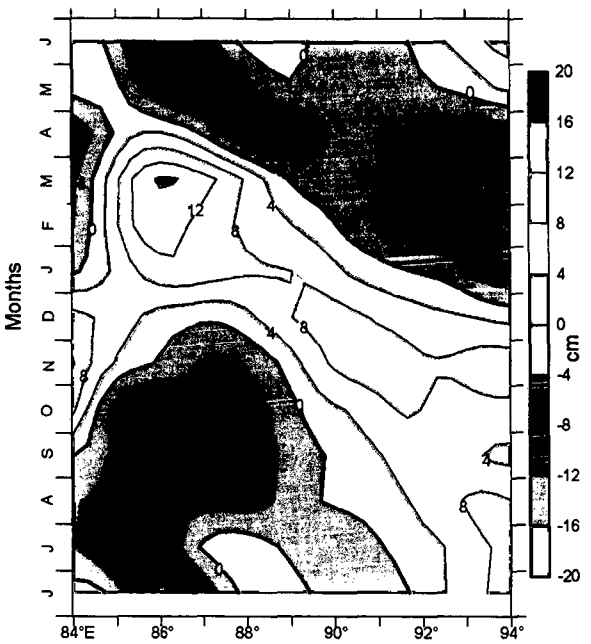

Figure 3.4.6. Time-longitude plot of monthly mean (1992-October to 2004-January) sea-level anomaly climatology derived from merged sea-level anomalies of Topex/Poseidon and ERS 1/2 satellites obtained from AVISO CNES, along 18°N starting from June. See text for details.

3.5. Summary

The present chapter deals with the cyclonic eddies observed in the BOB from the thermohaline structure during summer (July-August, 2001), fall intermonsoon (September-October, 2002) and spring intermonsoon (April-May, 2003) along the western boundary and describes its structure, evolution and possible generation mechanisms based on *in situ* and remote sensing data . The doming of isolines in the vertical distribution of temperature/salinity/density manifested the signature of eddy and was most pronounced in the northern part of the western boundary during spring intermonsoon. Accordingly, this eddy depressed the ambient temperature of upper-thermocline by 6°C and increased the near-surface salinity by 0.8 psu. The presence of these cyclonic eddies were confirmed using satellite derived sea-level anomaly maps,

which further indicated that the eddy observed in spring intermonsoon and summer originates as a meander in the WBC. However, the origin of the fall intermonsoon eddy was not clear from the sea-level anomaly maps. These cyclonic eddies encountered in the northern part of the western boundary (16°-19°N) in all the three seasons are designated as northern coastal eddy (NCE), while that in the southern part centered at 14°N and 12°N during spring and fall intermonsoons respectively is designated as southern coastal eddy (SCE). The NCE formed during the WBC regime of 2001 and 2003, had a complex life cycle undergoing offshore-onshore movements, southwestward translation, coalescence and splitting before they finally get dissipated; all of which occurred within a span of approximately 5 months. The time and space scales associated with the NCE during spring and summer suggested the role of baroclinic instability in generating them. With a suite of *in situ* and remote sensing data set, it has been found that a combination of remote and local forcing induced the baroclinic instability along the western boundary. They are 1) the positive wind-stress curl close to the western boundary 2) large negative wind-stress curl in the offshore region, and 3) westward propagating Rossby waves. The positive wind-stress curl close to the western boundary during January-February, between 14-20°N, drives divergence and upward Ekman pumping leading to upwelling of subsurface cold waters, while the large negative wind-stress curl in the offshore region combined with westward propagating Rossby waves drives convergence and down welling of warm surface waters.

Chapter 4 - Eddies in the central Bay of Bengal

4.1. Introduction

Previous chapter dealt with the characteristics, evolution and the generating mechanism of eddies along the western boundary of the BOB. In this chapter, the signature of eddies was explored using hydrographic data collected along the central BOB (88°E) onboard the ship during summer monsoon (10-22 July 2001), fall intermonsoon (17-27 September 2002) and spring intermonsoon (16-25 April 2003). Satellite sea-level anomaly is also used to track the origin and evolution of eddies identified from the hydrography.

4.2 Thermohaline structure

4.2.1 Summer Monsoon 2001

Examination of vertical thermal structure revealed several undulations. Doming of isotherms was noticed centered at 9°N, 16°N and 19°N, where as a depression was noticed at about 18°N. The displacement of isotherms was more prominent in the upper layers in the southern region. For example, 22 and 24°C isotherms underwent a displacement of ~50 m at 9°N (Figure 4.2.1.1a). The upward displacement of isotherms depressed the ambient temperature at 100 m by about 2.5°C, where as in the north the displacement of isotherms was more pronounced in the subsurface layers. At 19°N, 22°C and 24 °C isotherms underwent an upward displacement of ~25 m whereas deeper isotherms 13°C, 14°C, 15°C and 16°C were displaced upwards by about ~ 50 m. This

depressed the ambient temperature by about 2°C. Similarly at 16°N too deeper isotherms underwent maximum upheaval, though the magnitude of displacement was less. In the

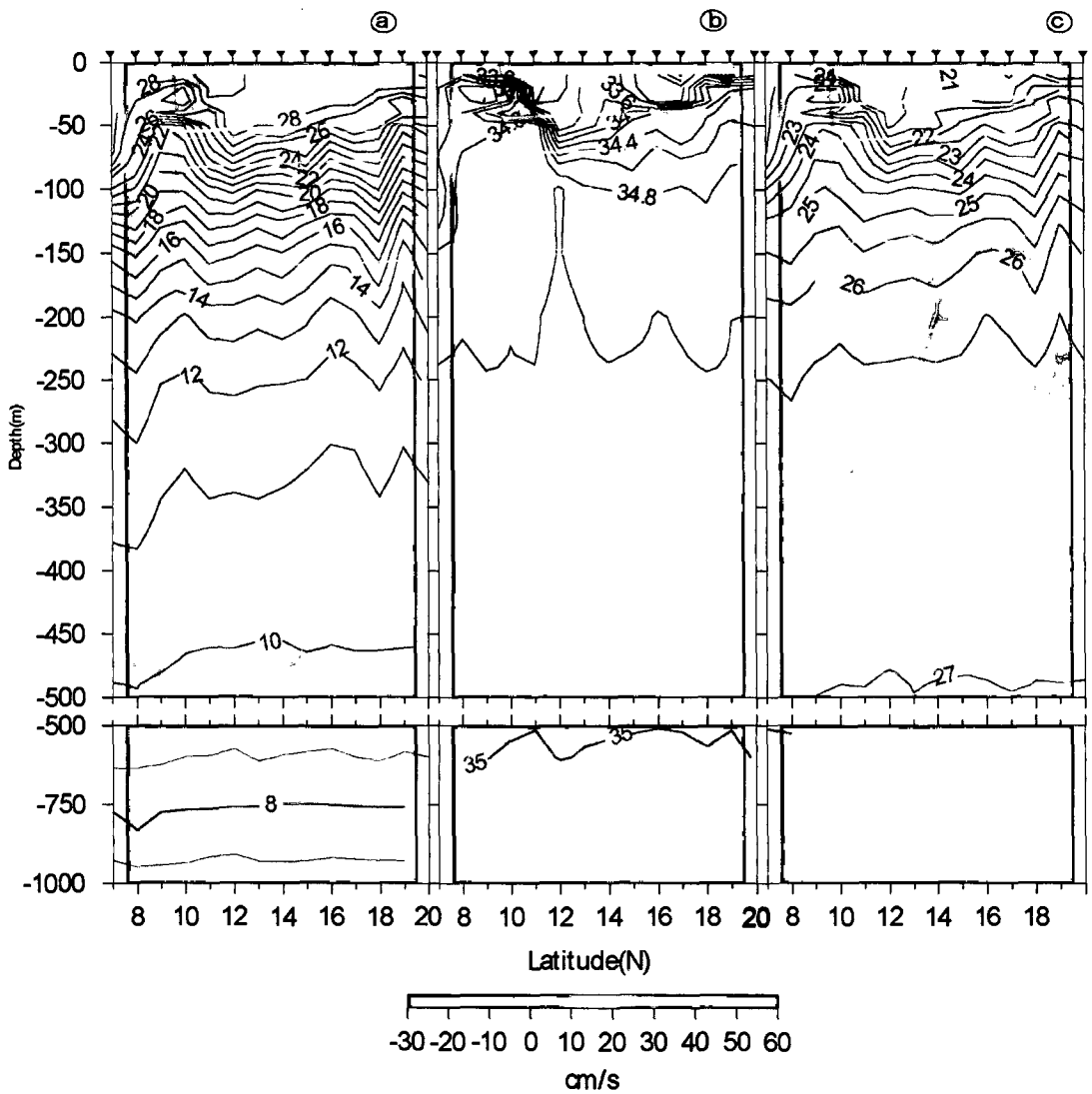

Figure 4.2.1.1 Vertical section of (a) temperature (°C), (b) Salinity (psu), and sigma-t (kg/m^3) overlaid on the geostrophic velocity (cm/s) w.r.t 1000 m along the central (88°E) BOB during summer monsoon (10-22 July) 2001. Filled inverted triangles indicate the position of CTD stations.

case of depression centered about 18°N, maximum displacement occurred for isotherms 13°C, 14°C, 15°C and 16°C (~30 m), which resulted in an increase of ambient temperature by about 1°C at 150 m depth. However, the 15°C isotherm underwent a

displacement of 40 m. Consistent with the isotherm displacement, the isohalines also showed undulations (Figure 4.2.1.1b). In the south 35 psu isohaline underwent an upward displacement of about 70 m. Though in the north isohalines showed tendencies similar to that of isotherms, the displacement was not prominent. The reason for this is the overwhelming impact of freshwater in the northern Bay, which is evident in the haline structure. The density structure essentially reflected the thermal structure, except in the north, where influence of salinity could be seen in the surface layers. In the south, 24 sigma-t surface displaced upward by about 60 m where as in the north, consistent with the thermal structure, the deeper isopycnals underwent maximum displacement (Figure 4.2.1.1c). For example, the 26 sigma-t isopleth was displaced by ~50 m at 19°N. Relative velocity computed w.r.t 1000 m (Figure 4.2.1.1 shading) showed alternate bands of eastward and westward velocities. In the south an east ward velocity of ~60 cm/s was noticed at 8°N which turned westward at about 11°N. At about 15°N again an eastward flow was noticed which turned to west after 16°N. An eastward flow followed this at 18°N which turned, west once again after 19°N. This turning of the flow coincided with the centers of doming and depression. Thus, centered about 9°, 16° and 19°N signatures of cyclonic flow and centered about 18°N one anticyclonic flow were detected.

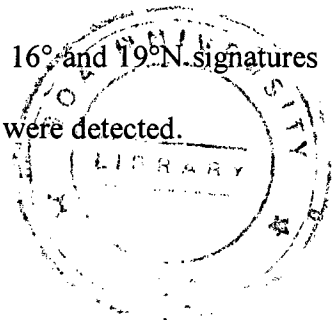

4.2.2. Fall intermonsoon 2002

Doming of isotherms was noted at three locations centered about 9°N, 14°N and 18°N (Figure 4.2.2.1a). Apart from these undulations, a depression centered about 12°N along the open ocean transect was also noticed. Similar to the observation during summer monsoon 2001 the isotherms underwent maximum displacement within the first 100 m

for the doming centered at 9°N. For example, the 26°, 27°, 28°C isotherms underwent displacements of about 40-50 m, where as for the depression centered about 12°N the maximum deformation was found to be associated with 16°, 17° and 18°C isotherms.

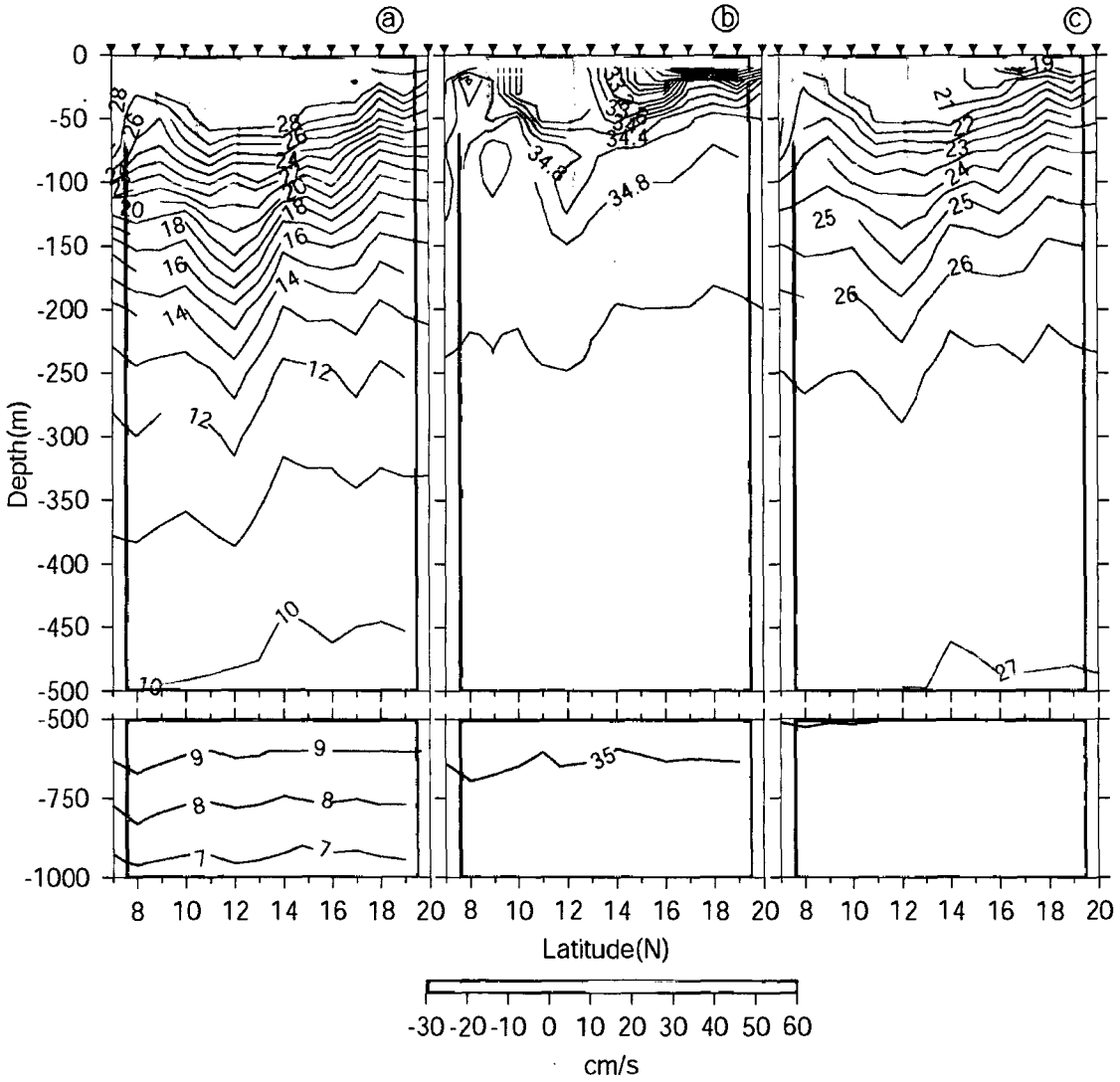

Figure 4.2.2.1 Vertical section of (a) temperature (°C), (b) Salinity (psu), and sigma-t (kg/m^3) overlaid on the geostrophic velocity (cm/s) w.r.t 1000 m along the central (88°E) BOB during fall intermonsoon (17-27 September) 2002. Filled inverted triangles indicate the position of CTD stations.

These doming/depressions decreased/increased the ambient temperature by about 2°C. The doming centered at 18°N was not very conspicuous. The upward and downward

displacements associated with the doming and depression was reflected in the salinity structure also (Figure 4.2.2.1b). The 34.8 psu isohaline displaced upward by about 80 m in the case of doming centered about 9°N and had a downward displacement of about the same amount in the case of depression centered about 12°N. The density structure also showed the salient features of the thermal structure except in the north where overwhelming signals of the fresh water was found. At 9°N the 22.5 sigma-t surface underwent a displacement of approximately 50 m whereas at 12°N the 25 sigma-t surface was depressed by about 40 m (Figure 4.2.2.1c). Consistent with the density structure the relative velocity computed with respect to 1000 m showed alternating bands of eastward and west ward velocities (Figure 4.2.2.1 shading). An eastward velocity of ~25 cm/s was found at 8°N which turned to west at about 10°N. This westward velocity started decreasing and turned east at about 13°N. This was followed by a weak westward flow at 15°N. Velocity was found to be eastward again at 17°N and turned west the north. Thus, consistent with the doming and depression in the temperature/salinity structure the velocities too underwent changes in direction signifying the presence cyclonic eddies centered about 9 , 14°N and 18°N and anticyclonic eddy at 12°N.

4.2.3 Spring intermonsoon 2003

Thermal structure showed many undulations within and beyond the thermocline. Prominent doming was noticed at 11°N, 16°N and 19°N, where as two regions of depression at 13°N and 18°N were also seen (Figure 4.2.3.1a). Maximum displacement of isotherms occurred at three locations, centered at 16°, 18° and 19°N in the upper 500 m of the water column. However, the displacements at 11° and 13°N were confined

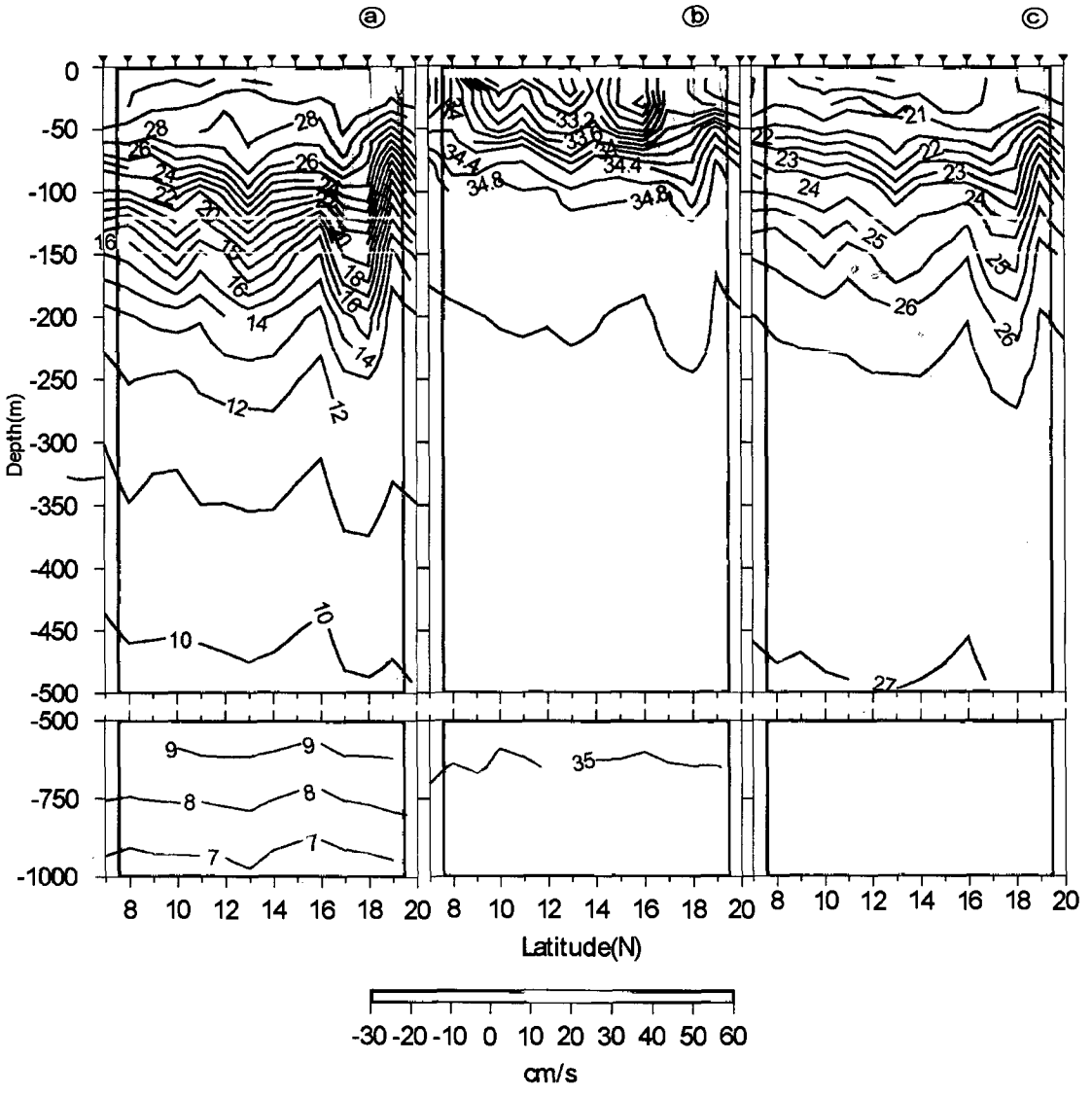

Figure 4.2.3.1 Vertical section of (a) temperature (°C), (b) Salinity (psu), and sigma-t (kg/m^3) overlaid on the geostrophic velocity (cm/s) w.r.t 1000 m along the central (88°E) BOB during spring intermonsoon (16-25 Aprilr) 2003. Filled inverted triangles indicate the position of CTD stations.

within the thermocline. The 16°C isotherm underwent an upheaval of about 40 m at 16°N while it was depressed by about 60 m at 18°N. Once again the isotherm had undergone an upheaval of about 60 m at 19 °N. Salinity structure showed low saline waters even in the southern most part of the transect (Figure 4.2.3.1b). However, it does not exactly mimic the thermal structure except at a few locations. The depression at 13°N and 18°N

and the doming centered about 19°N was conspicuous in the haline structure. However, maximum displacement of isohalines occurred at 18° and 19°N, where 35 psu isohaline was depressed by 60 m at 18 °N and was uplifted by the same distance at 19°N. The density structure essentially reflected the thermal structure with doming at 11°, 16° and 19°N and depressions at 13° and 15°N (Figure 4.2.3.1c).

Geostrophic velocities computed w.r.t 1000 m showed alternate bands of positive and negative velocities. The direction was generally westward in the southern part of the transect, however, at about 12°N this westward velocity increased to about 15 cm/s then turned eastward at 14°N. Velocity decreased further north and turned westward again at 17°N with velocity increasing towards north. Once again, the current changed its direction towards east at 19°N and subsequently decreases further north. Thus, from the thermohaline structure and the geostrophic velocity structure the signatures of three cyclonic eddies centered about 11°, 16° and 19°N, and two anticyclonic eddies centered about 14° and 18°N were deciphered during spring intermonsoon 2003.

In summary a total number of 13 cyclonic/ant-cyclonic features were identified from the thermohaline structure along the open ocean transect during the 3 seasons. Of this there were 4 eddies each in summer and fall intermonsoon (3 cyclonic and 1 anticyclonic), and 5 eddies (3 cyclonic and 2 anticyclonic) in spring intermonsoon. To confirm these features and to further understand their evolution, satellite altimeter data were utilized. The Topex/Poseidon, ERS merged sea-level anomalies obtained from AVISO-CNES were analyzed and in the following section.

4.3 Evolution of eddies from T/P ERS merged sea-level anomalies.

From the above analysis it is clear that the doming found at 18°N in the thermohaline structure during summer monsoon was not evident in the SLA snapshots. Again, the doming found at 18°N in the thermohaline structure during fall intermonsoon was found to be a part of the large scale negative sea-level anomaly, and not a mesoscale feature. Similarly, the depression found at 18°N during spring intermonsoon too was a part of the large scale positive sea-level anomaly. Hence no attempt was made to describe these 3 features out of the 13.

4.3.1 Summer monsoon 2001

4.3.1.1 Cyclonic eddy centered at 9°N (CES1)

Important features in the southern BOB during summer monsoon 2001 was the Sri Lankan dome formed by the positive wind-stress curl [*Vinayachandran et al., 1998*] and the westward propagating anticyclonic vortices [*Sengupta et al., 2001*]. These anticyclonic vortices are hypothesized to be formed by the interaction of south west Monsoon currents with the west ward propagating Rossby waves [*Sengupta et al., 2001*]. The cyclonic eddy at 9°N (CES1) was formed during the last week of June 2001 centered about 9°N, 87°E (Figure 3.3.2.5). As the anticyclonic vortex approached closer the SLD, CES1 got intensified and moved northeast following the contours of the anticyclonic vortex during the first week of July and then to southeastward This cyclonic eddy was sampled in the hydrographic section when it was centered approximately on 10°N, 88°E during the second week of July (Figure 3.3.2.6, top left). The CES1 dissipated by the

first week of August (Figure 3.3.2.6, bottom left). Through out its life time the CES1was characterized by a sea-level anomaly of –2 to –16 cm and geostrophic velocity anomaly of ~ 10-20 cm/s. However, the southern limb of CES1 was characterized by higher velocities (~ 60 cm/s) because the eastward velocity augmented by the eastward velocity component of the anticyclonic vortex.

4.3.1.2 Cyclonic eddy centered at 16°N (CES2)

Signature of a cyclonic circulation was found centered about 15°N 89.5°E during the first week of May 2001 (Figure 3.3.2.3). This was characterized by a negative SLA of 6 cm and geostrophic velocity anomaly of ~ 20 cm/s. However, the western limb of this cyclonic circulation was characterized by higher velocities due to an anticyclonic circulation was found west of it, and the cyclonic circulation intensified in the following weeks. One cyclonic eddy centered about 17°N 88°E, splitted from NCE appeared to have coalesced with this by the third week of May (Figure 3.3.2.4). This forms the CES2 during summer monsoon 2001. Subsequently, CES2 increased in size and displaced northward by 0.5 degrees by last week of June (Figure 3.3.2.5). During this time CES2 was characterized by a SLA of ~ -30 cm and geostrophic velocity anomaly of 40-50 cm/s. Subsequently, it moved northwestward and was found to coalesce with NCE 2001 centered at 16.5°N 84°N. This made it into an elongated structure extending from 15 to 17°N meridionally and 83 to 88°E zonally with two distinct centers (Figure 3.3.2.6). During the time of sampling (Figure 3.3.2.6, last week of July] CES2 was characterized by an SLA of ~ -30 cm and geostrophic velocity anomaly of ~ 40-50 cm/s.

4.3.1.3 Cyclonic eddy centered at 19°N (CES3)

A cyclonic circulation was formed centered about 18.6°N 91.5°E during the last week of May 2001 (Figure 3.3.2.4) and was characterized by a sea-level anomaly of -6 cm and geostrophic velocity anomaly of approximately 20-30 cm/s. This cyclonic circulation propagated into the western BOB. During the second week of July this was intensified and characterized by a sea-level anomaly of approximately -12 cm and geostrophic velocity anomaly of ~ 30-40 cm/s (Figure 3.3.2.6) and progressed further westwards to reach 86°E by September 2001. This feature was characterized by a sea-level anomaly of -8 cm and geostrophic velocity anomaly of approximately 20-30 cm/s. In the last week of July when the eddy was sampled it was elongated and extended approximately from 88° to 92°E zonally and 18° to 20°N meridionally (Figure 3.3.2.6, bottom left). By August this feature started diminishing.

4.3.2 Fall intermonsoon 2002

4.3.2.1 Cyclonic eddy centered at 9°N (CEF1)

In the first week of September 2002, a weak cyclonic circulation was observed in the northeast of an anticyclonic vortex centered about 9.5°N 87°E and close to SLD (Figure 3.3.3.1, top left). As the anticyclonic vortex moved further westward by the second week of September, the cyclonic circulation got intensified and moved southeastward. Unlike the CES1, this became a fully developed cyclonic circulation during the second week of September and was characterized by a sea-level anomaly of -14 cm and geostrophic velocity anomalies of approximately 30-40 cm/s (Figure 3.3.3.1, bottom left). This was the closest date matching with the hydrographic sampling from the ship. By 3rd week of

September, another weak anticyclonic circulation was seen approaching the western Bay and with this the cyclonic circulation dissipated.

4.3.2.2 Anticyclonic eddy centered at 12°N (ACF2)

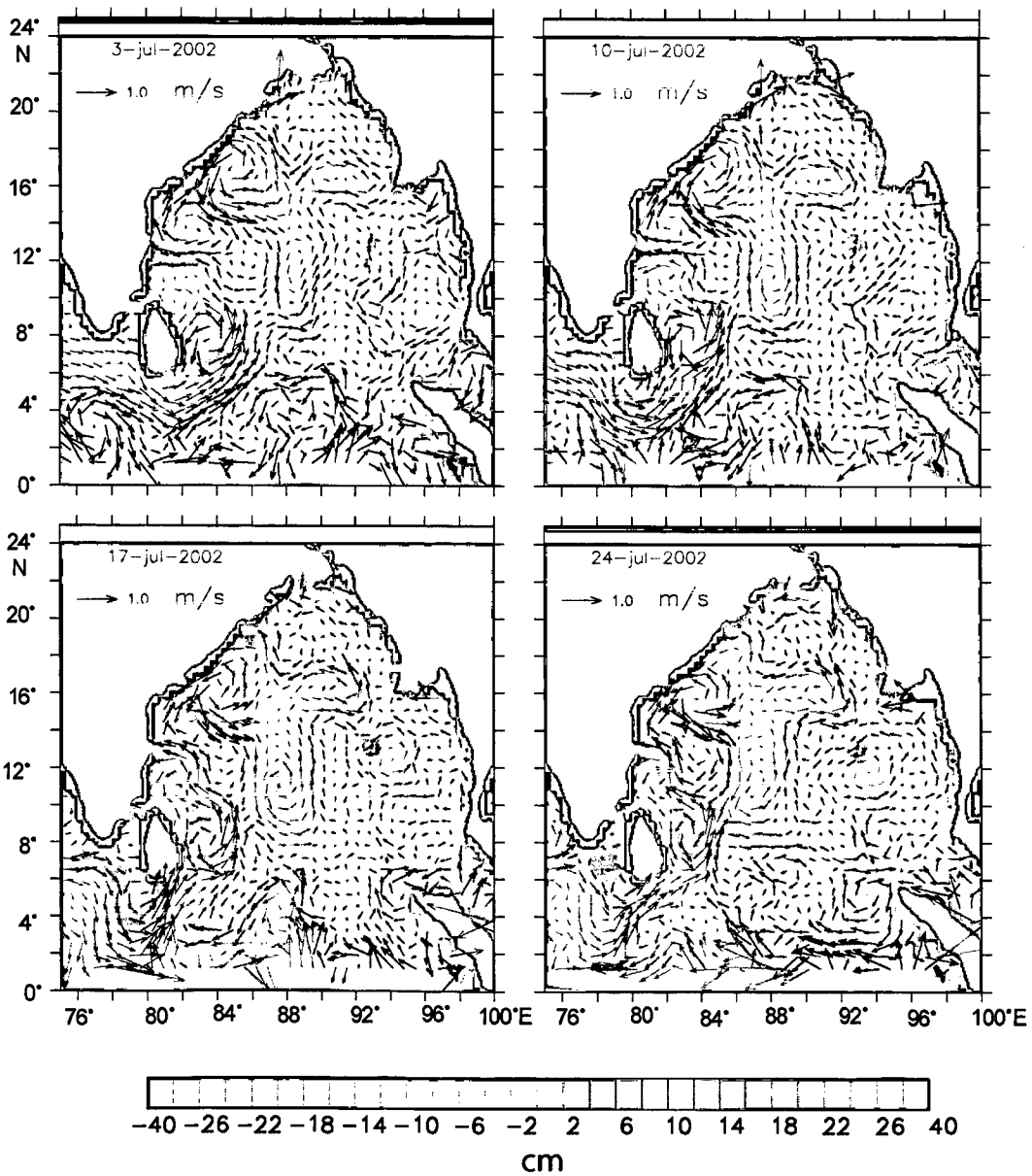

Figure 4.3.2.2.1 7-day snap-shots of Topex/Poseidon ERS1/2 merged sea-level anomalies overlaid with geostrophic velocities during July 2002.

The depression noted in the thermohaline structure was an anticyclonic eddy pinched-off from a large positive sea-level anomaly formed in the western Andaman region during last week of July 2002 (Figure 4.3.2.2.1) and was characterized by a positive sea-level anomaly of 16 cm and geostrophic velocity anomaly of ~30-40 cm/s. This anticyclonic eddy propagated into the western BOB and was sampled during the third week of September (Figure 3.3.3.1), when it was characterized by a sea-level anomaly of 12 cm and geostrophic velocity anomaly of 20-30 cm/s. By the last week of October the feature started dissipating (Figure 3.3.3.2).

4.3.2.3 Cyclonic centered at 14°N (CEF3)

A cyclonic circulation was developed during the first week of June centered about 17°N and 91°E with a negative SLA of about 8 cm and geostrophic velocity anomaly of about 20 cm/s (Figure 4.3.2.3.1). SLA picture showed that this cyclonic circulation got elongated by last week of June. This elongation appeared to be a result of coalescence of this cyclonic eddy with another one centered at 16°N, 93°E. This forms the CEF3 during fall intermonsoon. Two centers of low SLA could be seen in this elongated CEF3. One centered about 90°E 17°N another one centered about 93°E 16°N. By the first week of July these two centers disappeared and appeared as an elongated cyclonic circulation (Figure 4.3.2.2.1) extending from 89° to 93°E and from 15° to 18°N. The center of CEF3 shifted eastwards to 16°N 91°E by second week of July and was characterized by a SLA of about -30 cm and geostrophic velocity anomaly of ~40 cm/s. By third week of August it intensified and moved westwards (Figure 4.3.2.3.2). Later, by last week of

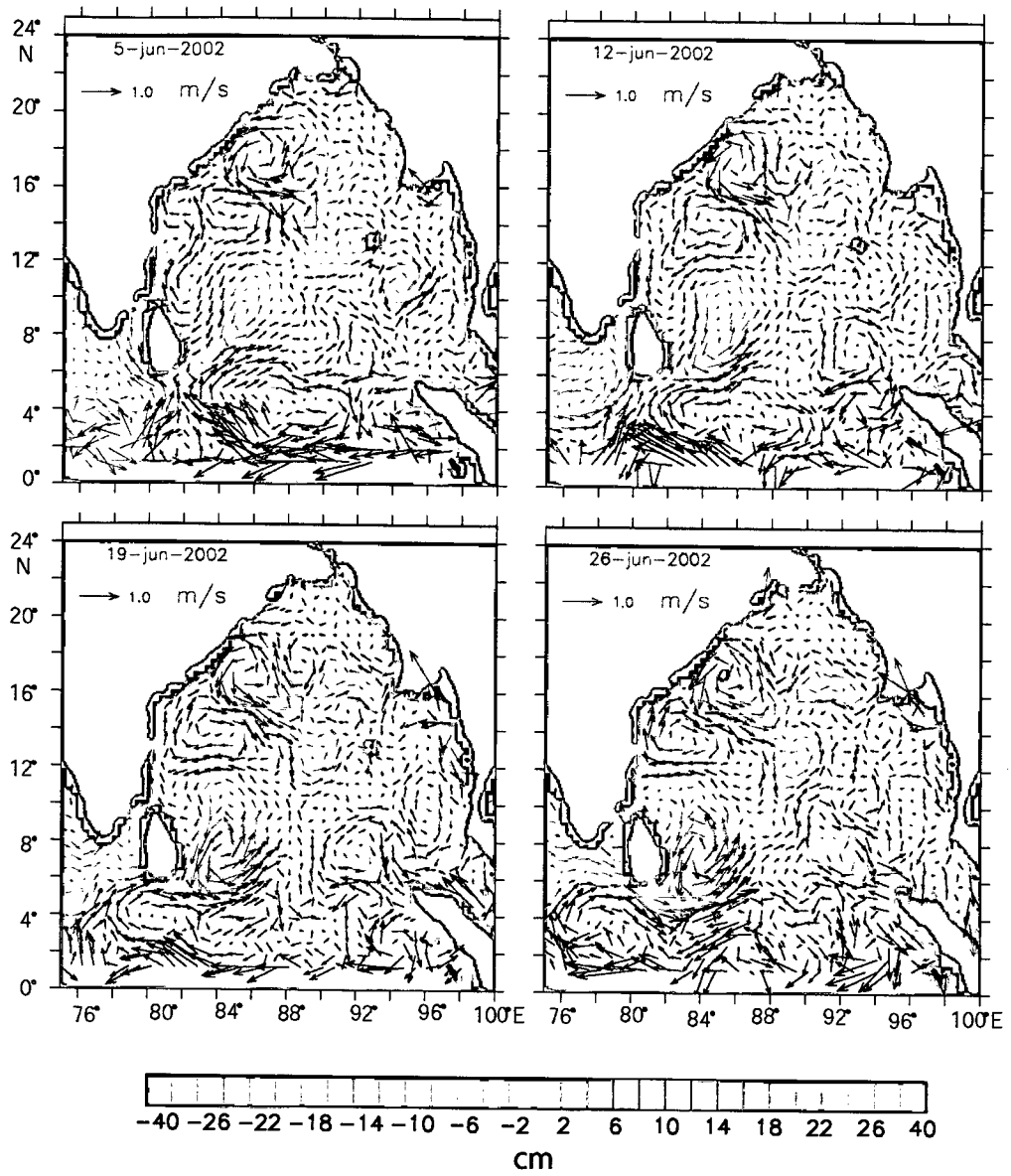

Figure 4.3.2.3.1 7-day snap-shots of Topex/Poseidon ERS1/2 merged sea-level anomalies overlaid with geostrophic velocities during June 2002.

September CEF3 coalesced with a cyclonic eddy and became a part of large cyclonic circulation that prevailed in the western BOB during fall intermonsoon 2002.

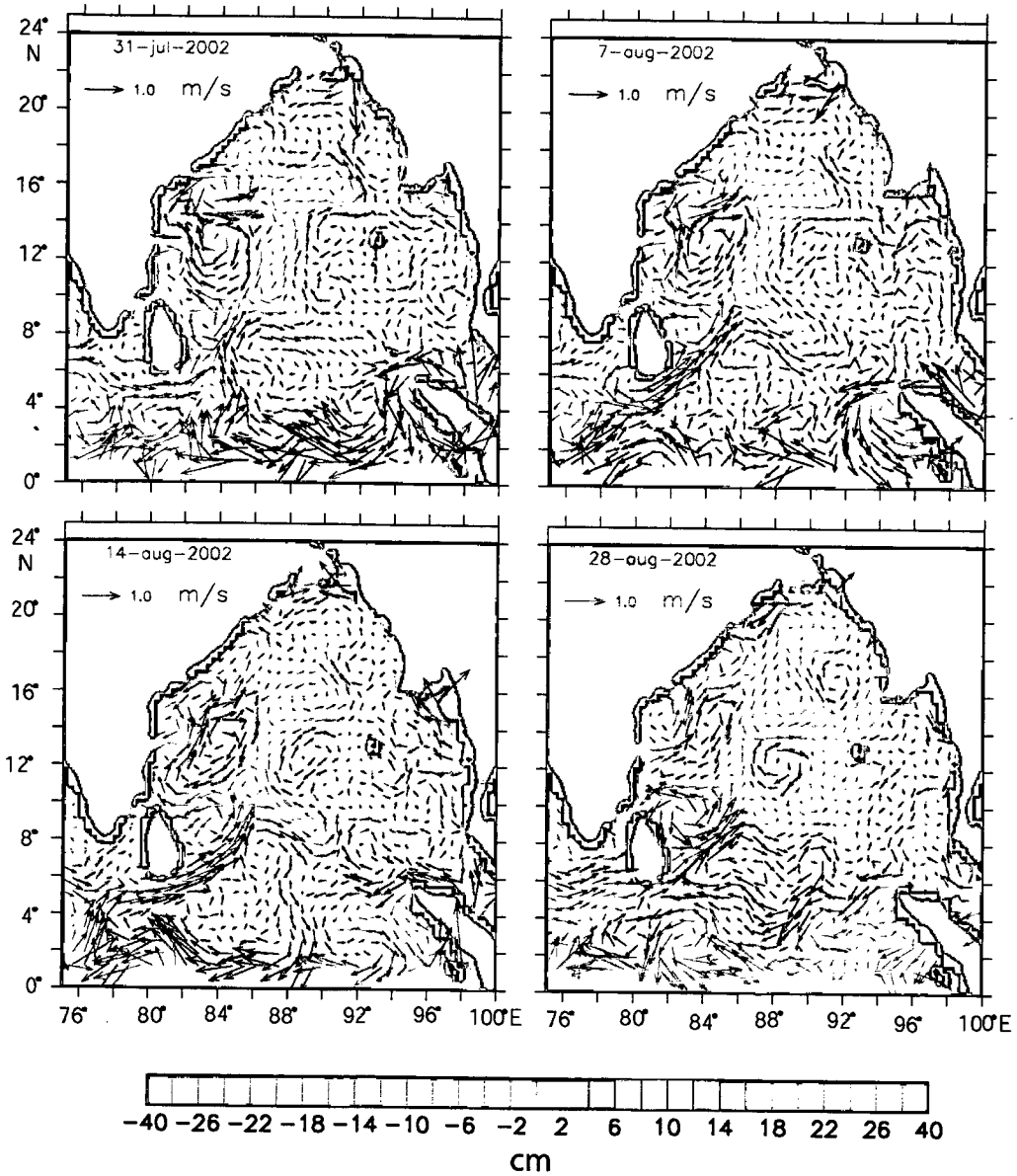

Figure 4.3.2.3.2 7-day snap-shots of Topex/Poseidon ERS1/2 merged sea-level anomalies overlaid with geostrophic velocities during August 2002.

4.3.3. Spring intermonsoon 2003

4.3.3.1. Cyclonic eddy centered at 11°N (CESP1)

Signatures of a cyclonic circulation could be seen centered about 11°N 90.5°E by first week of April 2003 (CESP1) (Figure 3.3.1.3, top left). During this time CESP1 was

characterized by a SLA of −10 cm and geostrophic velocity anomaly of ~25 cm/s. This translated westward and was sampled on 19th April (Figure 3.3.1.3, bottom left). This feature disappeared completely by the end of April 2003 (Figure 3.3.1.4, top left).

4.3.3.2 Anticyclonic eddy centered at 13°N (ACSP2)

An anticyclonic circulation (ACSP2) was developed centered about 15°N and 91.5°E by third week of February 2003 (Figure 3.3.1.1) with a positive SLA of 8 cm and geostrophic velocity anomaly of ~25 cm/s. Subsequently it moved southwestward and intensified by early April (Figure 3.3.1.3, top left). During this time it was centered at 14°N and 90°E and characterized by a SLA of 12 cm and geostrophic velocity anomaly of ~30 cm/s. By the end of April, ACSP2 moved southwest ward and reached 88°E. During the time of sampling its center was located at 13.5°N and 88.5°E. ACSP2 later merged with the large scale positive sea-level anomaly (figure 3.3.1.4, bottom left).

4.3.3.3 Cyclonic eddy centered at 16°N (CESP3)

A cyclonic circulation was formed with its centre at 17.5°N 93°E during the first week of Jan 2003 (CESP3) (Figure 4.3.3.3.1). This was characterized by a SLA of -16 cm and geostrophic velocity anomalies of about 25 cm/s. West to this negative SLA, prominent anticyclonic circulation was seen. After formation, CESP3moved westwards and reached 92°E by third week of January 2003. As it continued its westward movement it elongated meridionally during February (Figure 3.3.1.1) and reduced its meridional extent during March (Figure 3.3.1.2). By the end of March CESP3 was located at 17°N 89°E with an SLA of -14 cm and with geostrophic velocity anomaly of about 25 cm/s.

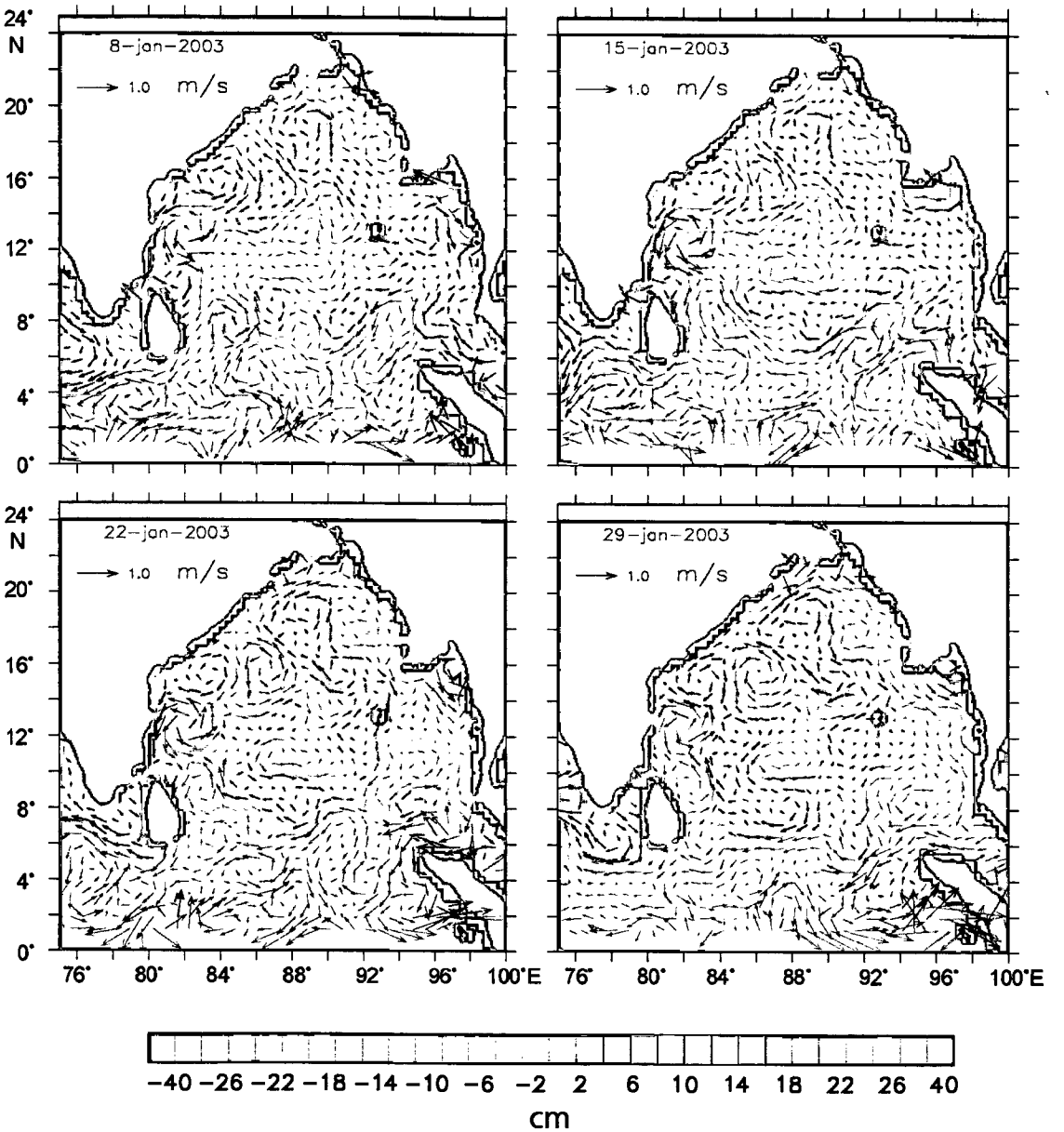

Figure 4.3.3.3.1 7-day snap-shots of Topex/Poseidon ERS1/2 merged sea-level anomalies overlaid with geostrophic velocities during January 2003.

The eddy showed a prominent southwestward translation during March possibly because of the southward flow associated with the anticyclonic circulation to its west. It was centered at 16°N 89°E during 23 April 2003, when eddy was sampled from the ship (Figure 3.3.1.3). It moved southwestward and coalesced with the northern coastal eddy (NCE) by the third week of May.

4.3.3.4. Cyclonic eddy centered at 19°N (CESP4)

The observed cyclonic circulation (CESP4) in the temperature/salinity field centered at 19°N was found to be formed during second week of April 2003 (Figure 3.3.1.3). This was centered at 19.75°N and 89.5°E and was characterized by SLA of -16 cm and geostrophic velocity anomay of 25cm/s. This moved westwards and was centered at 19°N 88°E by third week of April. By first week of May this was intensified and was found to have a SLA of -40 cm and geostrophic velocity anomaly of 40-50 cm/s Figure 3.3.1.4). CESP3 further moved westward and reached the east coast by second week of July.

4.4. Mechanisms of generation

In the previous sections 10 eddies have been delineated and their evolution described based on the thermohaline structure as well as sea-level anomaly maps. From the analysis of hydrographic data during summer, fall intermonsoon and spring intermonsoon as well as the sea-level anomaly maps during 2001 to 2003 it has been found that eddies are ubiquitous in the BOB. A synopsis of the ten eddies studied in the previous sections of this chapter is given in the following Table.4.4.1. In chapter 3 (section 3.4) generating mechanism of eddies from the western boundary current has been examined. In the open BOB no such strong current exists any time of the year, except in the south during summer monsoon. In summer the southwest monsoon current enters the southern BOB via south of Sri Lanka as a strong and narrow jet (Figure 1.2.5). However, unlike the generation of NCE from the WBC, the formation

Table.4.4.1 Synopsis of the eddies encountered along central (88°E) BOB track during 2001 July to 2003 April obtained from the thermohaline structure and confirmed by satellite derived sea-level anomaly data .

Name of eddy	Time and year of formation	Location of formation	Type of eddy	Lifespan (months)
CESP3	January 2003	17.5°N, 93°E	Cyclonic	5
ACPS2	February 2003	15°N, 91.5°E	Anticyclonic	2
CESP1	April 2003	11°N, 91°E	Cyclonic	1
CESP4	April 2003	19.75°N, 89.5°E	Cyclonic	4
CES2	May 2001	15°N, 89.5°E	Cyclonic	3
CES3	May 2001	18.5°N, 91.5°E	Cyclonic	3
CES1	June 2001	9°, 87°E	Cyclonic	1
CEF3	June 2002	17°N, 91°E	Cyclonic	2
ACF2	August 2002	Western Andaman Sea	Anticyclonic	3
CEF1	September 2002	9.5°N, 87°E	Cyclonic	1

of CES1 and CEF1 was not associated with any meander in this jet (Figure 3.3.2.5 & Figure 3.3.3.1, and also see Figure 4.3.2.3.2). The factors responsible for the generation of eddy in the open BOB could be (1) direct atmospheric forcing, (2) topographic effect, and (3) breaking of Rossby waves [*La Casce and Pedlosky*, 2004; *Chelton et al.*, 2007]. Since all the eddies discussed above were found to occur in the upper 500 m of the water column, well away from the influence of the bottom topography, the possibility of topographic effect in generating these eddies may be discounted. In order to examine the role of direct wind forcing in the generation of eddies, the curl of the wind-stress was examined. In summer monsoon the curl of the wind-stress during June is positive (Figure 4.4.1). This large-scale cyclonic wind-stress curl drives the formation of SLD [*Vinayachandran et al.*, 1998]. During the same period, the downwelling Rossby wave propagates from eastern BOB towards west [*Sengupta et al.*, 2001] and could be located at ~ 90°E in the sea-level anomaly map as a high (Figure 3.3.2.5). Thus, the juxtaposition

of the cyclonic wind-stress curl driving the colder water towards the surface and the anticyclonic circulation

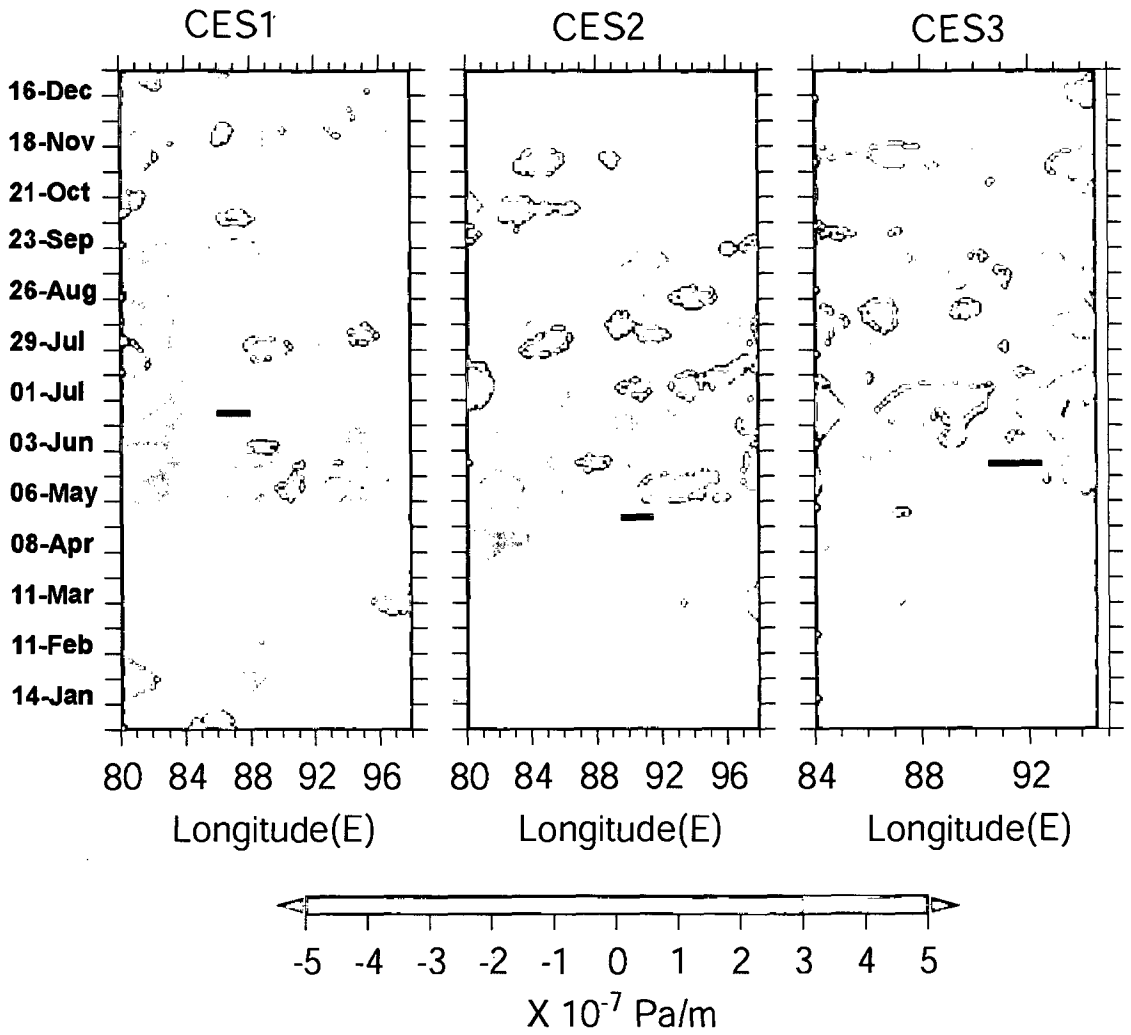

Figure 4.4.1 Curl of wind-stress obtained from QuickSCAT wind-stress (see chapter 2 for details) at the latitude of formation of eddies CES1(9°N), CES2 (15°N), and CES3 (18.5°N) for 2001. Thick horizontal line indicates the location and approximate zonal dimension of eddy.

associated with the Rossby waves driving the warm surface waters towards deeper levels, creates a strong horizontal density gradient leading to vertical shear, a necessary condition for the generation of baroclinic instability. Hence, it would seem that the formation of CES1 in June 2001, as inferred from the time evolution of sea-level

anomaly maps and the wind-stress curl, was linked to this process. The plausible mechanism of generation of CES2 and CES3 in the north (~15°N & 18.5°N) during May 2001 is the following. At both these locations a strong positive sea-level anomaly adjacent to a weak negative sea-level anomaly was noticed (Figure 3.3.2.4). The wind-stress curl changed from negative to positive at the locations of CES2 and CES3 at the first and last week of May 2001 respectively (Figure 4.4.1). This cyclonic wind-stress curl augments the negative sea-level anomaly which in turn can intensify the horizontal density gradient and can lead to vertical shear leading to baroclinic instability, and generates the cyclonic eddy.

During the formation of CEF1 in September 2002, though the wind-stress curl was anticyclonic (Figure 4.4.2), the negative sea-level anomaly associated with SLD was most intense (-40 cm). Adjacent to SLD, a strong positive sea-level anomaly (25 cm) associated with the Rossby wave propagation was also seen (Figure 3.3.3.1). Thus, it appeared that the strong horizontal density gradient necessary for the formation of cyclonic eddy in September 2002 arises due to the strong upward pumping of colder waters by the SLD and downwelling of warmer surface waters under the influence of anticyclonic circulation associated with Rossby waves. This condition was similar to that of the formation of CES1, except that the wind-stress curl in the latter case was cyclonic and strength of SLD was much weaker.

The formation of ACF2 in July 2002 can be explained in the context of curl of the wind-stress and sea-level anomaly. During the formation of the anticyclonic eddy (ACF2) in the mid of July, curl of the wind-stress was negative (Figure 4.4.2) and the sea-level

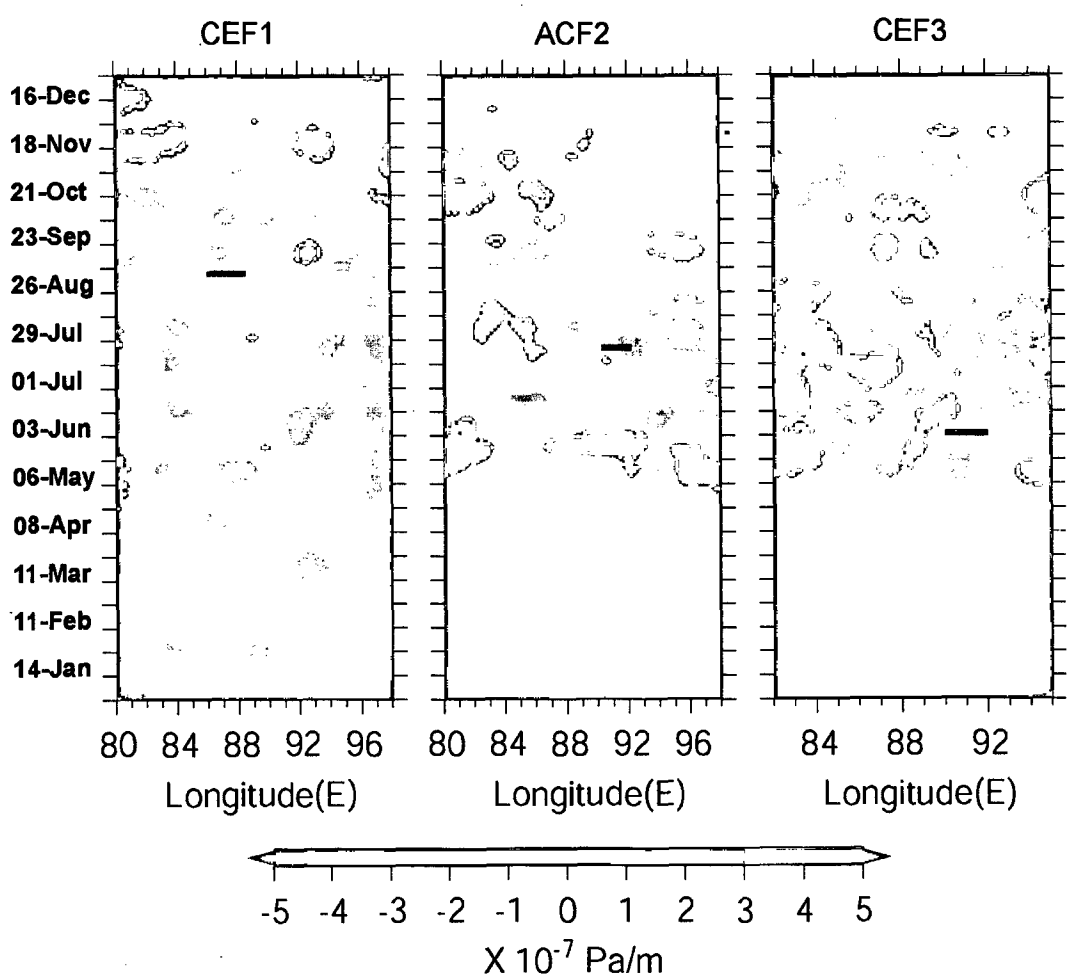

Figure 4.4.2 Curl of wind-stress obtained from QuickSCAT wind-stress (see chapter 2 for details) at the latitude of formation of eddies CEF1(9.5°N), ACF2 (13.5°N), and CEF3 (17°N) for 2002. Thick horizontal line indicates the location and approximate zonal dimension of eddy.

anomaly was positive (Figure 4.3.2.3.2). However, towards the west of the positive sea-level anomaly a negative sea-level anomaly was noticed. Thus, the zonally organized positive and negative sea-level anomaly drives a horizontal gradient in density field and the anticyclonic wind-stress curl further augments the positive sea-level anomaly, there by creating the necessary instability for the generation of the ACF2.

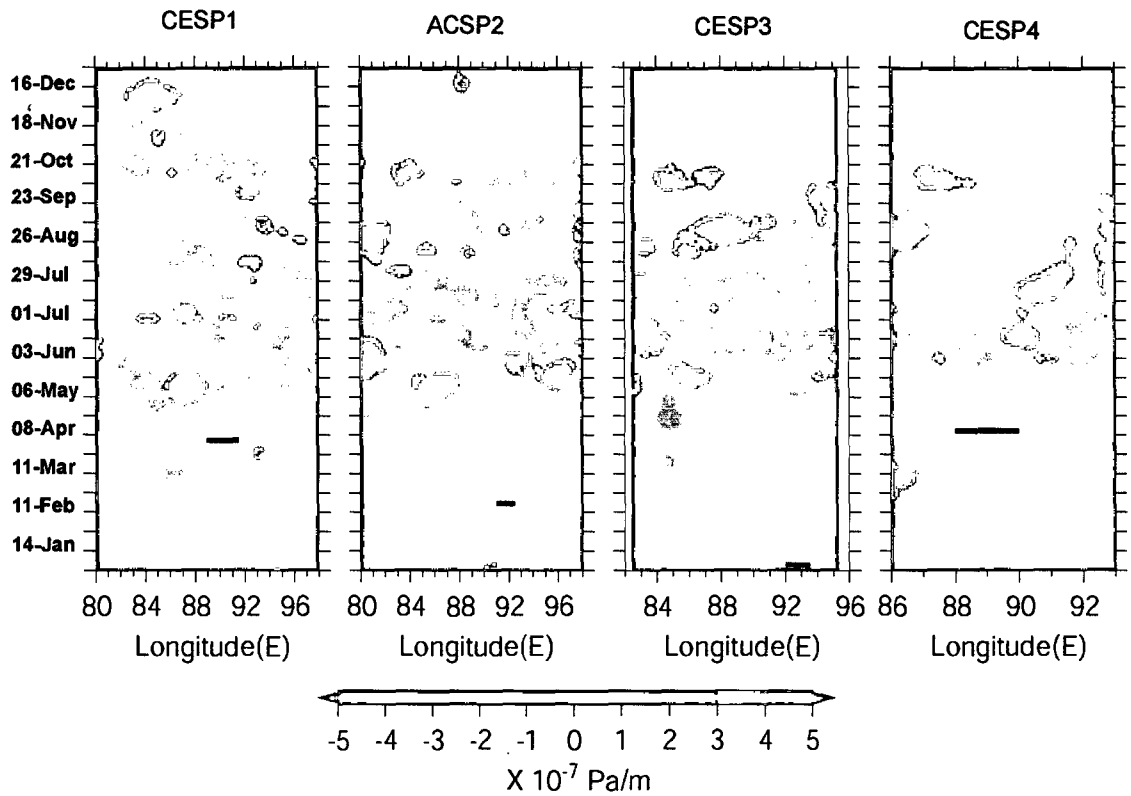

Figure 4.4.3 Curl of wind-stress obtained from QuickSCAT wind-stress (see chapter 2 for details) at the latitude of formation of eddies CESP1 (11°N), ACSP2 (15°N), CESP3 (17.5°N), and CESP4 (19.75°N) for 2003. Thick horizontal line indicates the location and approximate zonal dimension of eddy.

In the case of CEF3, the condition that existed during the formative period is the following. At the latitude where CEF3 was developed, a negative sea-level anomaly co-existed with positive sea-level anomaly to its east. Note that the magnitude of the negative sea-level anomaly is small (Figure 4.3.2.3.1). This condition could give rise to a horizontal density gradient in the zonal direction. However, the anticyclonic wind-stress

curl at this time near the generating region of CEF3 (Figure 4.4.2) would decrease the gradient by weakening the negative sea-level anomaly. Hence, it is not clear what would have caused the generation of CEF3. The condition is similar to that existed during the formation of CES3, except that the wind-stress curl was augmenting the negative sea-level anomaly.

The wind-stress curl in the region of formation of CESP1, ACSP2, CESP3 and CESP4 was weakly negative (0 to -1 x 10^{-7} Pa/m) during January to April (Figure 4.4.3). During this period propagation of an upwelling Rossby wave was discernible in the form of low sea-level anomaly (Figure 4.4.4). This would induce a cyclonic vorticity into the water column which is acted upon by a weak anticyclonic wind-stress curl. Thus it is not possible to attribute an instability mechanism based on the action of wind-stress curl and propagating Rossby wave during January till April 2003. This warrants other mechanisms such as breaking of Rossby waves [*La Casce, 2004, Isachsen et a.,l 2006*] to explain the eddy formation in the open waters of the BOB. An examination of the time-latitude plot of the sea-level anomaly, where the CESP3 and CESP1 were generated, showed that the Rossby wave propagation is not continuous (Figure 4.4.4), which could be an indication of this.

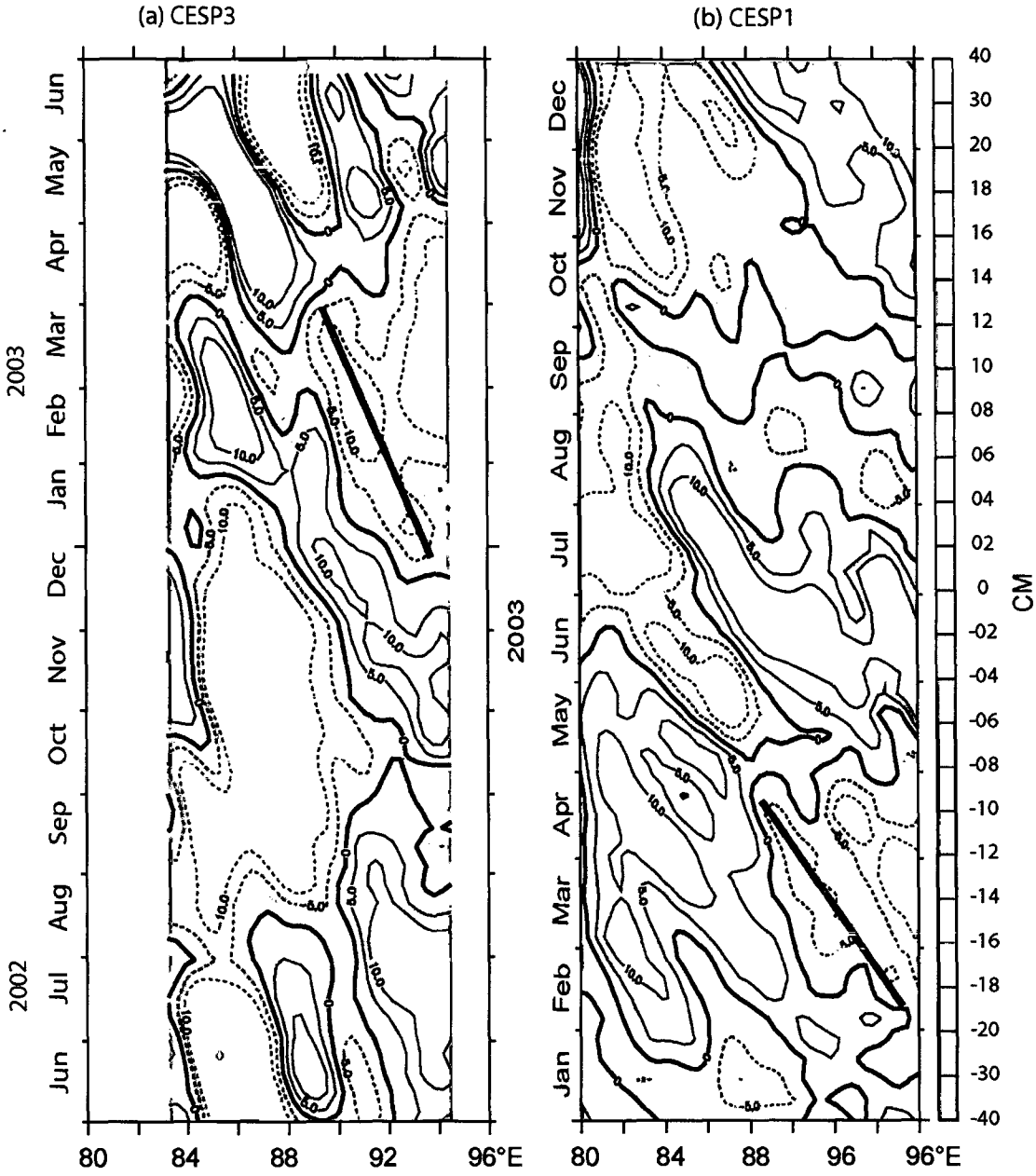

Figure. 4.4 4. Rossby wave propagation at the location of formation of (a) CESP3 (17.5°N) and (b) CESP1 (11°N).

4.5 Summary

Based on the thermohaline structure along the central BOB 10 mesoscale features (both cyclonic and anticyclonic eddies) were identified and confirmed with the satellite derived sea-level anomaly maps. These eddies changed the ambient temperature by about 2°C.

However, the changes in the salinity field due to these eddies were much smaller, < 1 psu. In the north, where the influence of river discharge dominates, the eddy was confined below the strongly stratified upper layer. The life span of eddies varied from a month as in the case of southern eddies to about 4-5 months as in the case of cyclonic eddy during spring intermosoon in the north (CESP3).

The time evolution of these eddies based on sea-level anomaly maps showed that, in general, they originated east of the central BOB transect and moved in a westward direction. However, the eddy encountered in the SLD region, was found to be generated locally. Unlike their coastal counterparts, eddies encountered in the open waters of the BOB were not formed from any meander of current. It has been found that direct wind forcing alone cannot explain the formation of all eddies. The generation of eddy in most of the observed 10 cases could be explained in the context of the interaction between the wind-stress curl and propagating Rossby wave. In the southern BOB, during summer and fall intermonsoon the upward pumping of cold and high salinity waters within the Sri Lanka dome (SLD) under the influence of cyclonic wind-stress curl and the sinking of warm and low salinity waters under the influence of high sea-level anomaly (Rossby wave) creates the necessary horizontal density gradient to cause baroclinic instability and generate cyclonic eddy. In the northern BOB, during summer monsoon, CES2 and CES3 was generated under the presence of cyclonic wind-stress curl acting upon the existing large-scale positive and negative seal-level anomaly. The large scale positive and negative sea-level anomaly preconditions and creates initial zonal gradient in density and the action of cyclonic wind-stress curl provides the necessary trigger for the instability

and generation of eddy. This large scale positive and negative sea-level anomaly may arises due to several reasons. In the case of CES2 it was the propagating upwelling Rossby wave and the anticyclonic circulation to its west, while in the case of CES3 it was the coastally trapped Kelvin wave in the eastern region and the relatively weak negative sea-level anomaly to the west. During fall intermonsoon the generation ACF2 is similar to that of CES2 with the difference that a positive sea-level anomaly (downweling Rossby wave) towards the east and negative sea-level anomaly towards the west. The wind-stress curl at the location of eddy changes to anticyclonic. In the spring intermonsoon, the wind-stress curl and the sea-level anomaly created by the propagating Rossby wave cannot explain the generation of observed eddies.

Chapter 5 - Role of eddies in hydrography and circulation

5.1. Introduction

Examination of thermohaline structure and the satellite sea- level anomaly in the previous chapters showed that eddies are ubiquitous in the BOB. Thermohaline structure showed that the isopycnals can be displaced significantly within the eddy. This result in increase/decrease of temperature (average of 2°C, in case of NCE 2003 this was 6°C) and salinity (~0.3 to 1 psu) at the locations of anticyclonic and cyclonic eddies. Evolution of these features studied using satellite sea-level anomalies showed that they have a life span of 1-5 months. In all ten such eddies in the open ocean, three during summer monsoon- CES1(9°N), CES2 (16°N), CES3(19°N), three during fall intermonsoon- CEF1(10°N), ACF2 (12°N), CEF3(14°N) and four during spring intermonsoon- CESP1 (11°N), ACSP2(13°N), CESP3 (16°N) and CESP4 (19°N), have been studied. In addition 5 cyclonic eddies were identified along the western boundary, 2 (NCE & SCE) each during spring and fall intermonsoons and one in summer (NCE). The aim of this chapter is to examine the impact of eddy-induced changes in heat and salt content and transport. Heat and salt content were calculated as $\iint \rho CpT \, dz \, dy$ and $\iint \rho S \, dz \, dy$ respectively, where ρ=1023 kg/m^3 , Cp = 4187 J/Kg/C, T is the temperature and S salinity. In addition to this heat and salt content anomaly also was calculated using $\iint \rho Cp(T-Tr) \, dz \, dy$ and $\iint \rho(S-Sr) \, dz \, dy$, where Tr and Sr are climatological monthly mean corresponding to the time period of observation obtained from WOA01 climatology [*Conkright et al., 2002*]. The volume transport was estimated as $\iint v \, dz \, dy$, while the heat and salt transport by $\iint v \, \rho CpT \, dz \, dy$ and $\iint v \, \rho S \, dz \, dy$ respectively, where v is the cross track velocity, dz and dy are the depth interval and along-track station spacing.

The uncertainty associated with the temperature and conductivity measurements are 0.001°C and 0.0003 S/m respectively. This would translate into an error of 0.003 psu in salinity measurements and would result in an error of approximately 1.7 cm/s in velocity in the south and about 1 cm/s in the north. When integrated over the top 150 m, this would result in an error of ~ 0.2 Sv (Sv=10^6 m^3/s) in volume computations. The errors in the temperature and salinity would result in an error of ~ 7 x 10^{10} J/m and 5 x 10^4 Kg/m in the heat and salt content respectively, which are ~4-5 orders of magnitude less than the variability.

The Ekman transport along the transects was also computed to examine the wind-driven part of the volume transport. The wind for this purpose was taken from the surface meteorological data collected onboard at stations. The methodology of Ekman transport computation is described in chapter 2. As the geostrophic volume transport yields only the cross-track component, in the case of the Ekman volume transport also only across-track component is presented. Along the central BOB track this is $\int(\tau_y/\rho f)dy$ where τ_y is the meridional component of the wind stress dy the distance between the stations ρ, and f mean sea water density for upper 150 m of water column and the corioilis parameter respectively. However, along the western boundary between 19°N and 15°N τ_y is rotated to about 45 degrees anticlockwise since the cruise track is roughly oriented in a northeast-southwest direction in this region. The results obtained are summarized in the following section.

5.2. Results

Heat content along the central BOB and western boundary are presented in Figure 5.2.1. and Figure 5.2.2. In general, the heat content integrated over 150 meters in the central

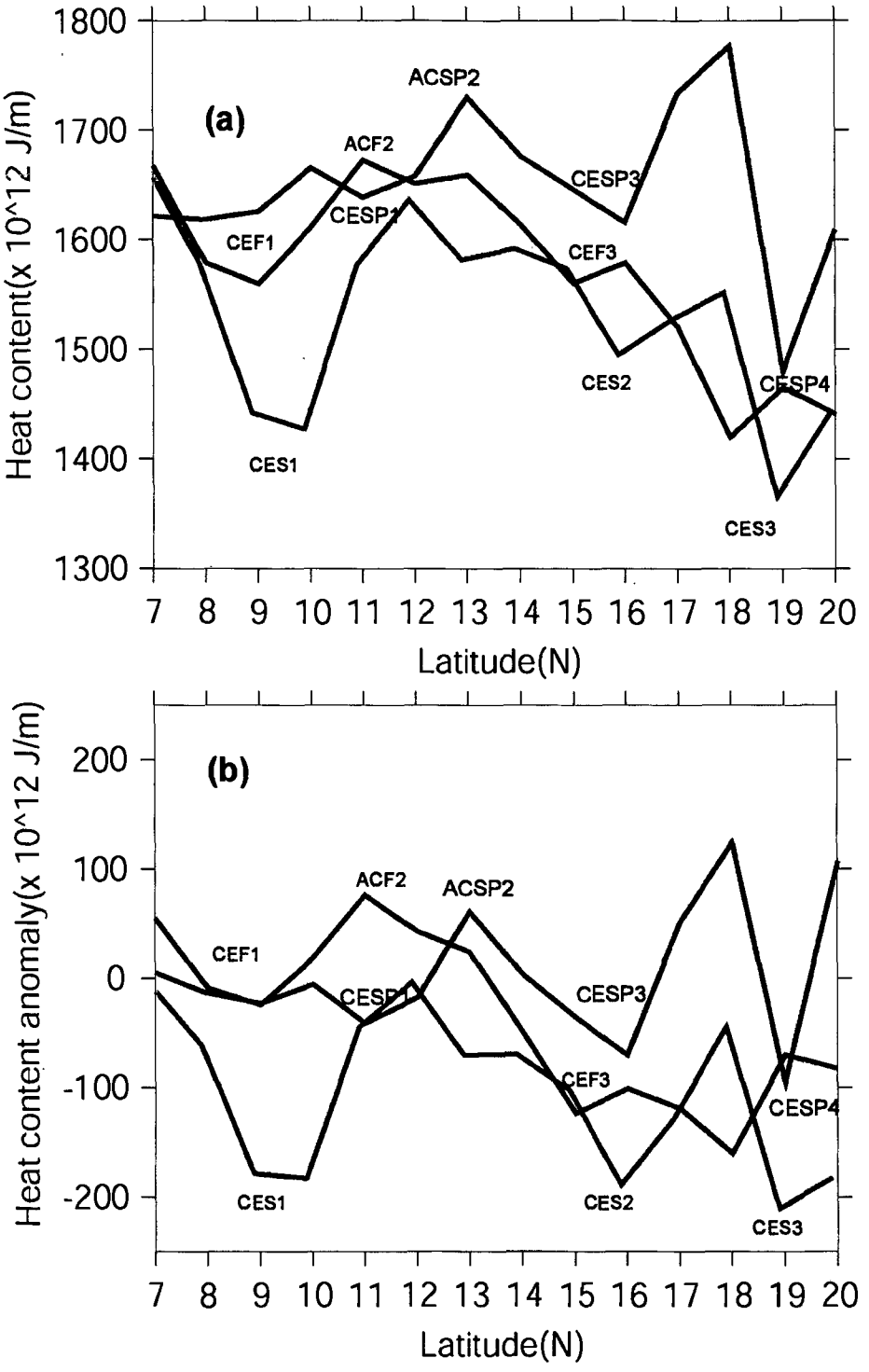

Figure 5.2.1. (a) Heat content and (b) heat content anomaly along the central (88°E) during ——summer monsoon,——fall inter-monsoon,—— spring intermonsoon

BOB showed a northward decrease of about $200x10^{12}$ J/m (Figure 5.2.1a), except during spring intermonsoon. Apart from this general south – north decrease, the heat content varied dramatically at locations where the presence of eddies were identified in the earlier chapters. During summer monsoon a heat content deficit of about 200 x 10^{12} J/m (Figure 5.2.2) was encountered at the location of cyclonic eddies CES1, CES2 and CES3. During fall intermonsoon, however, the heat content deficit exhibited by the cyclonic eddies was much smaller, ~ 50 x 10^{12} J/m for CEF1 and ~ 100 x 10^{12} J/m for CEF3. In the case of anticyclonic eddy ACF2 the heat content increased by about 100 x 10^{12} J/m. The general south – north decrease in heat content found during summer and fall intermonsoon was not discernable during spring intermonsoon. Again, unlike that during summer and fall intermonsoon, the heat content during spring intermonsoon did not exhibit any significant variability in the south (south of 15°N), except that eddy ACSP2 has increased the heat content by about 50 x 10^{12} J/m. In the north the heat content deficit associated with cyclonic eddy CESP3 and CESP4 were ~ 70 and 100 x 10^{12} J/m respectively. The northward decrease in the heat content during summer and fall intermonsoon is associated with the general northward shoaling of isotherms along with the occurrence of cyclonic eddies which dominate the thermohaline structure. Another striking feature is an increase of ~ 150 x 10^{12} J/m in the heat content at 18°N associated with an anticyclonic circulation as inferred from the SLA. The heat content along the western boundary did not show any definite south-north trend as in the case of the central BOB. However, in spring intermonsoon the heat content showed a southward decrease of about 150 to 200 x 10^{12} J/m (Figure 5.2.2). The most prominent feature in the heat content distribution in any season is the heat loss in the north (north of 16°N) in the upper 150 m under the influence of the cyclonic eddy NCE and heat gain in the south associated with high SLA.

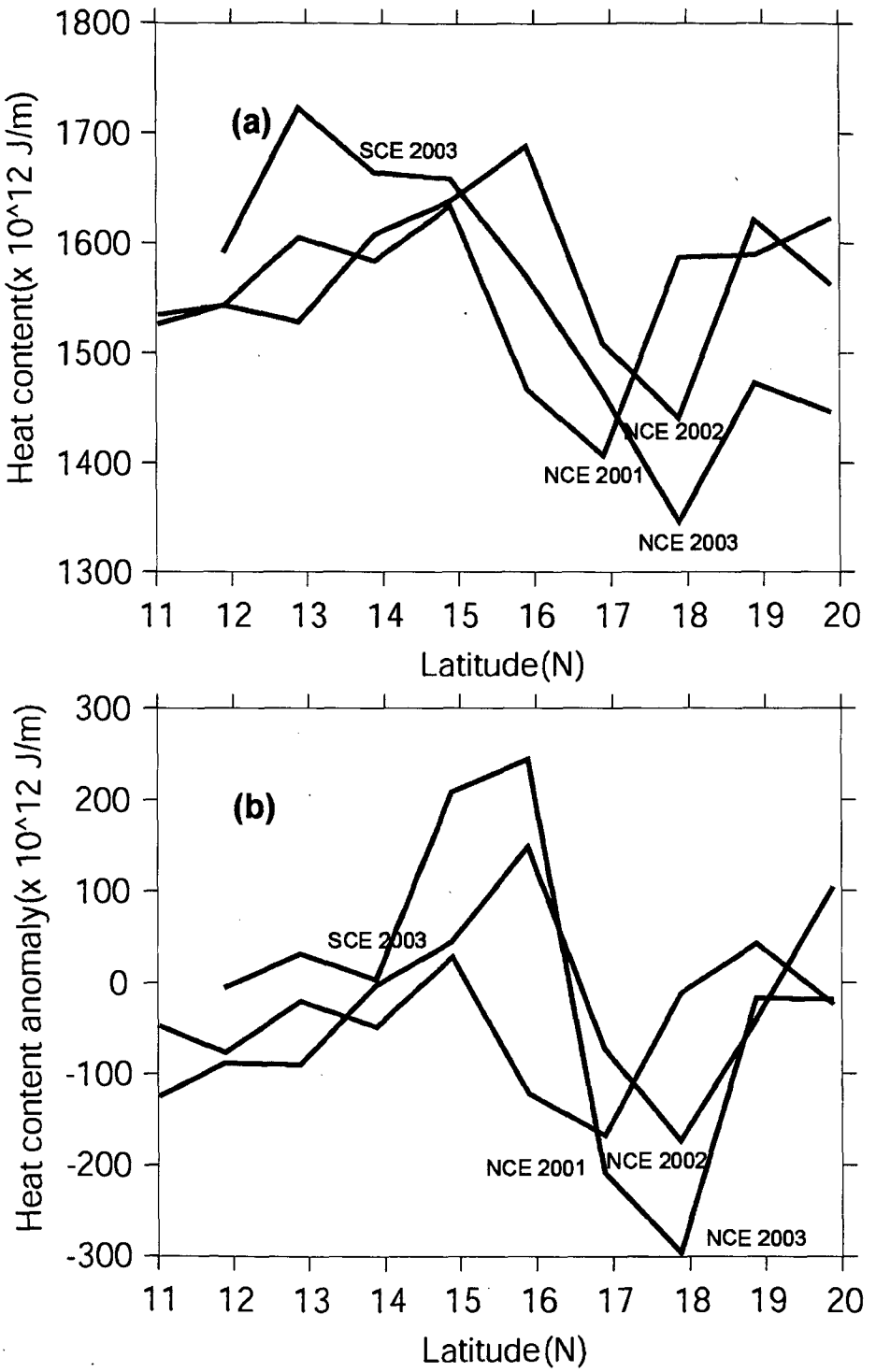

Figure 5.2.2. (a)Heat content and (b) heat content anomaly along the Western boundary BOB during ——Summer monsoon, ——Fall intermonsoon and ——Spring intermonsoon.

Note that both heat gain and heat loss is almost of the same magnitude. Thus, along the western boundary, the cyclonic eddy NCE which is seen in the SLA in all the 3 seasons reduced the heat content of the upper water column. The gain in the heat content in the north during spring intermonsoon was associated with the large-sale circulation while that in summer and fall intermonsoon was associated with anticyclonic circulation which was the reminiscent of spring intermonsoon.

The salt content in the central BOB showed a progressive decrease from south to north in all the 3 seasons, except during spring where an increasing trend was noticed towards the north from 16°N onwards (Figure 5.2.3). The salt content during summer and fall intermonsoon was about 5 to 10 x 10^6 kg/m higher than that during spring intermonsoon in the south. However, towards the north (north of 16°N) salt content did not show much variability with season. The salt content anomaly predominantly showed the variability associated with eddy. The eddy-induced variability was highest during spring intermonsoon followed by fall intermonsoon. The northward increase of salt content anomaly (~20 x 10^6 kg/m) during fall intermonsoon was the effect of fresh water. However, the magnitude of the anomaly appears to be too large and it is because the WOA 2001 salinity is too fresher.

The salt content along the coast also showed a southward decrease, but only during summer and fall intermonsoon [Figure 5.2.4]. In spring intermonsoon no definite south-north trend was discernible. Two regions of large variability was noticed one centered at

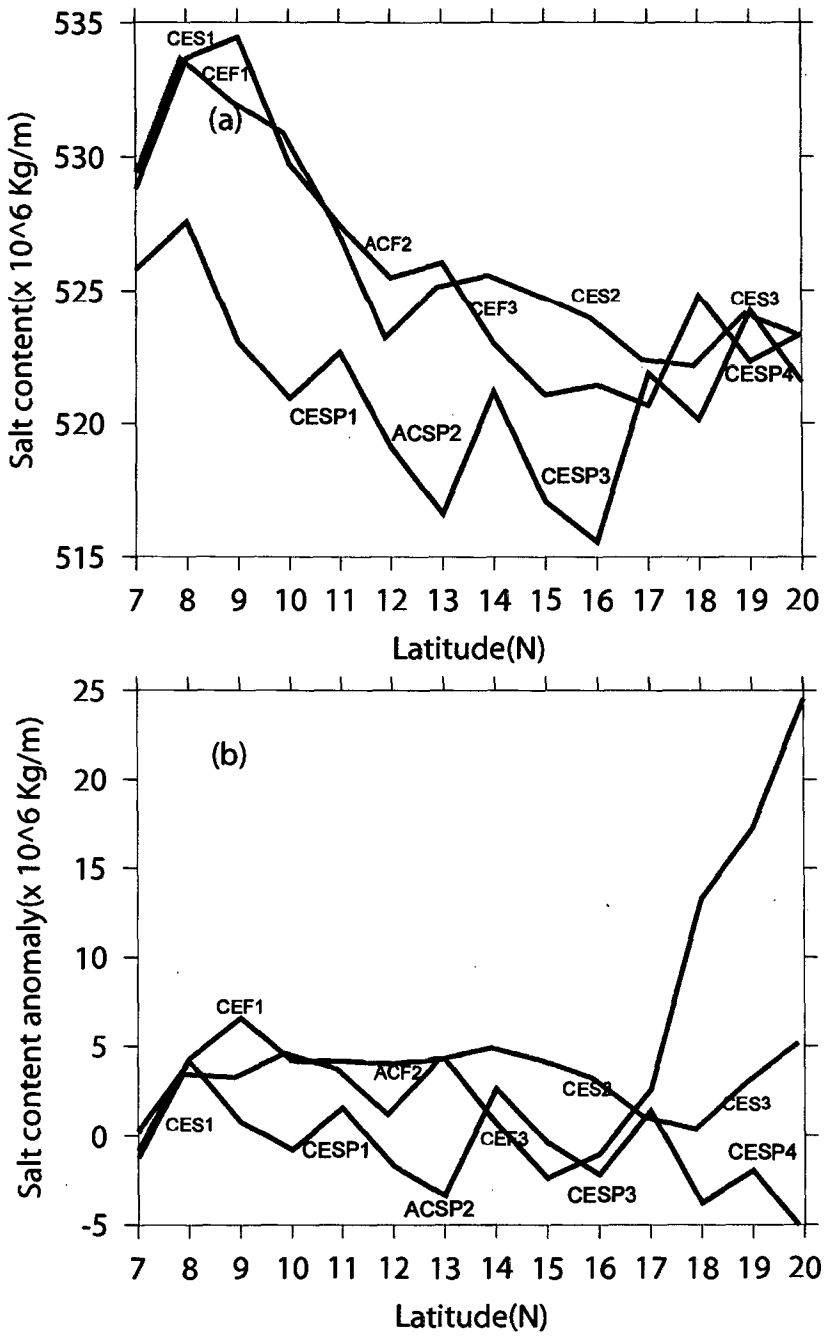

Figure 5.2.3. (a)Salt content and (b) salt content anomaly along central (88°E) BOB during —— Summer monsoon —— Fall intermonsoon and ——Spring intermonsoon.

13°N and the other one at 17°N. From the salt content anomaly it is clear that eddy-induced variability was of lesser magnitude, unlike that manifested in the heat content anomaly. The reason for this lies in the fact that these cyclonic eddies are subsurface

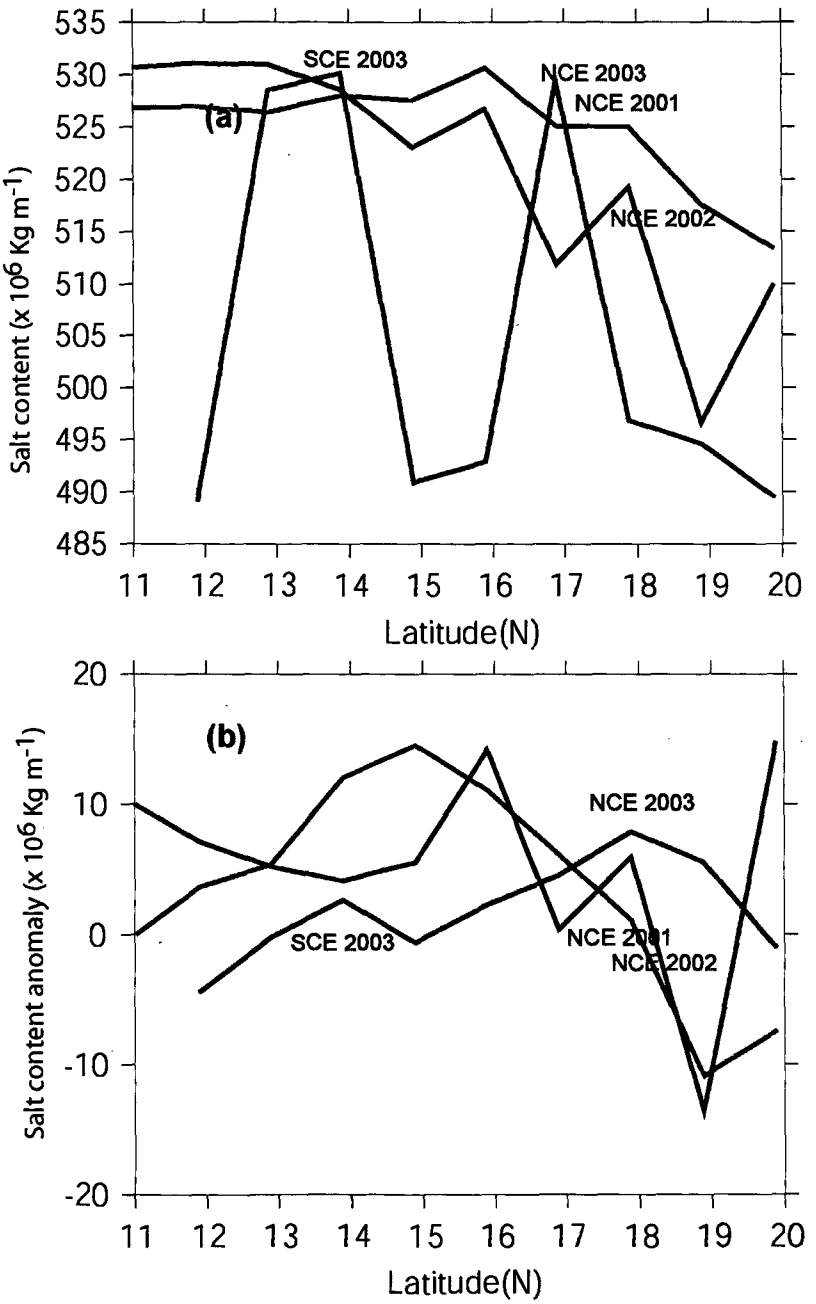

Figure 5.2.4. (a)Salt content and (b) salt content anomaly along western boundary of BOB during ___ Summer monsoon ___ Fall intermonsoon and ___ Spring intermonsoon.

features and lies below the upper halocline. Hence the up/down sloping of isohalines will not induce larger changes in the salt content of the water column due to eddy-pumping. During summer and fall intermonsoon the fresher water layer extends up to 15-16°N, while during spring intermonsoon it is confined to the north. Thus, the eddy-induced

changes were more pronounced in the heat content changes rather than salt content changes and the reason for this lies in the characteristics of the BOB.

Apart from the eddy-induced vertical motions and associated changes in the heat and salt contents, there can also be changes in the water column due to horizontal advection of water. To understand this, volume transport along the central and western boundary of the BOB was computed and discussed below.

Volume transport due to wind-driven Ekman drift was much smaller compared (Figure 5.2.5 a & c) to the transport due to geostrophic currents, both along the central and the western boundary (Figure 5.2.5 b & d). The geostrophic volume transport (zonal) showed alternate bands of eastward and westward transports along the central BOB track (Figure 5.2.5d). These alternating bands are associated with the cyclonic/anticyclonic circulation of eddies as could be seen from their location. During summer monsoon enhanced transport of 7 Sv eastward and 5 Sv westward was noticed between 8 and 10°N. Another major fluctuation in the volume transport was noticed between 18 and 20°N. Both these locations coincides with the locations of eddies CES1 and CES3. During fall intermonsoon the eastward transport associated with CEF1 located at 9°N was less compared to the summer monsoon period. However, the westward transport was comparable to that of summer. Enhancement of transport can also be seen between 12 and 13°N, and 14 and 15°N, both coinciding with the location of eddies ACF2 and CEF3

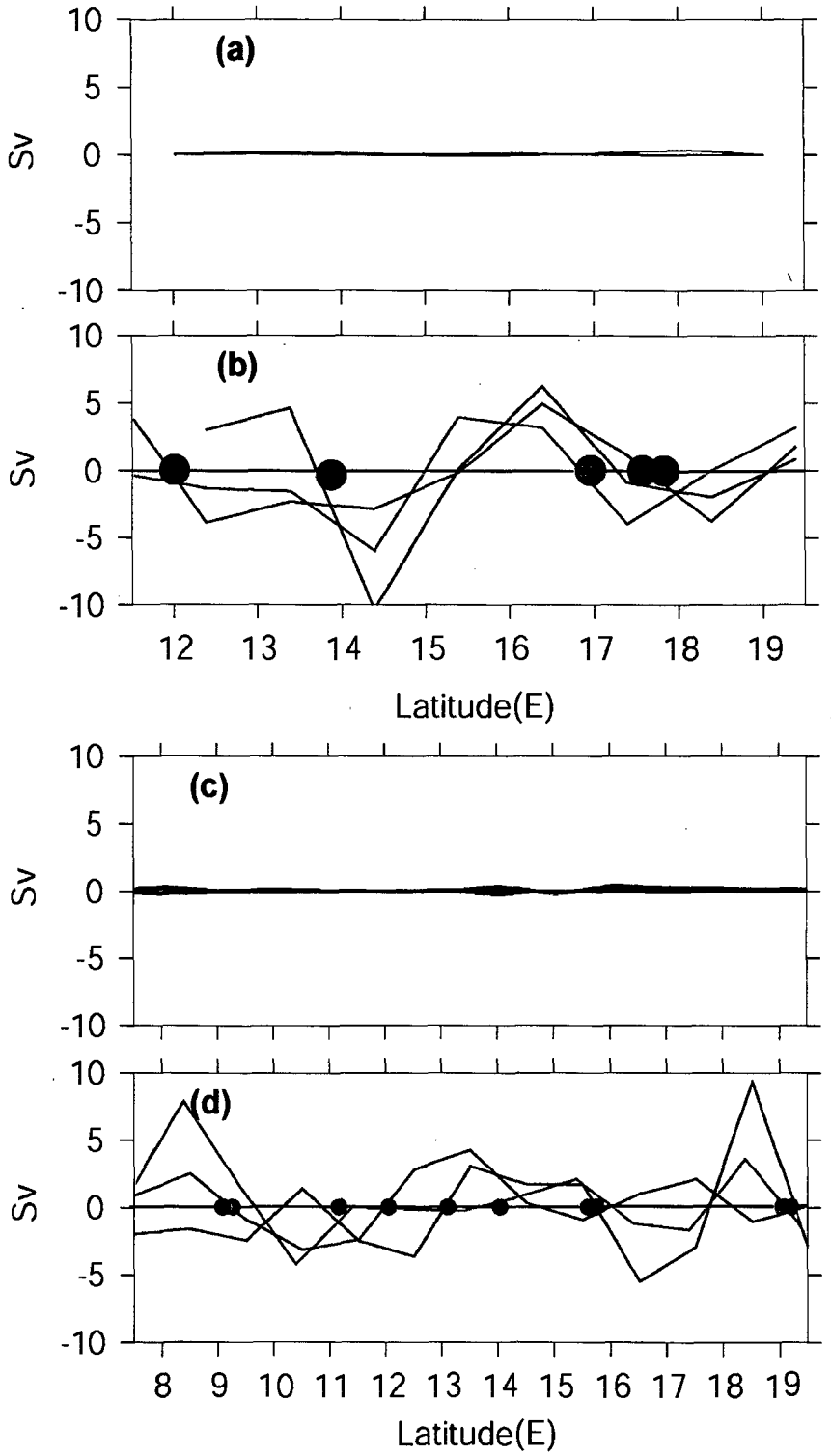

Figure 5.2.5. Volume transport integrated upto 150 m along central BOB(d), along the western boundary (b) along with the ekman transport along central BOB(c) and along the western boundary (a) during —— summer monsoon, —— fall intermonsoon and ——spring inter monsoon. coloured circles indicate the centres of eddies during each season.

respectively. During spring intermonsoon, an increase in transport was found in the north between 18 and 20°N coinciding with the location of CESP4. Here the eastward transport was higher (~8 Sv) than the westward transport (~3 Sv). Another fluctuation in transport can also be found between 15 and 17°N coinciding with the location of CESP3. Along the coast (Figure 5.2.5b) also fluctuations can be seen w.r.t the center of NCE which had an eastward transport during spring (~2 Sv) and fall (~3 Sv) intermonsoons.

Another enhanced region of westward transport was found between 14 and 15°N during spring intermonsoon and summer. During spring intermonsoon this was associated with an anticyclonic circulation, which later developed into an anticyclonic eddy (see figure 3.3.1.4). There was another large variability in volume transport in the north between 13 and 14°N, associated with cyclonic eddy SCE. During summer also this onshore transport was noticed because of another anticyclonic circulation which persisted in the BOB from spring intermonsoon 2001 onwards (see figures3.3.2). Thus, during all the seasons the geostrophic transport was dominated by eddies.

The heat and salt transport also followed the pattern of high variability (Figure 5.2.6) seen in the volume transport associated with eddies. The maximum heat transport in the open ocean transect (Figure 5.2.6b) was in the vicinity if CES1, CES3 during summer, and CESP4 in spring intermonsoon. CES1 had an eastward transport of about 600 x 10^{12} J/m/day and a westward transport of about 300 x 10^{12} J/m/day, where as CES3 had an east ward and westward transport of about 300 and 100 x 10^{12} J/m/day respectively. In summer, the cyclonic eddy CES2 had an almost equal eastward and westward transport of 100 x 10^{12} J/m/day.

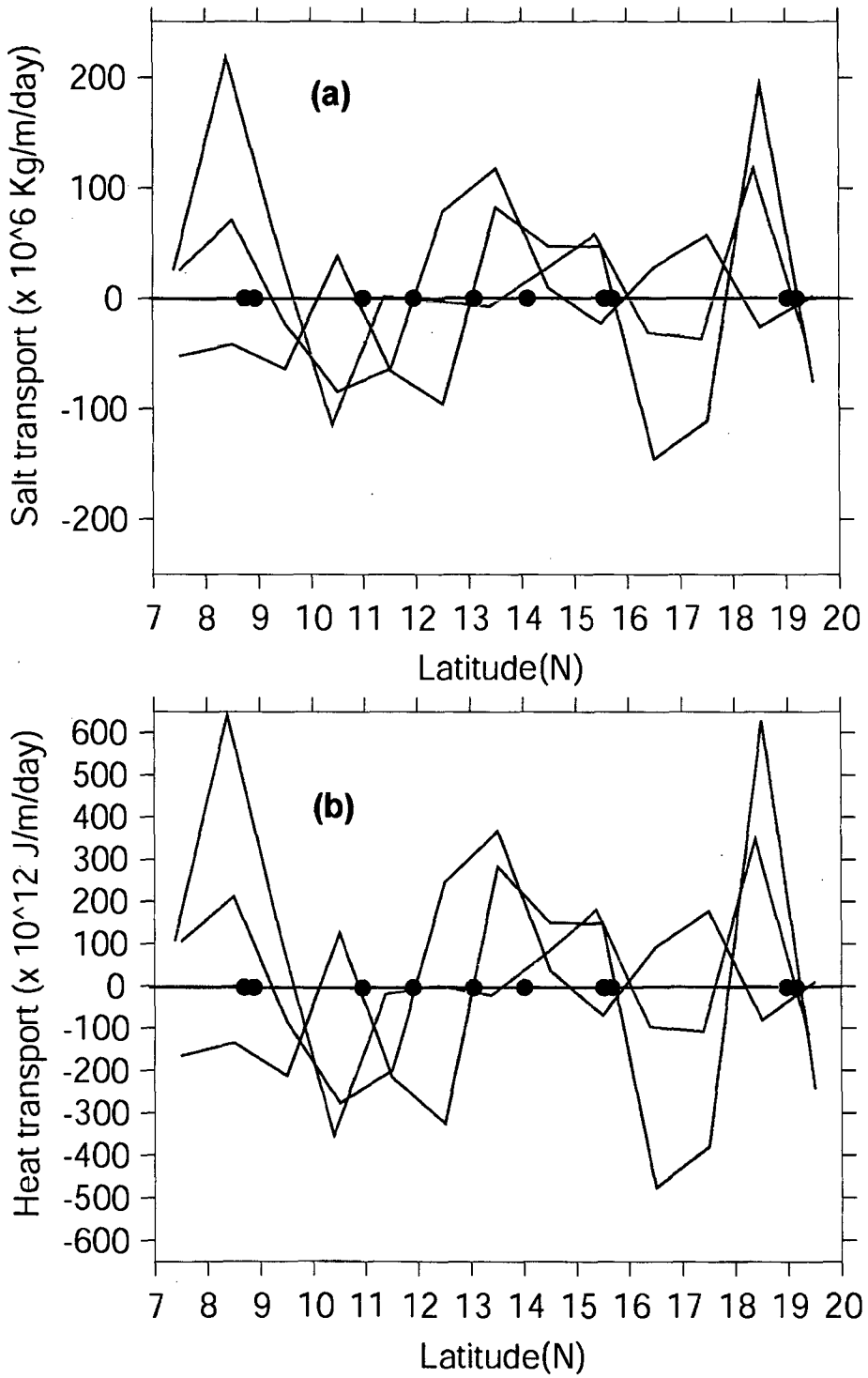

Figure.5.2.6. (a) Salt transport and (b) Heat transport along the central BOB during —— Summer monsoon, —— Fall inter monsoon and —— spring intermonsoon. The coloured circles shows the approximate locations of eddies during each season.

During fall intermonsoon the eastward transport by CEF1 (200 x 10^{12} J/m/day) (both eddies were formed by the same mechanism) was lesser than CES1 of summer, but the westward transport remained the same (300 x 10^{12} J/m/day). Similarly, the heat transport associated with the anticyclonic eddy ACF2 was ~ 300 x 10^{12} J/m/day. The highest heat transport was noticed during spring intermonsoon with the cyclonic eddy CESP4, which had an eastward and westward transport of 600 and 300 x 10^{12} J/m/day respectively. The pattern of salt transport (Figure 5.2.6a) was exactly similar to that of heat transport. The maximum values occurred during summer monsoon in the south and during spring intermonsoon in the north. In summer monsoon an eastward salt transport of ~ 200 kg/m/day was associated with cyclonic eddy CES1 (9°N) while during spring intermonsoon it was with CESP4 (19°N).

Along the coast also the heat and salt transports were greatly influenced by the presence of eddies (Figure 5.2.7). During spring intermonsoon the cyclonic eddy NCE had an offshore heat and salt transport of ~ 400 x 10^{12} J/m/day and 100 x 10^{6} Kg/m/day respectively. During summer and fall intermonsoon also the transport of heat and salt associated with NCE was the dominant with values of ~ 300 x 10^{12} J/m/day and 100 x 10^{6} Kg/m/day respectively. The large variability in the south (~ 13°N) in spring intermonsoon was associated with the cyclonic eddy SCE which was situated adjacent to an anticyclonic circulation as revealed from the SLA (Figure 3.3.1.3).

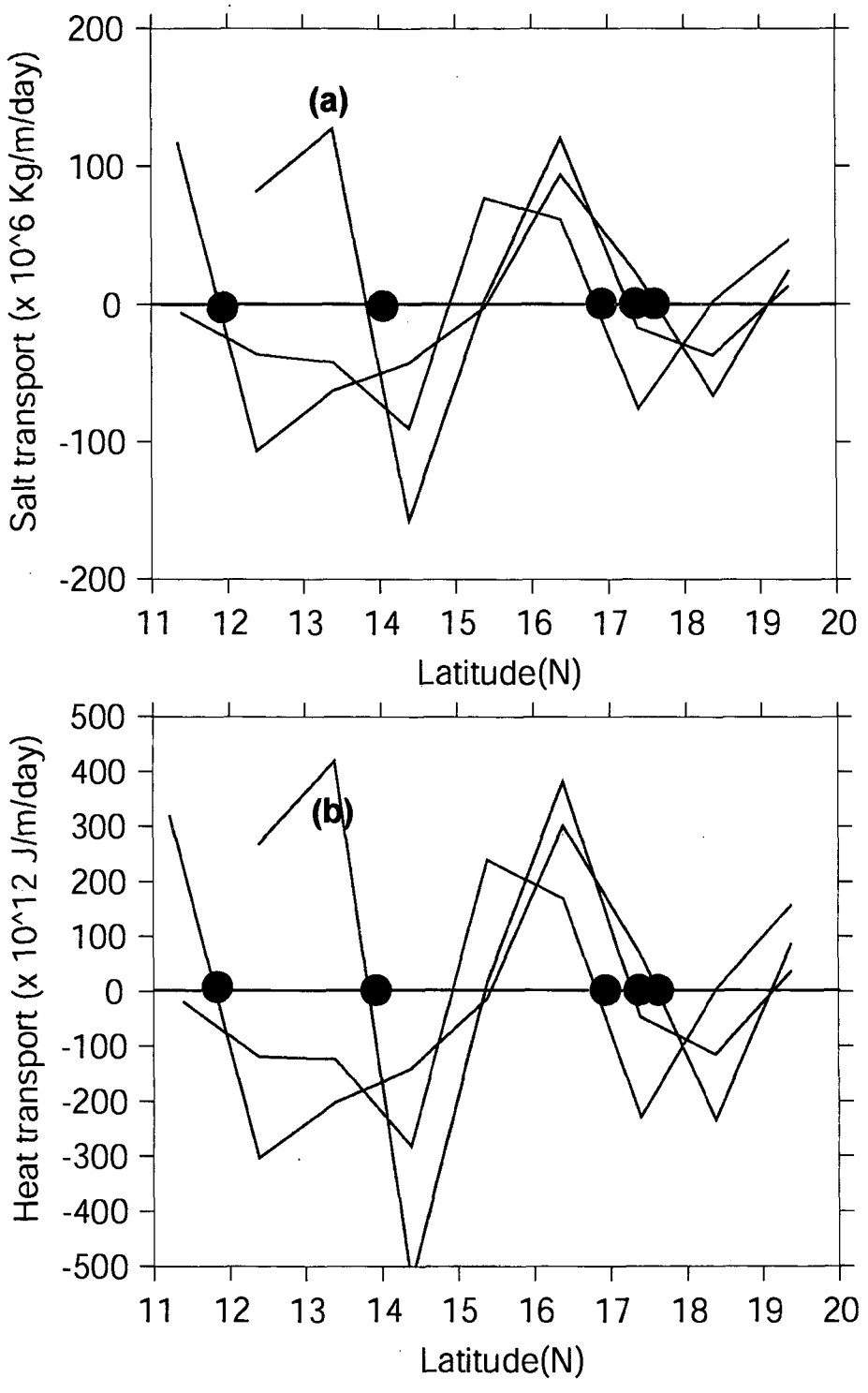

Figure.5.2.7. (a) Salt transport and (b) Heat transport along the western boundary during —— Summer monsoon, —— Fall inter monsoon and —— spring intermonsoon. Coloured circles indicate the centres of the NCE observed during the three seasons.

5.3. Summary

The heat content in the upper 150 m of the water column along the central Bay of Bengal showed a northward decrease of about 200 x 10^{12} J/m in summer and fall intermonsoon. This was associated with the northward shoaling of thermocline seen in the thermal structure. However, along the western boundary the heat content did not show any definite trend as in the case of central BOB, except in spring intermonsoon. During spring intermonsoon the northward decrease of heat content by a bout 200 x 10^{12} J/m was also associated with the thermocline shoaling. The most dominant change in the heat content, in addition to the south-north variability, was associated with the cyclonic/anticyclonic eddies. The salt content along the central and western BOB showed a progressive decrease from south to north in all the 3 seasons except in spring intermonsoon along the western boundary. This northward decrease is associated with the freshening of the northern BOB under the influence of precipitation as well as river discharge. The dominant variability in the salt content was associated with eddies, ~ 5 x 10^{6} Kg/m, especially during spring intermonsoon. However, the eddy-induced changes were more pronounced in the heat content changes rather than salt content changes. The reason for this lies in the characteristics of the BOB. The BOB has a very strong halocline in a very thin upper layer and the cyclonic eddies are unable to break the strong stratification associated with this halocline. Hence eddy-pumping cannot alter the salinity structure as dramatically as that of temperature. The volume transport computation showed that the contribution from wind-driven Ekman transport was far too small compared to geostrophic transport. The geostrophic volume transport in the top 150 m also showed the influence of eddies as alternate bands of eastward and westward transport in the region of eddies. The eddy-induced volume transport varied from 2 to 8

Sv. The heat and salt transport also showed maximum variability in the region of eddies. The eddy-induced heat transport varied from 100 to 650 x 10^{12} J/m/day, while the salt transport varied from 20 to 200 x 10^{6} Kg/m/day. Thus, from the above it is clear that eddy plays an important role in the east-west exchange of heat and salt in the BOB.

Chapter 6 – Role of eddies in the distribution of nutrients and Chlorophyll

6.1. Introduction

It has been found that from the previous chapters that eddy displaced the isopycnals, which were uplifted/depressed at the center of cyclonic/anticyclonic eddies. The up-sloping of the isopycnals due to eddy-pumping are known to enrich the oligotrophic surface layers [*Falkowski et al., 1991, Olaisala et al., 1993, Mc Gillicudy and Robinson, 1997, Mc Gillicuddy et al., 1998, Seki et al., 2001*]. In the presence of adequate sunlight this will lead to enhanced rates of biological productivity. In the case of anticyclonic eddies, the nutrient poor surface waters are pushed down to deeper layers and do not result in any ecosystem response [*Siegel et al., 1999*].

In the north Indian Ocean, which lies in the tropics, light is usually not a limiting factor that determines biological productivity. Hence, any mechanism that brings or take away the nutrients from the euphotic zone would determine the biological productivity of the region. In the Arabian Sea, biological productivity is tightly coupled to the atmospheric forcing. In winter, it is the convective mixing that result in high productivity [*Madhupratap et al.*, 1996, *Prasanna Kumar et al.*, 2001], while in summer it is through the coastal upwelling along the western margin as well as cyclonic wind-stress curl-driven open ocean upwelling in the north of the Findlater Jet [*Prasanna Kumar et al.*, 2000]. The two transition seasons, fall and spring intermonsoons, represents the least productive regime. The BOB, however, is traditionally considered to be a low productive basin. The recent measurements showed that it is 8 times less productive compared to the Arabian Sea [*Prasanna Kumar et al., 2002*] and marked with feeble seasonality. This

primarily stems from the fact that processes operating in the Arabian Sea such as convective mixing and upwelling are not known to operate here. Upwelling along the western margins of the BOB was reported earlier, but confined very close to the coast [*Shetye et al.*, 1991]. Heavy sediment load brought in by the rivers would suppress whatsoever little effect of upwelling by inhibiting the penetration of light to deeper layers. Not withstanding this, comparable rates of annual export of organic carbon by the BOB to the deep with that of Arabian sea [*Ramaswamy and Nair, 1994*] seems to be a puzzle. In this chapter the role of eddies is explored, which is expected to shed some light on this paradox.

6.2. Summer monsoon 2001

Nutrient structure along the central BOB showed that the concentrations were below detectable levels in the upper 40 m of the water column (Figure 6.2.1). However, centered at 9°N a doming in the isopleths was noticed. This doming was consistent with the thermohaline structure and the satellite derived sea-level anomaly, which showed the presence of a cyclonic eddy (CES1) at this location. Under the influence of CES1 the 1 μ mol nitrate isopleth was uplifted by about 45 meters (from 80 to 35 m). Similar doming can be seen for phosphate as well as silicate. However, two other eddies CES2 (16°N) and CES3 (19°N) that were prominently present in the thermohaline structure did not show its signature distinctly by way of upward displacement of isopleths at these location. In addition to the doming of isopleths, the nutrient distribution showed a general northward shoaling.

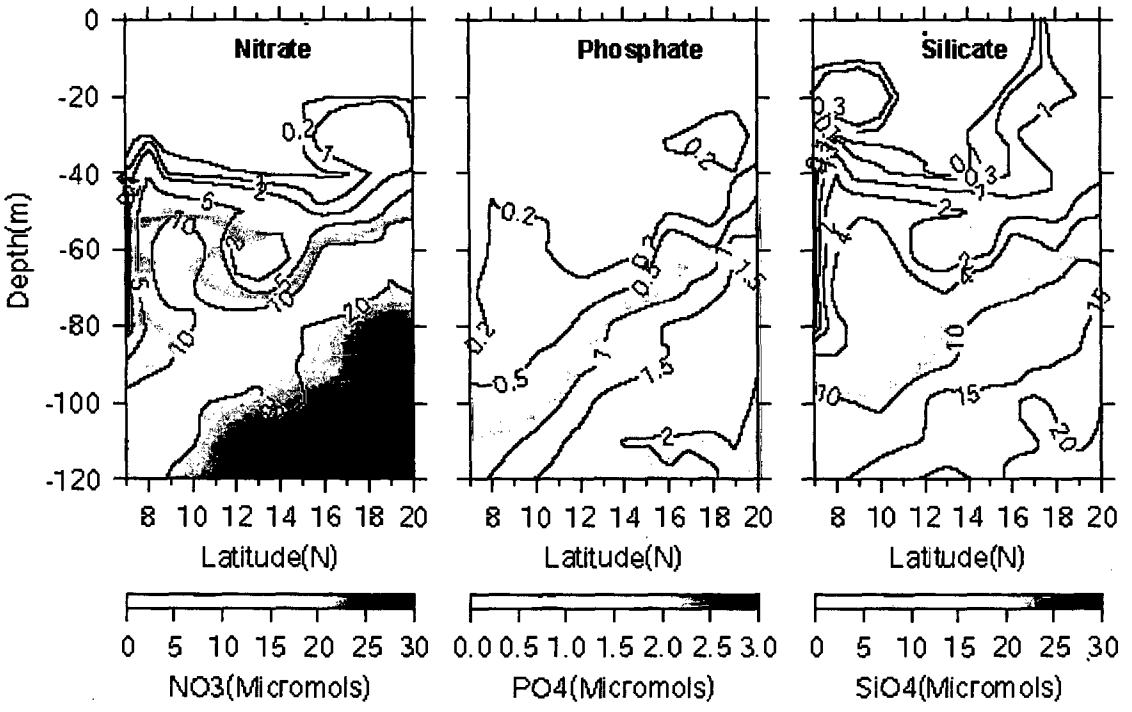

Figure 6.2.1. Vertical structure of nutrients in the central BOB (88°E) during summer monsoon (July-August, 2001). Shoaling of isopleths can be seen centered about 9°N coinciding with the location of the cyclonic eddy CES1. Also a surface enhancement of nutrients can be seen in the northern part of the transect. Note that only selected contours are drawn.

Chlorophyll *a* distribution showed a subsurface chlorophyll maxima (SCM) located at about 40 m depth in the south with a concentration of 0.3 mg/m^3 which showed a gradual shoaling towards north (Figure 6.2.2a), consistent with the thermohaline and the nutrient structure. Enhanced level of chlorophyll was noticed at three locations between 9 and 12°N, between 16 and 18°N, and between 18 and 20 °N. The first one was linked to the cyclonic eddy CES1 which pumped nutrient-rich subsurface waters into the euphotic zone and the second one with the CES2, whereas the third region of high chlorophyll was found to be at the surface (> 0.2 mg/m^3), coinciding with the location of CES3. But CES3 was mainly confined below 50 m (see Figure 4.2.1.1). In such case one would expect an enhanced level of nutrient and chlorophyll *a* some where in that depth region. Though nutrient was higher at the location of CES3, enhanced levels of chlorophyll was noticed at the surface. Surface enrichment of the nutrients was also noted in this location,

which indicates a riverine source, since this last sampling location along the central BOB falls close to the Ganges-Bhramaputra discharge region. Thus, the enhanced level of chlorophyll resulted from a combination of riverine input, eddy pumping and by the northward shoaling of the nutrient isopleths.

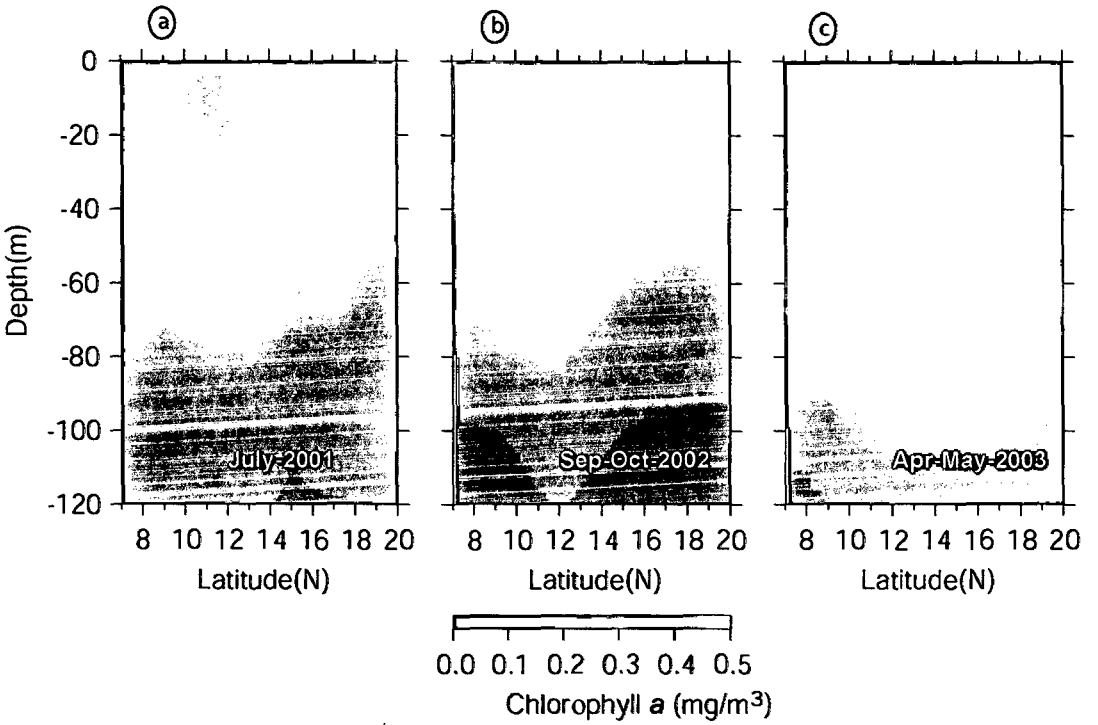

Figure.6.2.2. Chlorophyll *a* concentration during the three seasons a) summer monsoon b) fall inter monsoon and c) spring intermonson along the central BOB (88°E). Enhancement of chlorophyll *a* concentration can be seen coinciding with the location of cyclonic eddies. CES1(9°N) during summer monsoon, CEF1(9°N), CEF3(14°N) during fall inter-monsoon, and CESP1 (11°N), CESP3 (16°N) and CESP4 (19°N) during spring intermonsoon. Subsurface chlorophyll maxima centered at 12°N was depressed during fall intermonsoon (Sept-Oct, 2002) under the influence of anticyclonic eddy ACF2 (12°N).

However, the lack of a subsurface chlorophyll maximum in the north where CES3 was located indicated the possibility of limitation of light due to the enormous quantity of sediment load brought-in by the river discharge.

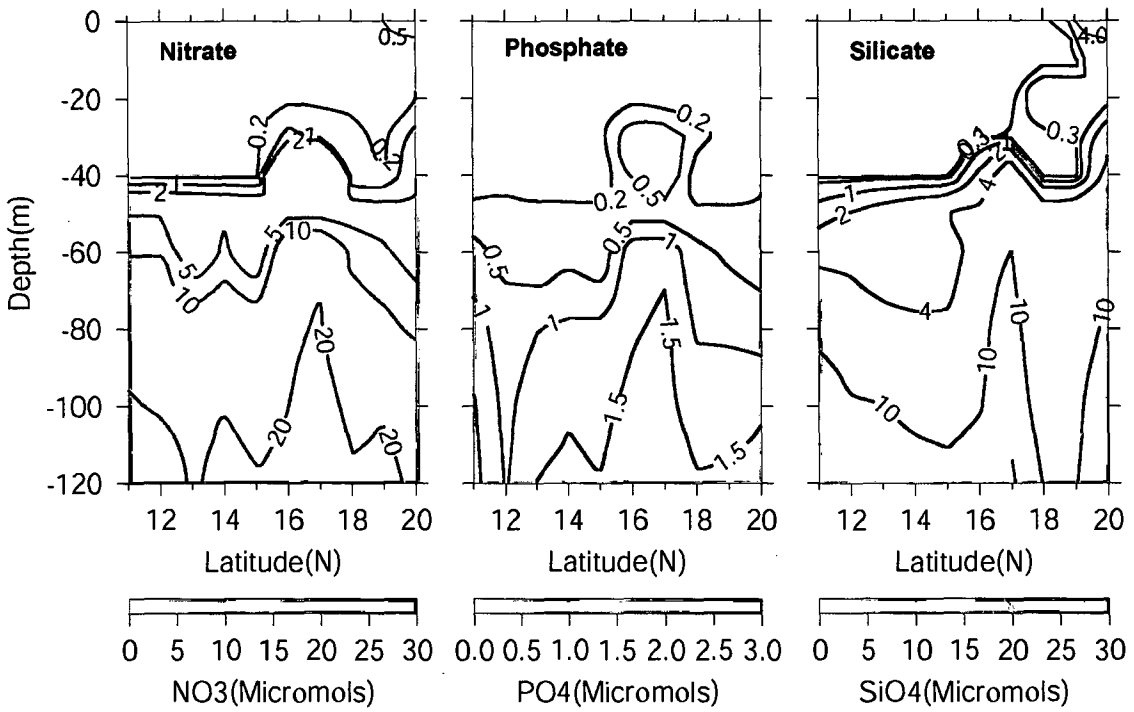

Figure.6.2.3. Nutrients along the western boundary of the BOB during summer monsoon (July-August, 2001). The region between 16 and 18°N is enriched with nutrients because of the upward eddy pumping associated with NCE-2001. Note that only selected contours are drawn.

Surface nutrient concentration, in general, was found to be below detection limits along the western boundary too [Figure 6.2.3]. However, in the north the nitrate as well as silicate showed a surface enhancement up to 0.5 and 4 μ mol. The most prominent feature was the doming of nutrient isopleths centered about 17°N, which forms the center of NCE during 2001. Under the influence of the NCE, 1 μ mol contour for nitrate shoaled to about 30 m. Similar enhancements were also seen in the phosphate as well as silicate distribution. Concurrent with this nutrient enrichment, chlorophyll *a* concentrations also showed enhancement from 0.25 mg/m^3 within the SCM in the south to 0.35 mg/m^3 in the location of NCE. Apart from the enhancement of chlorophyll within the SCM, the SCM itself shoaled under the influence of NCE (Figure 6.2.4).

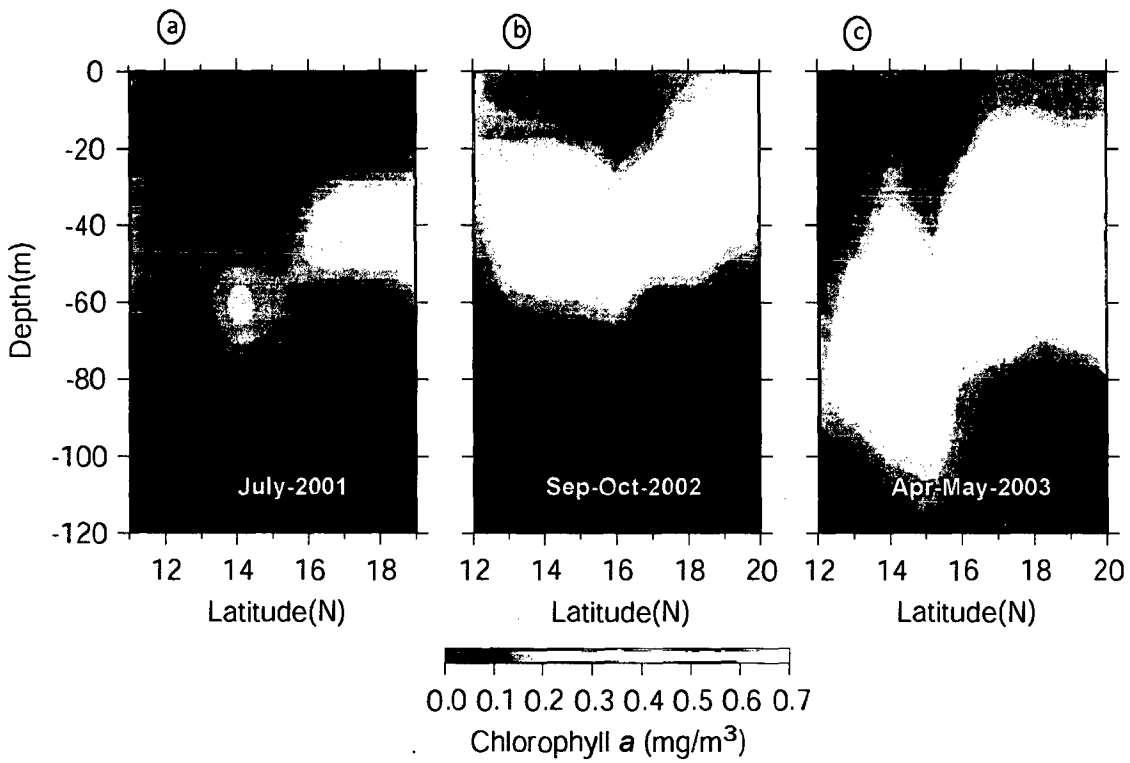

Figure.6.2.4 Chlorophyll *a* concentration during the three seasons a) summer monsoon b) fall inter monsoon c) spring intermonson along the westem boundary of BOB. Enhancement of chlorophyll *a* concentration can be seen between 16 and 19°N coinciding with the location of NCE.

6.3. Fall intermonsoon 2002

Prominent features in the nutrient structure during fall intermonsoon were the undulations in the isopleths (Figure 6.3.1). Doming of isopleths was noticed centered at 9 (CEF1) and 14°N (CEF3) and a depression can be found centered at 11°N (ACF2). The upper 20 meters along the central BOB was oligotrophic, however, the undulations enhanced the level of nutrients along the track. For example, 1μ mol contour reached 20 m depth under the influence of cyclonic eddy CEF1, corresponding enrichment was found for CEF3 also. However, the anticyclonic eddy ACF2 has pushed down the nutrient

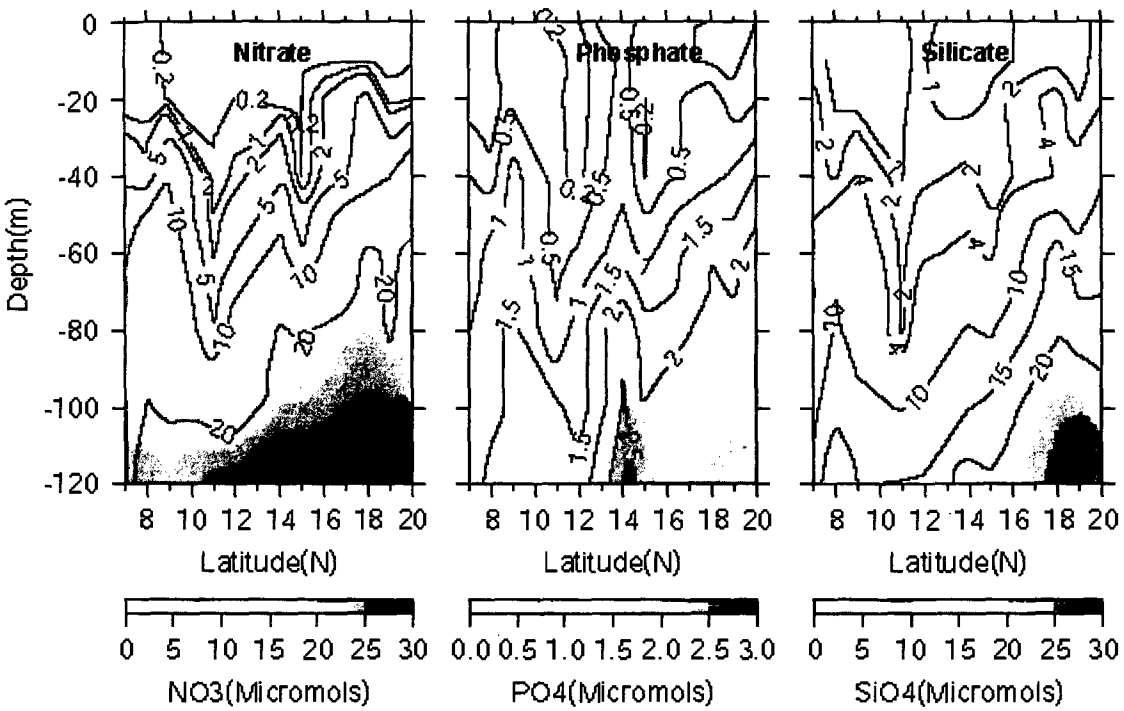

Figure 6.3.1. Vertical structure of nutrients in the central BOB (88°E) during fall inter monsoon (Sep-Oct, 2002). under the influence of the cyclonic eddies CEF1and CEF3 centered at 9 and 14°N the nutrient isopleths domed while that under the influence of anticylonic eddy ACF2 near 12°N isopleths are depressed.Note that only selected contours are drawn.

isopleths resulting in the depletion of nutrients in the euphotic zone. The general south-north shoaling noted during summer monsoon along in the central BOB was present during this season also. Along the western boundary also enhanced nutrient concentration was found at the location of NCE (18°N), whereas an anticyclonic eddy, which is a remnant of spring time circulation pushed the isopleths down resulting in nutrient depletion (Figure 6.3.2).

Variability in the chlorophyll *a* concentration followed the variability in the nutrient structure. Enhanced levels of chlorophyll *a* were noticed between 7-10°N, 13-15°N and 16-18°N. The first zone corresponds to the location of CEF1, second one with CEF3 and the third one with a large cyclonic circulation in which CEF3 was a part (Figure 6.2.2b).

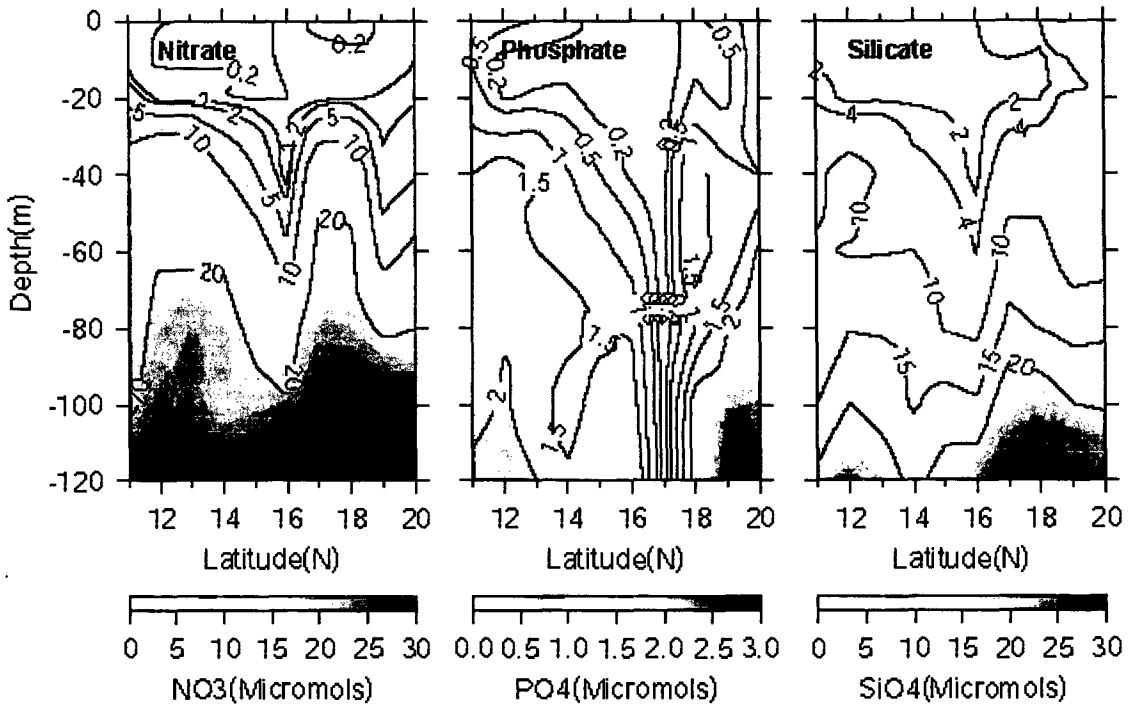

Figure.6.3.2. Nutrients along the western boundary of the BOB during fall inter monsoon (Sep-Oct, 2002). The region between 16 and 18°N is enriched with nutrients because of the upward eddy-pumping associated with NCE-2002. Depression in nutrient isopleth seen between 14-16°N can be linked to the anticyclonic circulation. Note that only selected contours are drawn.

Along the western boundary, enhanced levels of chlorophyll *a* were noticed at 14° and at 18°N. Both corresponds to the location of cyclonic eddies SCE and NCE (Figure 6.2.4b). No significant decrease in the chlorophyll *a* concentration was noticed at 16°N where a remnant anticyclonic circulation was found.

6.4. Spring intermonsoon 2003

One large scale feature in the distribution of nutrients along the central BOB was a depression in the vertical structure. This depression rendered the top 30 m of the water column oligotrophic during this season. However, the vertical nutrient structure was characterized by several undulations that domed and depressed at several locations where

eddies were present (Figure 6.4.1). Noticeable domings were found between 11-12°N (CESP1), 14-16°N(CESP3) and 18-20°N(CESP4) and depressions at 12-14°N(ACSP2) and 16-18°N. These locations were close to the cyclonic and anticyclonic eddies described in chapter 4. Vertical structure showed that the doming resulted in enhancing the levels of nutrients in the upper 50 m of the water column. For example 2 μ mol nitrate contour has shoaled to about 35 m for CESP4. Corresponding enrichment in phosphate can also be seen, however concentration of silicate does not vary much because of the high ambient concentration. Another noteworthy feature was the high surface concentration of silicate, 2 μ mol, situated near 13°N (Figure 6.4.1), which indicated the advection of surface waters from source region such as Ganges-Brahmaputra or Irawaddy river out flows.

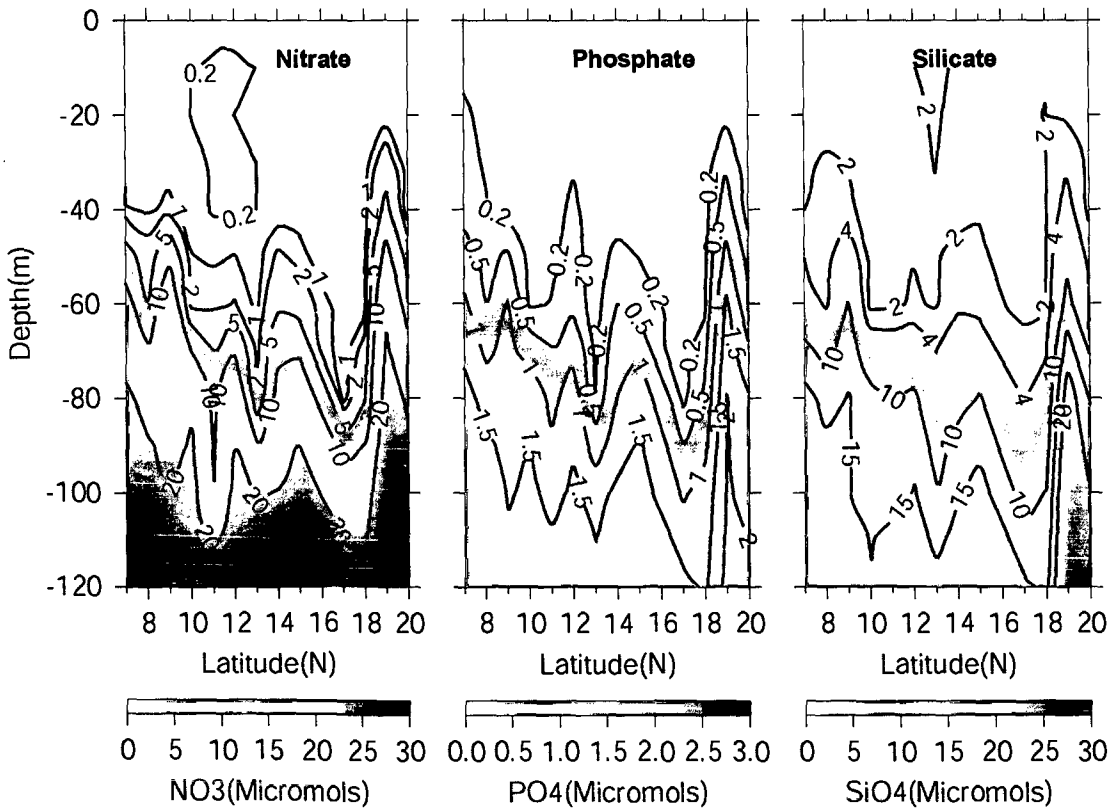

Figure 6.4.1. Vertical structure of nutrients in the central BOB (88°E) during Spring inter monsoon (Apr-May, 2003). Note that only selected contours are drawn.

Chlorophyll structure also showed elevated a level coinciding with the location of eddies. A major enhancement (0.6 mg/m^3) along the track occurred at 19°N corresponding with the location of CESP4. Elevated values in SCM could be seen centered about 16°N, 11°N and 9°N which corresponds to the location of CESP3, CESP1 and a large cyclonic circulation which had not been sampled as it fell outside the track (Figure 6.2.2c).

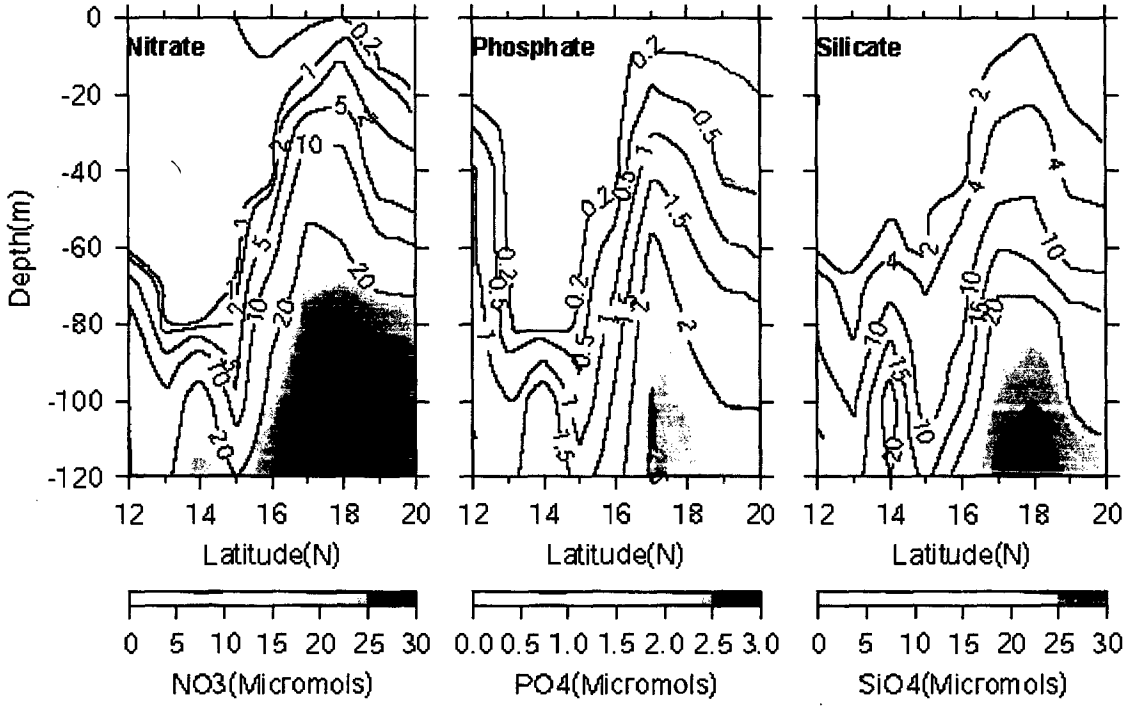

Figure.6.4.2. Nutrients along the western boundary of the BOB during spring inter monsoon (Apr-May, 2003). The region between 16 and 18°N was enriched with nutrients because of the upward eddy-pumping associated with NCE-2003. Depression in nutrient isopleth seen between 14-16°N can be linked to the anticyclonic circulation. Note that only selected contours are drawn.

Along the western boundaryalso the undulation in the nutrient structure coincided with the location of eddies (Figure 6.4.2). Maximum upsloping of nutrient isopleths occurred between 17-20°N coinciding with the location of NCE. Another upsloping was noticed at 14°, again corresponding with the location of a cyclonic circulation. In the case of NCE, the 2 μ mol contour reached 20 m depth which was located at a depth of 60 m outside the eddy. Similar doming coinciding with the location of eddies could be seen for phosphate and silicate.

Chlorophyll profile also showed enhanced concentrations coinciding with the locations of eddies along the western boundary (Figure 6.2.4c). Two such regions were between 16-18°N and 13-15°N, the first one was the location of NCE and the second one was the location of a transient cyclonic eddy SCE discussed in chapter 3.

6.5. Summary

Variability in the nutrient and the chlorophyll concentrations have been discussed in this chapter in the context of cyclonic and anticyclonic eddies. Under normal situation, the upper 20 m of the water column in all the 3 seasons were devoid of nutrients, except in the north. Accordingly, the chlorophyll distribution showed the surface chlorophyll was, in general, about 0.1 mg/m^3 and subsurface chlorophyll maximum (SCM) existed in all the seasons. During summer and fall intermonsoon, surface enrichment of nutrients occurred in the north due to the riverine input from Ganges-Brahmaputa river system. Hence the surface chlorophyll concentration also showed an increase in this region. In all the 3 seasons studied, large enhancement of nutrient was noticed in the locations of eddies both along the central as well as the western boundary of the BOB. This was mediated by the upward eddy-pumping which resulted in enhanced chlorophyll concentration. The upward eddy-pumping not only enhanced the chlorophyll content in the SCM, but moved it towards the surface. During summer the highest chlorophyll concentration was associated with cyclonic eddy NCE at 17°N along the western boundary and CES1 at 9°N with values in excess of 0.3 mg/m^3. The highest eddy-induced chlorophyll concentration during fall intermonsoon was 0.4 mg/m^3 which was associated with cyclonic eddy CEF1. The highest eddy-induced chlorophyll concentration

among all the 3 seasons occurred during spring intermonsoon at 18°N along the western boundary associated with NCE and in the central BOB at 19°N associated with CESP4. In both cases the chlorophyll a concentrations were in excess of 0.6 mg/m^3.

In summary, eddies enhanced the chlorophyll by 2 to 6 times by eddy-pumping of subsurface nutrient to upper water column. In addition to these eddy-mediated changes, perceptible enhancement of chlorophyll due to seasonally changing atmospheric forcing was not discernible. Thus, eddy-induced chlorophyll enhancement offers an alternate /additional mechanism to ballast theory and could at least partially resolve the issue of comparable rates of annual organic flux to deep in the high productive Arabian Sea and the low productive BOB.

Chapter 7 – Summary and Conclusions

Eddies in the Bay of Bengal (BOB) have been studied for their thermohaline characteristics, formation and evolution, role in the hydrography, circulation and in the distribution of nutrients and chlorophyll using a suite of data set both *in situ* as well as remote sensing. The *in situ* data includes temperature and salinity profiles measured using CTD at 1-degree from 7°N to 20°N along the central BOB (88°E) transect and from 11°N to 20°N along the western BOB, in the upper 1000 m collected for 3 seasons - summer monsoon (10-July-2001 to 1-August-2001), fall intermonsoon (17-September-2002 to 11-October-2002) and spring intermonsoon (16-April-2003 to 6-May-2003). The nutrient and chlorophyll profiles were obtained from BOBPS CD-ROM (Indian Oceanographic Data Centre product, National Institute of Oceanography, Goa, March 2007). Remote sensing data includes the 7-day snap-shot of merged sea-level anomaly of Topex/Poseidon ERS1/2 satellites at $1/3^{rd}$ of a degree resolution and twice-daily QuickSCAT wind-stress at $1/4^{th}$ of a degree resolution, both from 2001 to 2003.

The thermohaline structure along the western boundary was dominated by the signature of eddies manifested by the doming (cyclonic) and depressions (anticyclonic) during all the 3 seasons. Two eddies along the western boundary, namely the northern coastal eddy (NCE) and the southern coastal eddy (SCE), were identified from the thermohaline structure and confirmed using satellite derived sea-level anomaly (SLA) maps. Out of these two, NCE was found in all the 3 seasons and all the 3 years analyzed (2001 to 2003). Hence NCE appeared as a robust feature occurring seasonally every year within

the latitudinal belt 16° – 19°N and had alie span of about 5 months. The NCE cooled the ambient temperature of upper-thermocline, which was maximum during spring intermonsoon by about 6°C and increased the near-surface salinity by 0.8 psu. However, SCE was found only during spring and fall intermonsoons and was located at 14°N and 12°N respectively. The SCE during fall intermonsoon was advected from the Sri Lankan Dome region, while during spring intermonsoon it was formed locally. The SCE cooled the upper thermocline by 3°C and increased the ambient salinity by 0.5 psu. Unlike the NCE, SEC was transient feature which lasted only for a month. Since NCE was a robust feature which appeared yearly during spring intermonsoon, its evolution and generating mechanism was explored further.

Based on the 7-day SLA maps of 2001 and 2003, it was found that the NCE was formed during the western boundary current (WBC) regime. The WBC starts flowing northward along the western boundary of BOB during the first week of February. A meander centered at 17°N appeared in the WBC during this period and develops into a cyclonic eddy, NCE, in the last week of March. The NCE had a complex life cycle undergoing offshore-onshore movements, southwestward translation, coalescence and splitting before it finally gets dissipated. All of this occurred within a span of approximately 5 months. From the above, it appeared that the trigger for the generation of the cyclonic eddy NCE could be the instability of the WBC. The cross-shore density gradient accompanied by vertical shear in the horizontal velocity field is a necessary condition for baroclinic instability [*Pedlosky*, 1979]. The possible mechanisms that can lead to this cross-shore density gradient could be (1) topographic changes, (2) wind forcing, and (3) remote

forcing, either individually or in combination. A careful examination of the bathymetry and the location of meander in the WBC rules out the possibility of topographic changes as a trigger for the instability of WBC. Based on the analysis of curl of the wind-stress as well as from the time-longitude plot of zonally de-meaned SLA indicated that both wind forcing as well as remote forcing by Rossby waves plays a key role in generating NCE.

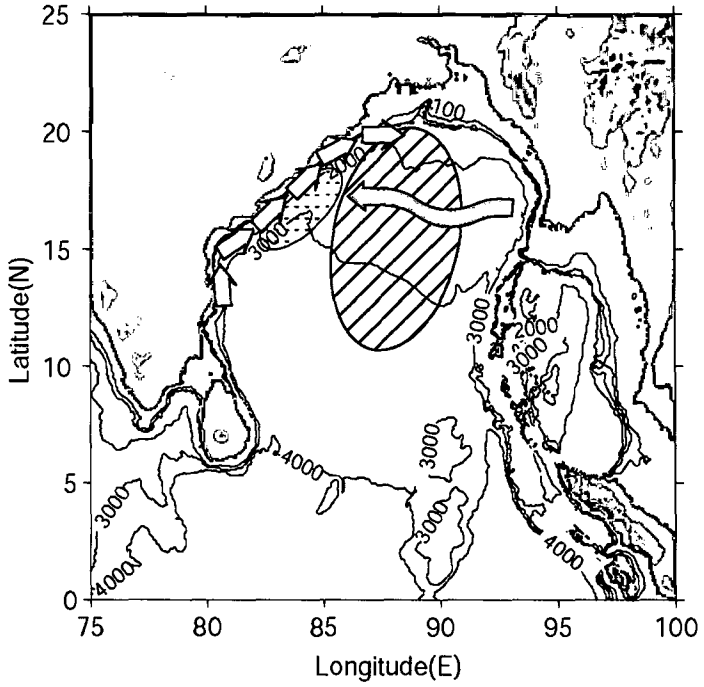

Figure 7.1. Schematic showing the mechanism of generation of northern coastal eddy (NCE) under the influence of wind-stress curl and the Rossby wave. Smaller (bigger) ellipse filled with dots (slanting lines) represents the positive (negative) wind-stress curl. The arrows along the western boundary represents the WBC, while the zonal band with the arrow-head indicates the Rossby wave propagation. Labled contours indicate bathymetry in meters.

Large-scale wind-stress curl was negative in the offshore region and showed a positive curl close to the western boundary where the meander in the WBC was noticed. In response to this wind forcing, large-scale convergence and downwelling of warm surface waters will occur under the negative wind-stress curl, while divergence and upwelling of subsurface waters close to the coast under the positive wind-stress curl. In addition, the

westward propagating Rossby wave during this period augments the basin-wide negative wind-stress curl in deepening the pycnocline. Thus, the negative wind-stress curl and Rossby wave act in union to deepen the pycnocline in the offshore region, while the positive wind-stress curl shallows the pycnocline close to the coast. This in turn will generate strong cross-shore density gradient necessary for the baroclinic instability that leads to the generation of NCE. This is schematically represented in Figure 7.1.

The thermohaline structure along the central BOB showed the signature of 10 eddies, both cyclonic as well as anticyclonic, which were confirmed based on the SLA maps. The cyclonic eddies cooled the ambient temperature which ranged from 1 to 3°C, and increased the salinity which raged from 0.2 to 0.4 psu. The anticyclonic eddies warmed the ambient temperature which ranged from 1 to 2°C, while the decrease in salinity was about 0.2 psu. Unlike their coastal counter part, the eddies seen in the central BOB were not generated out of a process such as meandering of strong current but out of a variety of processes that has strong spatio-temporal dependence. Most of these eddies were formed in the eastern BOB and was advected westward into the central region and beyond (Figure 7.2). Eddies CES1 and CEF1, however, were formed in the western side of the central transect and were moved eastward during summer and fall intermonsoon under the influence of the eastward flowing summer monsoon current.

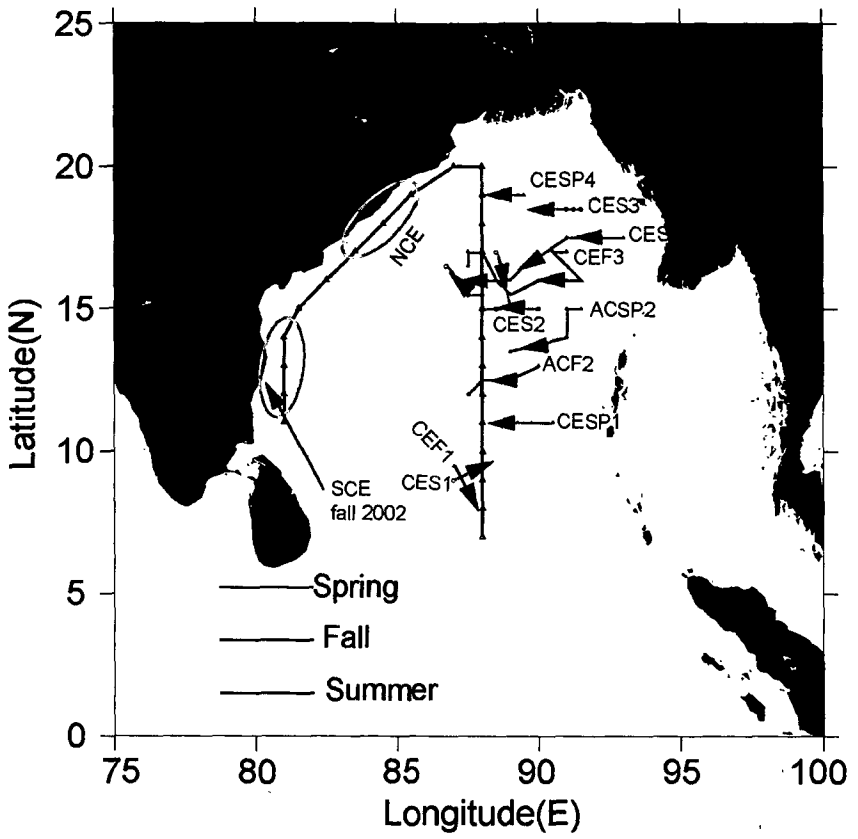

Figure 7.2. Movement of eddies in the Bay of Bengal. All the eddies encountered in the central BOB were formed east of 88°E. Whereas eddies were found to be locally formed along the western boundary, except the SCE found during fall intermonsoon, which was advected from north-east of Sri Lanka. Ellipses along the western boundary represents the region where NCE and SCE were encountered.

A common feature that was observed during the formation of eddies described above was the horizontal SLA gradient which generates the vertical shear, a necessary condition for the baroclinic instability. The horizontal SLA gradient was generated by a combination of processes. In the case of CES1 and CEF1 which forms in the vicinity of Sri Lankan dome during summer and fall intermonsoon respectively, the horizontal gradient was generated by the Sri Lankan dome (negative SLA) and the westward propagating anticyclonic vortices (positive SLA). The formation of cyclonic eddy CES2 in the early summer was due to the SLA gradient generated by a negative SLA adjacent to positive SLA driven by a large-scale anticyclonic circulation. The eddy was found to intensify

when the curl of the wind-stress changed from negative to positive in the month of May. A similar situation was observed during the generation of CES3, the only exception was the positive SLA towards east which was the manifestation of coastally trapped Kelvin wave. The anticyclonic eddy ACF2 formed during summer (July) when there was a a negative wind-stress curl overlying a positive SLA. Towards the west of this, there was a positive SLA and this created the horizontal density gradient necessary for the generation of ACF2. The condition during the formation of cyclonic eddy CEF3 during fall intermonsoon was similar to that of cyclonic eddy CES3 during summer (Figure 7.2), except that the wind-stress curl was negative at the location of CEF3.

The condition that existed during the generation spring time eddies CESP1, ACSP2, CESP3 and CESP4 was the following. The large-scale wind-stress over BOB was uniform and negative during April and underlying the wind field was the westward propagating upwelling Rossby wave manifested by the low SLA. The upwelling Rossby wave imparts a cyclonic motion to the water column whereas the negative wind-stress curl imparts an anticyclonic motion, and hence opposing each other. In such situation it is difficult to explain the development of horizontal gradient in SLA.

Thus, the formation of eddies observed in the central BOB takes place due to a combination of variety of processes that were specific to the space and season, all of which lead to the generation of horizontal gradient in the SLA. This has been represented schematically in Figure 7.3.

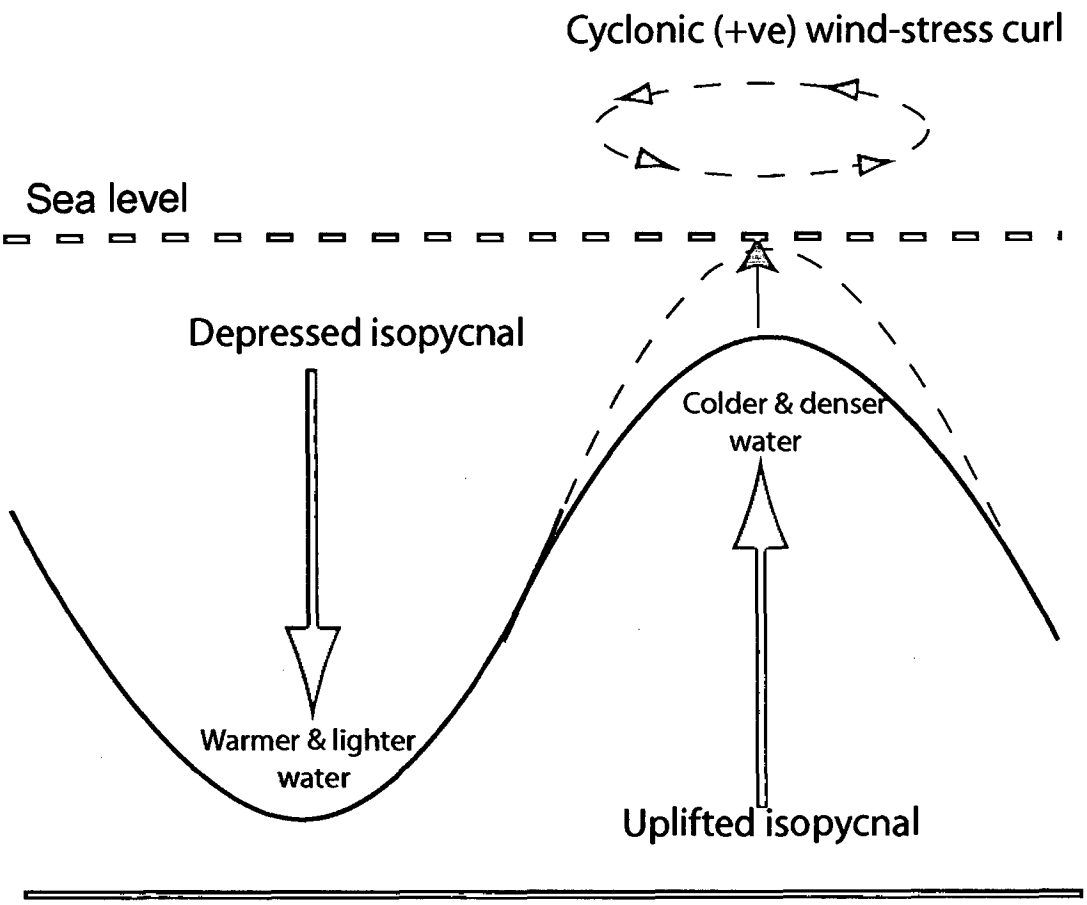

Figure 7.3. The figure depicts one of the mechanism that could generate an eddy in the BOB. The uplifted isopycnal towards the right and the depressed isopycnals towards the left. This contrasting effect will create a horizontal density gradient which can lead to vertical shear This is a necessary condition for baroclinic instability.

From the above discussion it is clear that eddies are ubiquitous in the BOB and present during all the seasons studied. Since eddies are ubiquitous, it natural to expect that these features would influence the hydrograhy and circulation of BOB. The estimation of heat and salt content in the upper 150 m of the water column showed the dominant effect of eddies over the seasonal variability, which amounted to 200-300 x 10^{12} J/m and 5 x 10^{6} Kg/m of heat and salt content respectively. These eddy-induced changes were more pronounced in the heat content rather than salt content. The reason for this lies in the

characteristics of the BOB which has a very strong halocline in a very thin upper layer. The cyclonic eddies are unable to break the strong stratification associated with this halocline. Hence, eddy-pumping cannot alter the salinity structure as dramatically as that of temperature. The volume transport computation showed that the contribution from wind-driven Ekman transport was far too small compared to geostrophic transport. The geostrophic volume transport in the top 150 m was dominated by eddies, which varied from 2 to 8 Sv. The heat and salt transport also showed maximum variability in the region of eddies. The eddy-induced heat transport varied from 100 to 650 x 10^{12} J/m/day, while the salt transport varied from 20 to 200 x 10^{6} Kg/m/day. Thus, in the BOB eddies play an important role in the transport and exchange of heat and salt.

Eddies not only influenced the thermohaline characteristics of the BOB but also showed its role in altering the water column nutrient as well as chlorophyll pigment concentrations. Eddy-pumping of nutrient was instrumental in enhancing the chlorophyll concentrations by 2 to 6 times the ambient values in the BOB. Thus, eddies plays a vital role in enhancing the biological productivity of BOB which was traditionally known for its low biological productivity. This may in part resolve the paradox of comparable rates of annual organic carbon flux to the deeper waters in the high productive Arabian Sea and low productive BOB.

Epilogue

The attempt in this thesis was to study the characteristics and role of eddies in the Bay of Bengal. A suite of data sets has been used to accomplish this objective. To this end the evolution and the generating mechanisms were studied first followed by their role in the hydrography, circulation and in the distribution of nutrients and chlorophyll. The study brings out the role eddy in mediating physical, chemical and biological changes. However some questions remain. The study has not been able to answer all the possible mechanisms of generation of eddy in the Bay of Bengal. The process of instabilities has to be tackled in a more quantitative fashion. A first step towards that will be eddy-specific observations to understand the processes involved so that it could be modelled. The next step will be the use of eddy resolving ocean circulation models coupled with good ecosystem dynamics. There is enough scope to explore the mechanisms of geophysical turbulence and associated energy cascade. Recent studies show that this is true even for baroclinic oceans. But the bottle neck is the length at which this cascade is arrested. For barotropic ocean this happens at the Rhines length. However there is no perfect analogy of this for a baroclinic ocean.

It is satisfying that the thesis has found answers to some of the questions posed but at the same time opens door to new avenues. Attempting such questions would add to the understanding of the underlying dynamics of the Bay of Bengal and kindle further excitement.

References

Babu, M.T., S. Prasanna Kumar, D.P. Rao,(1991), A subsurface cyclonic eddy in the Bay of Bengal, *J. Mar. Res.*, 49, 403-410.

Babu, M.T., Y.V.B. Sarma, V.S.N. Murty, P. Vethamony, (2003),On the circulation in the Bay of Bengal during northern spring inter-monsoon (March-April 1987), *Deep-Sea Res (II).*, 50, 855-865.

Bernstien, R.L., W.B.White, (1977), Zonal variability in the distribution of eddy energy in the midlatitude North Pacific Ocean, *J. Phys. Oceanogr.*, 4, 123-126.

Böning, C.W., R.G. Budich, (1992), Eddy dynamics in a primitive equation model: Sensitivity to horizontal resolution and friction, *J. Phys Oceanogr.*, 22, 361-381.

Bruce, J.G. (1979), Eddies off the Somali Coast during the southwest monsoon, *J. Geophys. Res.*, 84C, 7742-7748.

Chelton, D.B., Michael. G. Schlax., Roger. M. Samelson, Roland. A. de. Szoeke, (2007), Global observations of westward energy propagation in the ocean: Rossby waves or nonlinear eddies, submitted to *Science*.

Conkright, M.E., R.A. Locarnini, H.E. Garcia, T.D. O' Brien, T.P. Boyer, C. Stephens, J.I. Antonov, (2002), World Ocean Atlas 2001: Objective Analysis, Data statistics and Figures, CD-ROM documentation, National Oceanographic Data center, Silver Spring, MD, 17pp.

Cushman-Roisin, B., E. P. Chassignet and B. Tang, (1990), On the westward motion of mesoscale eddies. *J. Phys. Oceanogr.*, 20, 758-568.

Duncan. C.P., (1968), An eddy in the subtropical convergence southwest of South Africa, *J. Geophys. Res.*, 73C, 531-534.

Eady, E.T., (1949) Long waves and cyclones, *Tellus*,1, 33-52.

Falkowski, P.G., D. Zieman, Z. Kolber, P.K.Beingfang, (1991), Role of eddy pumping in enhancing primary production in the ocean, *Nature*, 352, 55-58.

Fuglister, F.C., L.V., Worthington (1947) Hydrography of the western Atlantic; meanders and velocities of the Gulf stream, *Woodshole Oceanogr.* Inst., Tech. Rep., No. WHOI 47-9.

Gopalan, A.K.S., V.V. GopalaKrishna, M.M. Ali, R. Sharma, (2000), Detection of Bay of Bengal eddies from TOPEX and insitu observations, *J. Mar. Res.*, 58, 721-734.

Grasshoff, K.; Ehrhardt, M.; Kremling, K. eds, (1983), *Methods of seawater analysis*, Verlag Chemie, Weinheim, Germany, 419pp.

Isachsen, P.E., La Casce. J.H., J.Pedlosky, Rossby wave instability and apparent phase speeds in large ocean basins,(2006), Submitted to *J. Phys. Oceanogr.*

Iselin, C'OD, (1936), A study of the circulation on the western north Atlantic. Pap Phys Oceanogr. Met., 4(4), 101pp.

Iselin, C'OD., F.C.Fuglister, (1948), some recent developments in the study of gulf stream, *J. Mar. Res.*, 7(3), 317-329.

Josey, S.A., E.C. Kent, P.K. Taylor, (2002), On the windstresss forcing of the ocean in SOC climatology: Comparisons with NCEP/NCAR, ECMWF, UWM/COADS and Hellerman and Rosenstein data sets, *J. Phys. Oceanogr.*, 32(7), 1993-2019.

Jet propulsion Laboratory, California Institute of Technology (2003), Sea winds on Quik SCAT Level-3 derived multi algorithm surface wind stress (JPL), Version 1, Guide document.

Kamenkovich, V.M., M. N. Koshlyakov, A.S. Monin, (Eds.), (1986), *Synoptic eddies in the ocean*, Reidel, Dordrecht, Holland, 433pp.

La Casce. J.H, Joseph. Pedlosky, (2004), The instability of rossby basin mode and the oceanic eddy field, *J. Phys. Oceanogr.*, 34, 2027-2041.

La Fond, E.C (1957), Oceanographic studies in the Bay of Bengal, *Proc. Indian. Acad. Sci.*, 46B, 1-43.

Legeckis. R., (1987), Satellite observation of a western boundary current in the Bay of Bengal, *J. Geophys. Res.*, 92C, 12974-12978.

Le Traon, P.Y., F. Nadal, N. Ducet, (1998), An improved mapping method of multisatellite altimeter data, *J. Atmos. Oceanic. Technol.*, 15, 522-534.

Le Traon P.Y., G. Dibarboure, (1999) Mesoscale mapping capabilities from multiple altimeter missions. *J. Atmos. Oceanic Technol.*, 16, 1208-1223.

Levitus, S., R. Burgett, and T. Boyer, 1994, *World Ocean Atlas 1994.*Vol 3, *Salinity*; Vol. 4, *Temperature,* NOAA Atlas NESDIS 3, 4,U.S. Dept. of Commerce, 117pp & 99pp

Lutjeharms, J.R.E., (2006), *The Agulhas Current*, Springer, Berlin, Germany, 329pp.

Madhupratap. M., S. Pasanna Kumar, P.M.A. Bhattathiri, M. Dileep Kumar, S. Raghukumar, K.K.C. Nair, N. Ramaiah, (1996), Mechanism of biological response to the winter cooling in the northeastern Arabiab sea, *Nature*, 384, 549-552.

McCreary, J.P. W. Han, D. Shankar, S.R, Shetye, (1996), Dynamics of the east India coastal current. 2. Numerical solutions, *J. Geophys. Res.*, 101C, 13993-14010.

McGillicuddy, D.J., A.R. Robinson, (1997), Eddy induced nutrient supply and new production in the Sargasso sea, *Deep. Sea. Res(1)*, 44, 1427-1449.

McGillicuddy, D.J., A.R. Robinson, D.A. Seigel, H.W.Jannasch, R. Johnson, T.D.Dickey, J. McNeil, A.F. Michaels, A.H. Knap, (1998), Influence of mesoscale eddies on new production in the Sargasso sea, *Nature*, 394, 263-266.

Murty, C.S., V.V.R. Varadachari, (1968), Upwelling along the east coast of India, *Bull. Natl. Inst. Sci.* India, 38, 80-86.

Murty, V.S.N., A. Suryanarayana, D.P. Rao, (1993), Current structure and volume transport across 12°N in the Bay of Bengal, *Indian. J. Mar. Sci.*, 22, 12-16.

Nilsson C.S., G.R. Cresswell, (1980), The formation and evolution of East australian current warm core eddies, *Prog. Oceanogr*, 9, 133-184.

Olaisala. M., D.A. Zeimann, P.K. Beingfang, W.A. Walsh, L.D. Conquest, (1993), Eddy induced oscillations of the pycnocline affect the florist composition and depth distribution of phytoplankton in the subtropical Pacific, *Marine Biology*, 116, 533-542.

Pedlosky, J., (1979),*Geophysical Fluid Dynamics*, Springer-Verlag., 624pp.

Pond, S., G.L. Pickard, (1978), *Introductory dynamic oceanography*, Pergamon Press, Oxford, UK., 241pp.

Potemra, J.T., M.E. Luther, J.J. O'brien, (1991),The seasonal circulation of the upper ocean in the Bay of Bengal, *J. Geophys. Res.*, 96 C, 12667-12683.

Prasad, T.G., (1997), Annual and seasonal mean buoyancy fluxes for the tropical Indian Ocean, *Curr. Sci.*, 73, 667-674.

Prasanna Kumar, S., M.T. Babu, D.P. Rao, (1992), Energy and generating mechanism of a subsurface, cold core eddy in the Bay of Bengal, *Indian J. Mar. Sci.*, 21, 140-142.

Prasanna Kumar, S., M. Nuncio, J. Narvekar, A. Kumar, S.Sardesai, S. N. De Souza, M. Gauns, N. Ramaiah, M. Madhupratap,(2004), Are eddies nature's trigger to enhance biological productivity in the Bay of Bengal?, *Geophys.Res Lett.*, 31, L07309, doi:10..1029/2003G1019274.

Prasanna Kumar, S., M. Madhupratap, M. Dileep Kumar, M. Gauns, P.M. Muraleedharan, V.V.S.S. Sharma, S.N.De. Souza, (2000), Physical control of primary productivity on a seasonal scale in central and eastern Arabian Sea, *Proc. Indian Acad. Sci., Earth Planet Sci.*, 109, 433-441.

PrasannaKumar, S., N. Ramaiah, M. Gauns, V.V.S.S, Sarma, P.M. Muraleedharan, S. Raghukumar, M. DileepKumar, M. Madhupratap, (2001), Physical forcing of biological productivity in the northern Arabian Sea during the northeast monsoon, *Deep-Sea Res., (II)*, 48(6-7), 2001, 1115-1126.

Prasanna Kumar, S., P.M.Muraleedharan, T.G.Prasad, M.Gauns, N.Ramaiah, S.N.de. Souza, S.Sardesai, M. Madhupratap (2002),Why is the Bay of Bengal less productive during summer monsoon compared to the Arabian Sea?, *Geophys.Res Lett.*, 29, doi:10.1029/2002GL016013.

Ramasastry. A.A., C. Balaramamurty, (1957), Thermal fields and oceanic circulation along the east coast of India, *Proc. Indian. Acad. Sci.*, 46, 293-323.

Rao, D.P., J.S. Sastry, (1981), Circulation and distribution of some hydrographical properties during the late winter in the Bay of Bengal, *Mahasagar-Bull. natn. inst. oceanogr.*, 14, 1-16.

Rao, T.V.N., D.P. Rao, B.P. Rao, V.S. Raju, (1986), Upwelling and sinking along Visakhapatnam coast, *Indian J. Mar.Sci.*, 18, 46-49.

Rao, T.V.N, (2002), Spatial distribution of upwelling off the central east coast of India, *Estuarine and Coastal shelf science*, 54, 141-156.

Ramaswamy, V., and R.R. Nair (1994), Fluxes of material in the Arabian sea and Bay of Bengal- Sediment trap studies, *Proc. Indian Acad. Sci. Earth Planet. Sci.*, 103, 189-210.

Richardson. P.L, (1983), "*Gulf stream rings*" in Eddies in Marine science, Eds A.R.Robinson, 19-43.

Richardson. P.L., R.E. Cheney, L.V. Worthington, (1978), A census of Gulf stream rings, Spring 1975, *J. Geophys. Res.*, 83(C12), 6136-6143.

Robinson, A.R, (1983), *Eddies in Marine science*, Springer-Verlag, Berlin, Germany, 609pp.

Schott, F., (1983), Monsoon response of the Somali Current and associated upwelling, *Prog. Oceanogr.*, 12, 357-381.

Sanilkumar, K.V., T.V. Kuruvilla, D. Jogendranath, R.R Rao, (1997), Observation of the western boundary current of the Bay of Bengal, *Deep-Sea Research(1)*, 44, 135-145.

Seigel. David. A., McGillicuddy, D.J., Fields, E.A., (1999), Mesoscale eddies, satellite altimetry, and new production in the Sargasso sea, *J. Geophys. Res*, 104C, 13359-13379.

Seiki. M.P., J.J. Polovina, R.E. Brainard, R.R, Bidigare, C.L. Leonard, D.G. Foley, (2001), Biological enhancement at cyclonic eddies tracked with GOES thermal imagery in the Hawaiian waters, *Geophys. Res. Lett.*, 28, 1583-1586.

Sengupta, D., R. Senan, B.N, Goswami, (2001), Origin of intra seasonal variability of circulation in the tropical central Indian Ocean, *Geophys. Res. Lett.*, 28(7) 1267-1270

Shankar, D., J.P. McCreary., W. Han., S.R. Shetye., (1996), Dynamics of East India Coastal Current 1. Analytic solutions forced by interior Ekman pumping and local alongshore winds., *J. Geophys. Res.*, 101C6., 13975-13991.

Shankar, D., P.N. Vinayachandran, A.S. Unnikrishnan, (2002), The monsoon currents in the north Indian Ocean, *Progr. Oceanogr*, 52, 63-120.

Shetye, S.R., S.S.C.Shenoi, A.D.Gouveia, G.S. Michael, D. Sundar, G. Nampoothiri, (1991), Wind-driven coastal upwelling along the western boundary of the Bay of Bengal during the southwest monsoon, *Cont. Shelf Res*,11, 1991, 1397-1408.

Shetye, S.R, A.D. Gouveia, S.S.C. Shenoi, D. Sundar, G.S. Michael, G. Nampoothiri, (1993), The western boundary current of the seasonal subtropical gyre in the Bay of Bengal, *J. Geophys. Res.*, 98, 945-954.

Stammer, D., (1997), Global characteristics of ocean variability estimated from regional TOPEX/POSEIDON altimeter measurements, *J. Phys. Oceanogr.*, 27(8), 1997, 1743-1769.

Stammer,D. (1998) On Eddy Characteristics, Eddy Transports, and Mean Flow Properties, *J. Phys. Oceanogr.*, 28, 727–739.

Stammer,D., C. Boning, (1992), Mesoscale variability in the Atlantic ocean from geosat altimetry and WOCE high-resolution nunmerical modeling, *J. Phys. Oceanogr.*, 22, 732-752.

Subramanian, V., (1993), Sediment load of Indian rivers, *Curr. Sci.*, 64, 928-930.

Swallow, J.C., J.G. Bruce, (1966), Current measurements off the Somali coast during the southwest monsoon of 1964, *Deep-Sea Res.*, 13, 861-888.

Tomsada, A., (1986), Generation and decay of Kuroshio warm core rings, *Deep. Sea. Res.*, 33, 1475-1486.

The MODE group, 1978, *Deep Sea Res.*, 25, 859-910.

The Ring Group, (1981) Gulf stream cold core rings: Their physics, chemistry, and biology, *Science*, 212 (4499), 1091-1100.

van Aken, H.M., A. K. van Veldhoven, C. Veth, W. P. M. de Ruijter, P. J. van Leeuwen, S. S. Drijfhout, C. P. Whittle and M. Rouault, (2003), Observations of a young Agulhas ring, Astrid, during MARE in March 2000, *Deep Sea Research (II),* 50, 167-195.

Vinayachandran, P.N., S.R. Shetye, D. Sengupta, S.Gadgil, (1996), Forcing mechanisms of the Bay of Bengal circulation, *Curr. Sci.,* 71, 753-763.

Vinayachandran, P. N., T. Yamagata, (1998), Monsoon response of the sea around Sri Lanka: generation of thermal domes and anticyclonic vortices, *J. Phys.Oceanogr.*, 28, 1946-1960.

Vinayachandran, P.N., Murty, V.S.N., RameshBabu, V. (2002), Observations of barrier layer formation in the Bay of Bengal during summer monsoon, *J. Geophys. Res.* 107 (C12), SRF19.1-SRF19.9.

Wyrtki, K., L. Magaard, and J. Hager, 1976, Eddy energy in the oceans, *J. Geophys. Res.*, 81, 2641-2646.

Yu, L., J J. Obrien, J, Yang, (1991), On the remote forcing of the circulation in the Bay of Bengal., *J. Geophy. Res.*, 96C11., 20449-20454.